

# Condition Assessment of the Insulation of On-Load Tap Changers by Partial Discharge Measurements

Vasileios Kanas

Supervisor: Dr. ir. Peter H.F. Morshuis

Daily supervisor: Dr. ir. Armando Rodrigo Mor

June 2013

INTELLIGENT ELECTRICAL POWER GRIDS

## ΙΘΑΚΗ

Σα βγεις στον πηγαιμό για την Ιθάκη,  
να εύχεσαι νάναι μακρύς ο δρόμος,  
γεμάτος περιπέτειες, γεμάτος γνώσεις.  
Τους Λαιστρυγόνες και τους Κύκλωπας,  
τον θυμωμένο Ποσειδώνα μη φοβάσαι,  
τέτοια στον δρόμο σου ποτέ σου δεν θα βρεις,  
αν μέν' η σκέψις σου υψηλή, αν εκλεκτή  
συγκίνησις το πνεύμα και το σώμα σου αγγίζει.  
Τους Λαιστρυγόνες και τους Κύκλωπας,  
τον άγριο Ποσειδώνα δεν θα συναντήσεις,  
αν δεν τους κουβανείς μες στην ψυχή σου,  
αν η ψυχή σου δεν τους στήνει εμπρός σου.

Να εύχεσαι νάναι μακρύς ο δρόμος.  
Πολλά τα καλοκαιρινά πρωιά να είναι  
που με τι ευχαρίστησι, με τι χαρά  
θα μπαίνεις σε λιμένας πρωτοειδωμένους·  
να σταματήσεις σ' εμπορεία Φοινικικά,  
και τες καλές πραγμάτειες ν' αποκτήσεις,  
σεντέφια και κοράλλια, κεχριμπάρια κ' έβενους,  
και ηδονικά μυρωδικά κάθε λογής,  
όσο μπορείς πιο άφθονα ηδονικά μυρωδικά·  
σε πόλεις Αιγυπτιακές πολλές να πας,  
να μάθεις και να μάθεις απ' τους σπουδασμένους.

Πάντα στον νου σου νάχεις την Ιθάκη.  
Το φθάσιμον εκεί είν' ο προορισμός σου.  
Αλλά μη βιάζεις το ταξείδι διόλου.  
Καλλίτερα χρόνια πολλά να διαρκέσει·  
και γέρος πια ν' αράξεις στο νησί,  
πλούσιος με όσα κέρδισες στον δρόμο,  
μη προσδοκώντας πλούτη να σε δώσει η Ιθάκη.

Η Ιθάκη σ' έδωσε τ' ωραίο ταξείδι.  
Χωρίς αυτήν δεν θάβγαινες στον δρόμο.  
Άλλα δεν έχει να σε δώσει πια.

Κι αν πτωχική την βρεις, η Ιθάκη δεν σε γέλασε.  
Έτσι σοφός που έγινες, με τόση πείρα,  
ήδη θα το κατάλαβες η Ιθάκες τι σημαίνουν.

Κ. Π. Καβάφης, 1863 - 1933

As you set out for Ithaca,  
hope that your journey is a long one,  
full of adventure, full of discovery.

C. P. Cavafy, 1863 - 1933

To my parents and my sister

# Abstract

During the last 50 years electricity demand has significantly increased. Large amounts of electricity are transported from the generation to the consumption sites. Overhead lines or underground cables are used to transport the required energy. High voltage levels are used to reduce the transmission losses. Power transformers are responsible for linking the different voltage levels. In addition, power transformers must regulate the voltage of the electricity grid when needed. To achieve the regulation of the voltage, power transformers are equipped with on-load tap changers (OLTC).

The winding of the transformer is equipped with tapped windings. The function of the tap changer is to adjust the output voltage of the power transformer by selecting the different tapped windings and without interrupting the load current. Different OLTC technologies are used in the market. The most commonly used technology of the last 50-60 years is the conventional oil type OLTC (OILTAP).

In the last few years, time based maintenance is systematically being replaced by condition based maintenance. Condition based maintenance aims to reduce the costs that are associated with the maintenance of high voltage equipment and prevent possible failures. On-load tap changers constitute a vulnerable part of the power transformer and there is a number of power transformer failures attributed to OLTC failures. Diagnostic tools are used to assess the condition of tap changers. The condition assessment of the tap changer leads to a decision about the appropriate maintenance.

This thesis investigates the possibility of a new diagnostic tool for on-load tap changers based on partial discharge (PD) measurements. The research project focuses on the major insulation defects that could hamper the operation of on-load tap changers. The differences between PD activity in star and delta connected tap changers are also investigated in this thesis.

The conditions that are present in on-load tap changers are initially modeled by the use of small scale set ups. Signature PD patterns associated with the major insulation defects are obtained from the small scale set up. In addition, PD measurements are also performed in a small, single phase tap changer and in a large three phase, star connected tap changer.

The main purpose of this research project is to investigate the applicability of PD measurements as a diagnostic tool to assess the condition of the insulation of on-load tap changers.

# Table of contents

<b>1</b>	<b>Introduction</b> .....	<b>1</b>
1.1	Power transformers equipped with on-load tap changers.....	1
1.2	Objectives of the research project.....	3
1.3	Outline of the thesis.....	4
<b>2</b>	<b>OLTC technologies and major electrical defects</b> .....	<b>6</b>
2.1	OLTC technologies.....	6
2.1.1	Selector switch tap changers.....	9
2.1.2	Diverter switch tap changers.....	13
2.1.3	Vacuum switch tap changers.....	14
2.2	OLTC connection schemes.....	16
2.2.1	Star-connected tap changers.....	16
2.2.2	Delta-connected tap changers.....	17
2.3	Insulation defects.....	19
2.3.1	Gas bubbles in oil.....	21
2.3.2	Sharp points in oil.....	24
2.3.3	Surface discharges.....	24
2.3.4	Tracking.....	25
<b>3</b>	<b>Insulation diagnosis</b> .....	<b>27</b>
3.1	Dissolved gas analysis (DGA).....	28
3.2	PD measurements by electrical methods.....	31
3.2.1	IEC 60270 test circuit.....	31
3.2.2	Calibration.....	32
3.2.3	Partial discharge patterns.....	39
3.3	Summary.....	41
<b>4</b>	<b>Small scale experiments: Part 1</b> .....	<b>42</b>
4.1	PD detector and additional equipment.....	43
4.1.1	PD detectors.....	43
4.2	Experiments on the small scale set up.....	48
4.2.1	Calibration.....	51
4.2.2	PD measurements.....	52
4.2.2.1	Corona discharges in oil.....	54
4.2.2.2	Surface discharges in oil.....	58
4.2.2.3	Tracking on the paper insulation.....	70
4.2.2.4	Gas bubbles in oil.....	75
4.3	Summary.....	80
<b>5</b>	<b>Small scale experiments: Part 2</b> .....	<b>82</b>
5.1	Single phase tap changer.....	82
5.1.1	Testing in air.....	82
5.1.1.1	Test procedure.....	83

5.1.2	Testing in oil.....	84
5.1.2.1	Test procedure.....	84
5.2	Detection of the discharges.....	92
5.3	Summary.....	97
<b>6</b>	<b>Testing the 3-phase OLTC.....</b>	<b>99</b>
6.1	Experimental procedure (IN AIR).....	99
6.1.1	Defects between adjacent tap positions.....	100
6.1.2	Defects between contacts of different phases.....	105
6.2	Experimental procedure (IN OIL).....	111
6.3	Summary.....	112
<b>7</b>	<b>Conclusions and Recommendations.....</b>	<b>114</b>
7.1	Conclusions.....	114
7.2	Recommendations.....	117
Appendix A.....		118
Appendix B.....		125
Appendix C.....		128
Bibliography.....		129



## Introduction

### 1.1 Power transformers equipped with on load tap changers

The role of the electricity grid is to transport and distribute energy to the consumers. The large distances between the generation of electricity and the consumption sites, force using overhead lines and cables for transportation of the electricity. In order to decrease the transmission losses, the voltage is increased up to higher levels. The power transformers are responsible for changing the voltage levels and thus constitute a very essential part of the electricity grid. The major functions of the power transformers can be summarized as:

- 1) Power transformers provide a link between the different voltage levels of the electricity grid. The link between the different levels must be performed in a way that the exchange of electrical power is ensured.
- 2) Power transformers must maintain the voltage level of the electricity grid at the required level or at an acceptable level during load fluctuations.

The latter can be accomplished by adjusting the transformation ratio of the power transformer. To achieve the regulation of the voltage, the transformer winding is equipped with tapped windings. Every time that a regulation of the voltage is required, a tapped winding is connected to or removed by the main transformer winding, thus adding or subtracting a defined voltage level which is called the step voltage. The on-load tap changer (OLTC) is responsible for selecting the different tapped windings along the main transformer winding without interrupting the load current. In addition, the active and reactive power of the transformer can be controlled by the OLTC.

## 1 Introduction

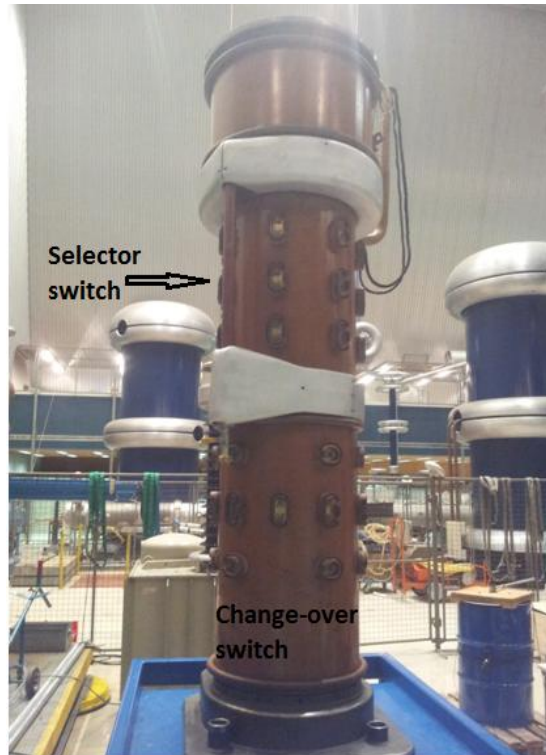


Figure 1.1. A selector switch type OLTC.

There are a number of different OLTC technologies in the market. The different types of tap changers can be categorized depending on:

- i) The location of the tap changer. Tap changers can be 'in-tank' when placed in the same enclosure as the power transformer or 'compartment type' when placed in a different enclosure than the one of the power transformer.
- ii) The electrical location of the tap changer. Tap changers can be connected either to the low voltage side of the transformer or to the high voltage side of the transformer. In Europe it is common to connect the OLTC to the high voltage side of the transformer whereas in the US the OLTC is usually connected to the low voltage side of the transformer.
- iii) The transition impedance. Tap changers can be categorized as reactor type or as resistor type.
- iv) The number of the contacts used for switching. The two types of tap changers include the diverter switch type and the selector switch type. The differences between the diverter switch type OLTC and the selector switch type OLTC are presented in chapter 2.
- v) The connection of the main transformer winding. Tap changers can be connected either in star or in delta depending on the connection of the main transformer winding.
- vi) The switching cycle of the transition contacts. The two types that can be distinguished in that way are the flag cycle and the pennant cycle. The flag switching cycle is described in detail in Appendix A.



## 1 Introduction

- vii) The capability of switching load. The types of the different tap changers are the on-load tap changer (OLTC) and the de-energized tap changer (DETC).
- viii) The insulating medium which is used to extinguish the arcs. The types of the different tap changers include the conventional oil type OLTC and the vacuum type OLTC.

The most common technology which dominates the market of tap changers is the '*in oil*' technology. In oil tap changers are mainly used in the last 50-60 years. This technology is commonly used because it is quite cheap.

### 1.2 Objectives of the research project

On-load tap changers constitute the most vulnerable part of a power transformer [1]. According to the experience, maintenance of tap changers takes place every 3 to 5 years depending on the OLTC technology and connection. The lifetime of the tap changer depends on the function and the location of the power transformer and can withstand up to 150,000 operations. The lifetime of power transformers, according to the experience, is defined by the manufacturer and it ranges between 40 and 50 years of operation. The long lifetime of power transformer increases the concern about the degradation mechanisms in tap changers. During the last few years, time based maintenance is gradually being replaced by condition based maintenance. Condition monitoring can be a useful tool in the future regarding OLTC technologies. Condition monitoring can increase the reliability and can ensure the safe operation of on-load tap changers. Different diagnostic tools are used to assess the condition of the tap changer. Condition based maintenance requires measurements of key diagnostic parameters. The monitoring of the diagnostic parameters provides valuable information about the condition of the tap changer. Then, a decision can be made about the required maintenance. Some of the existing diagnostic tools for on-load tap changers focus on the condition of the mechanical parts of the tap changer and the degradation of its contacts. The condition of the mechanical parts of an OLTC can be assessed by using vibration analysis and acoustic measurements. In addition, dynamic resistance measurements can be used to assess the degree of degradation of the contacts of an OLTC. Other diagnostic tools such as dissolved gas analysis (DGA) can provide information about the insulation of on-load tap changers.

However, there is little scientific research on partial discharge (PD) measurements as a possible diagnostic tool in on-load tap changers. In this research project, partial discharge measurements will be used as a diagnostic tool for assessing the condition of the insulation in on-load tap changers. Defects in the insulation of the tap changer can lead to OLTC failure. The objectives of this research project are:

## 1 Introduction

- Initially, to present the major insulation defects which can appear in star and delta-connected on-load tap changers.
- Then, to investigate the applicability of PD monitoring as a diagnostic tool for on-load tap changers. The principal purpose of this thesis is to investigate whether the major insulation defects in an OLTC can be identified by the use of PD measurements before leading to possible OLTC failure.
- To present a comparison between PD measurements by electrical methods and acoustic PD measurements. The purpose of the comparison is to investigate which detection system is more suitable for monitoring an OLTC.

### 1.3 Outline of the thesis

The aim of this thesis is to investigate the applicability of partial discharge measurements as a diagnostic tool for the condition assessment of on-load tap changers. More specifically, partial discharge activity caused by the major defects that can deteriorate the insulation quality of on-load tap changers is measured by means of electrical methods. The tap changers under investigation are conventional oil type tap changers which can be connected either in delta or in star. Then a comparison is made between the major insulation defects that can cause partial discharge activity in delta and star connected tap changers.

In **Chapter 2**, the different OLTC technologies are described. In addition, the different connection schemes (star and delta) of on-load tap changers are presented. Finally, the major insulation defects in on-load tap changers are discussed. In **Chapter 3**, DGA analysis for on-load tap changers and the most essential background information regarding partial discharge measurements by means of electrical detection are presented.

**Chapter 4** presents the equipment that was used for the partial discharge measurements. In addition, a small scale set up is used to simulate the conditions present in an OLTC. The major insulation defects are modeled in the small scale set up and PD measurements are performed. **Chapter 5** presents the experiments that were performed in a single phase tap changer. A comparison between PD measurements by electrical methods and acoustic PD measurements is also presented in chapter 5. The purpose of the experiments performed in chapter 4 and chapter 5 is to investigate which are the most probable defects to cause partial discharge activity in star and delta connected tap changers. In addition, the applicability of partial discharge measurements as a diagnostic tool for on load tap changers is investigated.

## 1 Introduction

**Chapter 6** presents the experiments that were finally performed in a three phase, star connected, selector switch type OLTC. The introduction of the defects, which were presented in chapter 4, to the OLTC, was attempted. Finally, **Chapter 7** presents the conclusions drawn from the experiments and some recommendations for future research.

# 2

## OLTC Technologies and Major Electrical Defects

The main function of an on-load tap changer (OLTC) is to regulate the voltage output of a power transformer. This voltage regulation is done through the different taps of the tap changer. The taps are contacts mounted on the circumference of the tap changer and are connected to different positions on the tapped winding. Every time the tap changer moves from one position to another, the voltage is increased or decreased (by including or removing a part of the tapped winding) by a fixed voltage level which is called step voltage. The OLTC must be able to select the different taps without interrupting the load current and in a safe way. This procedure can be performed in many ways, thus leading to different OLTC technologies [2-3]. This chapter focuses firstly on the different OLTC technologies. Then, the different ways of connecting the OLTC to the transformer are described and an overview is given of the star and delta connection of the OLTC. Finally, the major electrical defects that may hamper the operation of on-load tap changers are presented.

### 2.1 OLTC technologies

In all the existing technologies of on-load tap changers the load current must be transferred from one tap to another without interrupting it. For that reason, in every on-load tap changer the presence of an arcing switch is required. The arcing switch principles that are mainly in use include the diverter switch and the selector switch. On-load tap changers equipped with the diverter switch also include a tap selector. The tap selector selects the next tap position of the tap changer without switching any current. Then the diverter switch transfers the load from the previously selected tap to the next tap position.

On the other hand, in on-load tap changers equipped with a selector switch, the selection of the next tap position and the switching of the load current take

## 2 OLTC Technologies and Major Electrical Defects

place at the same time. In both technologies the regulating range of the tap changer can be increased by introducing a change over switch. There are several ways, in which the change over switch can be used, as a coarse change over switch, a reversing change over switch and a combination of the coarse and the reversing switch. The operation of the different OLTC technologies is presented in paragraphs 2.1.1, 2.1.2 and 2.1.3.

On-load tap changers can be connected to the low voltage side of the transformer or to the high voltage side of the transformer. In addition, another difference in the OLTC technologies can be found in the transition impedance. The transition impedance is used to control the circulating current. The circulating current is created when the contacts of the tap changer move from one tap position to another. The transition impedance can be a resistor, a reactor or a combination of both. The transition impedance is mounted on the rotor of the tap changer as shown in Figure 2.1. Reactor type on-load tap changers are usually connected to the low voltage side of the transformer whereas resistor type on-load tap changers are usually connected to the high voltage side of the transformer. The type and the value of the transition impedance must fulfill some requirements. These requirements are according to [4]:

- 1) The circulating current should not be excessive.
- 2) The voltage fluctuation during the switching cycle should not be large.
- 3) The arc duration during the transfer of the load should be kept as low as possible.

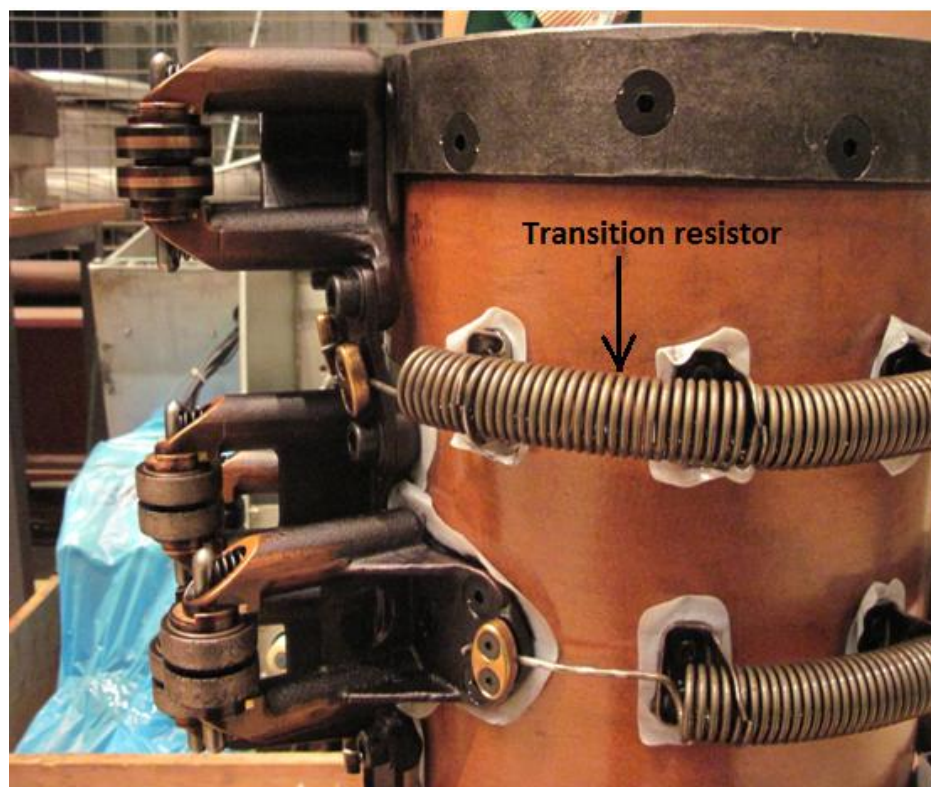


Figure 2.1. Transition resistors mounted on the rotor of the tap changer.

## 2 OLTC Technologies and Major Electrical Defects

On-load tap changers, which are equipped with reactor type transition impedance, are mainly used in the US. A reactor type OLTC, usually is equipped with a diverter switch. Additionally, reactor type on-load tap changers are placed in a separate compartment and not in the same tank with the transformer. In Europe, it is common that the OLTC uses a transition resistor (see Figure 2.1) and the OLTC is placed in the same tank with the transformer (in-tank). The advantages of placing the OLTC in a separate compartment are [4]:

- 1) The OLTC can be inspected without interfering with the transformer.
- 2) The tap changer can be dismantled which gives more flexibility to the transportation.
- 3) The transformer can operate at a constant and fixed ratio when problems are encountered with the OLTC.

On the other hand, three main disadvantages can arise when placing the OLTC in a separate compartment. The disadvantages include [4]:

- 1) Internal bushings between the tap changer and the transformer are required.
- 2) The dimensions of the system increase significantly when compared to in-tank tap changers.
- 3) The cost for this arrangement is increased.

All the technologies that were mentioned use oil as the switching medium. Tap changers, which use vacuum as the switching medium, have been developed and seem to have high performance and a lot of advantages compared to the other type of tap changers (see paragraph 2.1.3).

### 2.1.1 Selector switch tap changers

The selection of the next tap position and the switching of the load current are performed at the same time in tap changers, which are equipped with a selector switch. When the number of steps is limited, then only one selector switch can be used. In this case one selector switch contact is connected to each tap position. An OLTC using only one selector switch is presented in Figure 2.2.

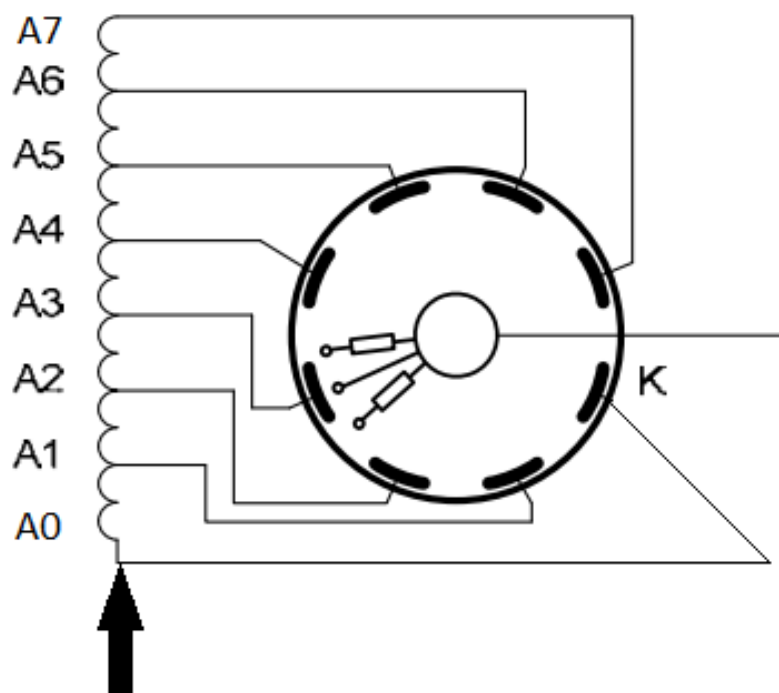


Figure 2.2. OLTC with one selector switch [5].

This design requires a limited number of steps. When the number of steps is increased, the size of the tap changer is also increased. For that reason, when the number of required steps exceeds a certain value, the regulating range of the tap changer is increased by using a second switch. This switch is called the change-over switch. Figure 2.3 presents an OLTC with a selector switch and a coarse change over switch.

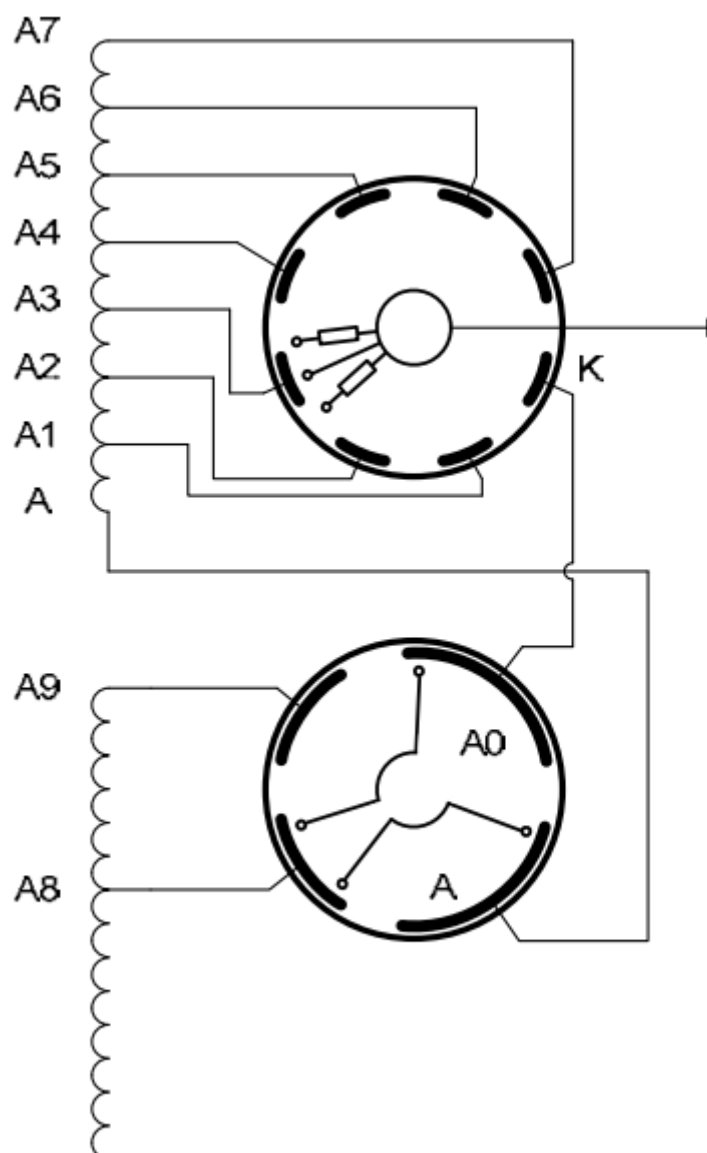


Figure 2.3. OLTC with a selector switch and a change-over switch [5].

When the selector switch has selected all the tap windings, which are connected to its contacts, then the coarse change-over switch operates and selects the next coarse tap winding (A8 to A9). When this process is complete, the selector switch can start selecting the tap windings once more. The selector switch is placed on the top part of the tap changer while the change-over switch is located on the bottom part of the tap changer. As a consequence, the selector switch is more easily accessible than the change-over switch. The rotor of the selector switch can be removed for inspection, the polluted oil can be replaced with new oil and the damaged contacts by the arcing phenomena can be replaced during the maintenance of the tap changer.

The tap changers built for power transformers are of the cylindrical type. The tap selector consists of two parts. The first part is the stator, which contains the static tapping contacts. These contacts are connected to the tapped winding of the



## 2 OLTC Technologies and Major Electrical Defects

transformer as shown on the left part of Figure 2.2 (A to A7). The second part is the rotor that is located inside the stator of the selector switch and contains the moving contacts and is rotated by a drive system. The rotor is responsible for making the connection between the static contacts of the stator, which are connected to the tapped windings, to the main transformer winding. Both the stator and the rotor are cylinders. They are made by hard paper of high mechanical and dielectric strength. The stator and the rotor of a selector switch are presented in Figure 2.4.

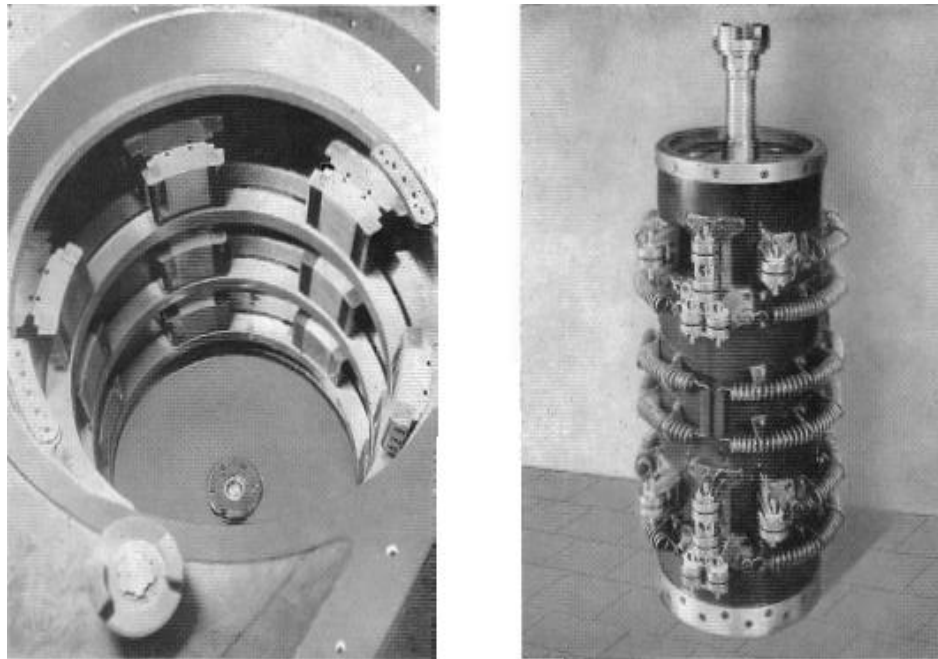


Figure 2.4. Stator contacts of a selector switch (left) [4] and the rotor of the selector switch (right) [4].

The contacts of the stator are placed across the circumference of the cylinder in three different planes, as shown on the left of Figure 2.3. The three planes are placed one above the other with each plane corresponding to one of the three phases. Under every phase of the tap changer there is a slipring. The slipring provides the connection of the rotor contacts to the line terminal. On the right of Figure 2.4, the rotor of the selector switch can be seen. The rotor consists of the moving contacts and the transition resistor. There are four contacts per phase and more specifically, two bridging contacts, one stationary contact and one slipring contact.

In the selector switch the load current is transferred from one tap position to another. During this process, arcs are created (see paragraph 2.3.1). For that reason the insulating oil of the selector switch must be separated from the insulating oil of the transformer. The contacts of the selector switch are made of copper-beryllium alloy and are equipped with arcing tips which are made of a copper-wolfram alloy. Gas, which is created by the arcing phenomenon, is released through a special ventilation system. The same ventilation system is also responsible for preventing the absorption of moisture.

## 2 OLTC Technologies and Major Electrical Defects

The change-over switch is built in the same way as the selector switch. The only differences are:

- 1) No arcing tips are required.
- 2) No transition resistors are required because the change-over switch does not switch the load current.

Every time the selector switch moves to the next / previous tap position, the voltage is increased / decreased by the step voltage. When all tap positions of the selector switch have been selected, the voltage has been increased by 7 times the step voltage, as shown in Figure 2.3 (contacts A1 to A7). Then the change-over switch will move its contacts from the position A8 to position A9 thus increasing the voltage by 8 times the step voltage. At the same time the contacts of the selector switch move to position A0.

When the tap changer moves its contacts from one position to the adjacent tap position, the transition resistors prevent the presence of a short-circuit between the adjacent contacts. Moreover, the transition resistors provide a path for the load current during the operation of the tap changer and limit the circulating current. The operation of an OLTC equipped with a selector switch and a coarse change-over switch is described in more detail in Appendix A.

### 2.1.2 Diverter switch tap changers

An OLTC equipped with a diverter switch is presented in Figure 2.5. This type of OLTC uses the diverter switch together with a tap selector.

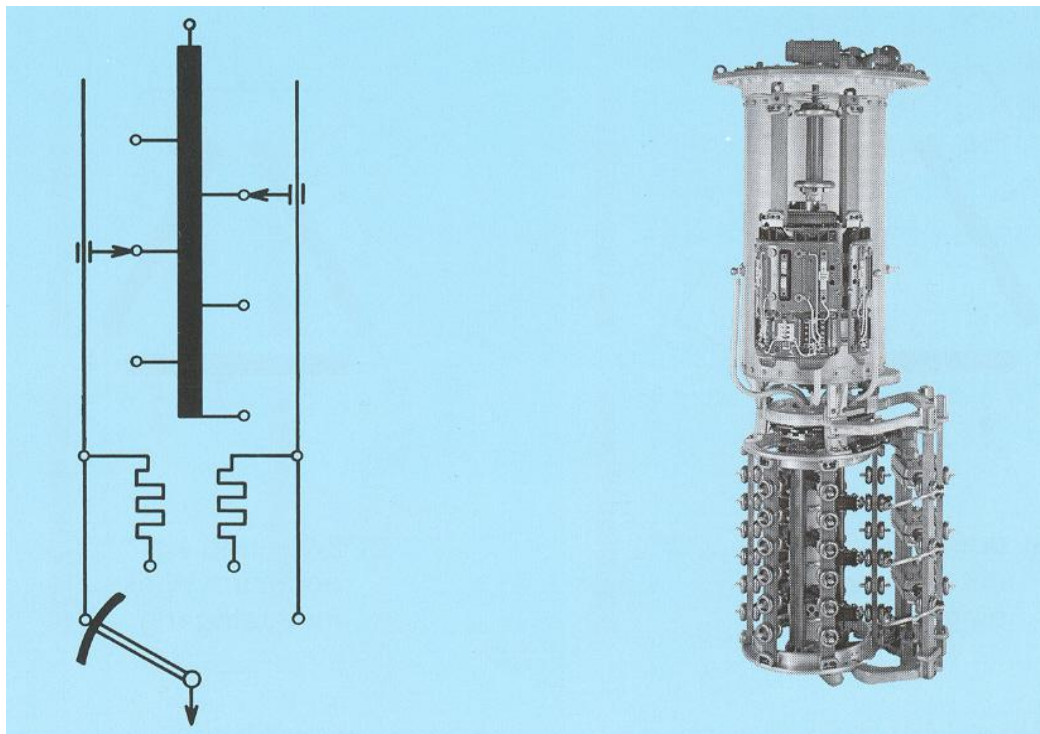


Figure 2.5. Diverter switch type OLTC [6].

The diverter switch can select between two different positions of the tap selector. The selected position will operate under load. The other contact of the tap selector determines the next tap position of the tap changer. This procedure is performed without any current switching. The diverter switch then moves its contact from the operating to the selected tap. The function of the transition resistors remains the same as in the case of the selector switch type OLTC.

The regulating range of the tap changer can be increased by introducing a change-over switch. The change-over switch can operate as, a coarse change-over switch, a reversing change-over switch or a combination of both. The main difference between the diverter switch and the selector switch is that the diverter switch type OLTC does not require the presence of the rotor in the arcing compartment. In Appendix A the operation of the diverter switch type OLTC is described in more detail.

### 2.1.3 Vacuum switch tap changers

Figure 2.6 presents a diverter switch of a vacuum type OLTC. In this type of tap changers the arcs are extinguished inside the vacuum compartment. Since 2000, 600 vacuum tap changers equipped with 3.300 vacuum switches are in operation [6].

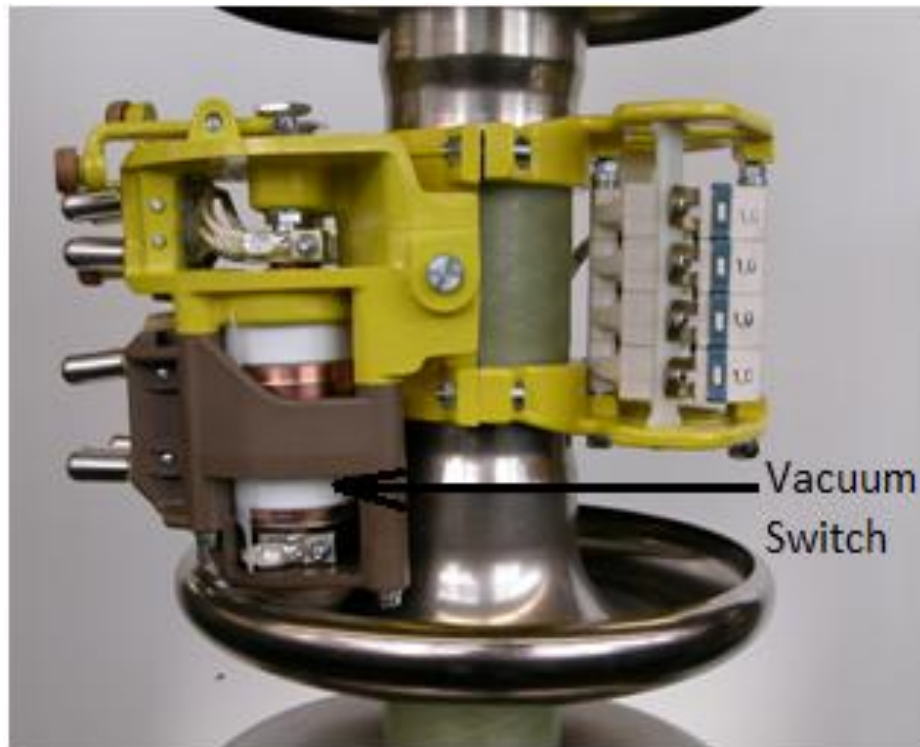


Figure 2.6. Vacuum switch OLTC [6].

Vacuum type tap changers have significant advantages when compared to conventional tap changers where the arc is extinguished in oil. The major advantages are [6]:

- 1) No arcing takes place in oil. As a result, the pollution of the oil is kept to a minimum.
- 2) The contact wear due to the arcing process is also reduced.
- 3) The inspection interval for the vacuum tap changers can be increased from 150,000 to 300,000 operations.
- 4) The maintenance costs and operating costs are reduced.
- 5) Only routine monitoring of the quality of the oil is required.

Vacuum tap changers have high performance and it is a very promising technology. Figure 2.7 presents the rotors of the conventional OLTC in which the extinguishing medium is oil and the vacuum type OLTC after the same number of operations.

## 2 OLTC Technologies and Major Electrical Defects

It is shown in Figure 2.7 that the rotor of the conventional OLTC is easily polluted. On the other hand, the rotor of the vacuum tap changer is in perfect condition. The operation of a vacuum type OLTC is described in more detail in Appendix A.

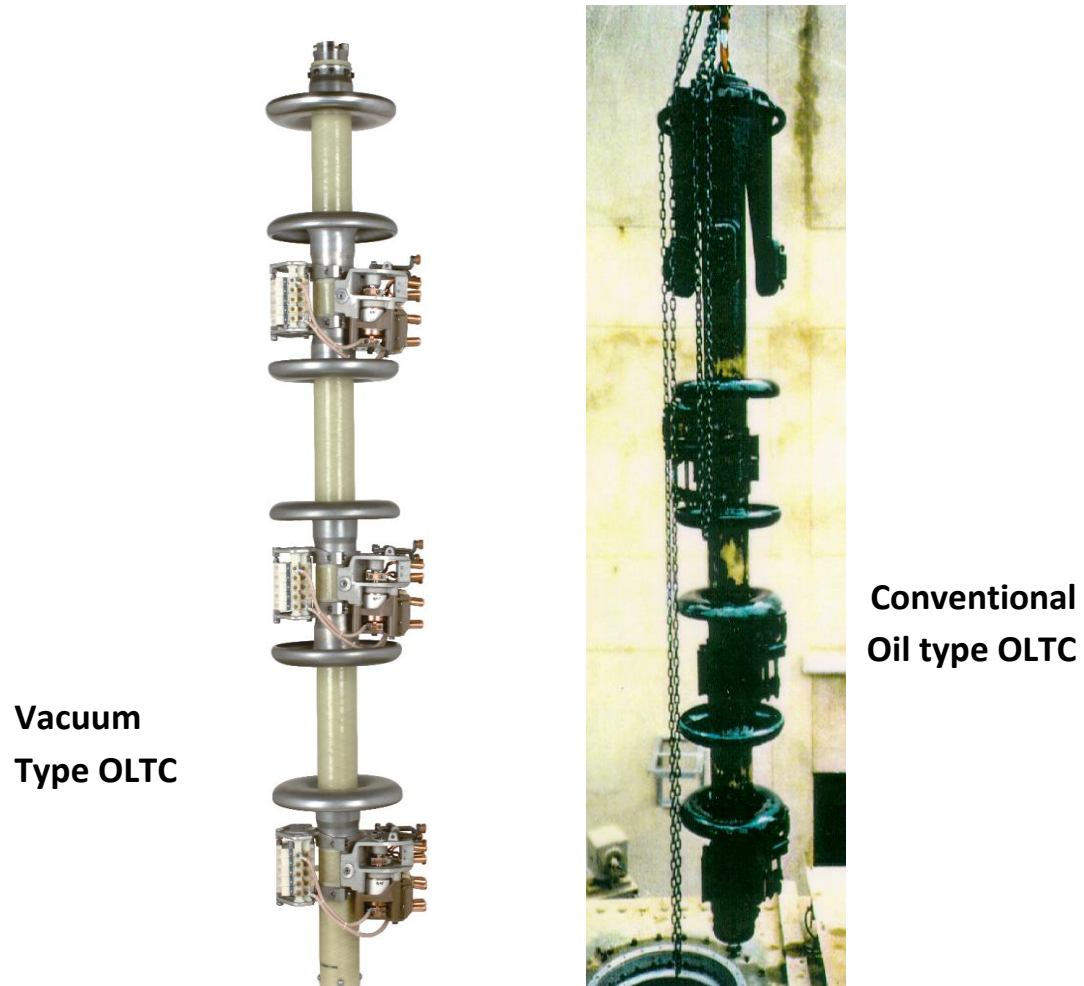


Figure 2.7. Comparison between the rotors of a vacuum OLTC and a conventional oil OLTC [6].

## 2.2 OLTC connection schemes

On-load tap changers can be connected -depending on the connection of the transformer windings- either in star or in delta. The major difference between the two connections is the electrical stress that the tap changer should withstand. Delta connected tap changers are located at the windings end and should insulate for the line to line voltage. On the other hand, tap changers which are installed in star-connected windings are located in the neutral side of the transformer and, therefore, insulate only a part of the line to neutral voltage. As a result, tap changers installed in delta connected windings are electrically stressed more than tap changers installed in star-connected windings.

### 2.2.1 Star-connected tap changers

A schematic diagram of a tap changer which is installed in star-connected windings is presented in Figure 2.8.

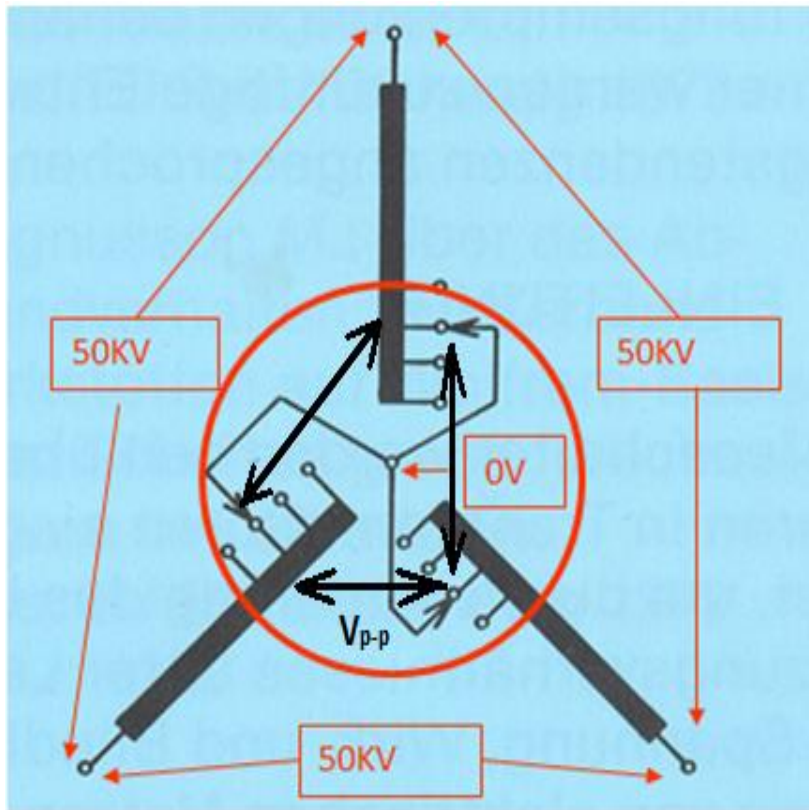


Figure 2.8. Schematic diagram of star-connected tap changers [6].

The switch in star-connected tap changers is located at the neutral point of the transformer. As a result, the tap changer insulates only for a part of the line to neutral voltage. In addition, the voltage difference between the contacts of different phases is low. The voltage difference between the phases of star-connected tap changers is:

$$V_{p-p} = \sqrt{3} \times n \times V_{step} , \quad \text{where,}$$

$V_{p-p}$ , is the voltage difference between two phases,



$n$ , is a number which depends on the number of steps that the tap changer has performed and

$V_{step}$ , is the step voltage of the tap changer.

In the example presented in Figure 2.8, the line voltage is 50 kV. If we assume a normal step voltage of 1.5 kV and that the tap changer has moved its contacts to the position of Figure 2.8, then the maximum voltage difference between adjacent contacts of different phases is

$$V_{p-p} = \sqrt{3} \times 3 \times 1.5 = 7.8 \text{ kV.}$$

The star point in this configuration is formed by the load switch. When tap changers have to operate with star-connected transformer windings, the neutral point is formed in the tap changer by using an extra slipping contact.

### 2.2.2 Delta-connected tap changers

Figure 2.9 presents the schematic diagram of a tap changer installed in delta-connected transformer windings. The line voltage in this example is 50 kV.

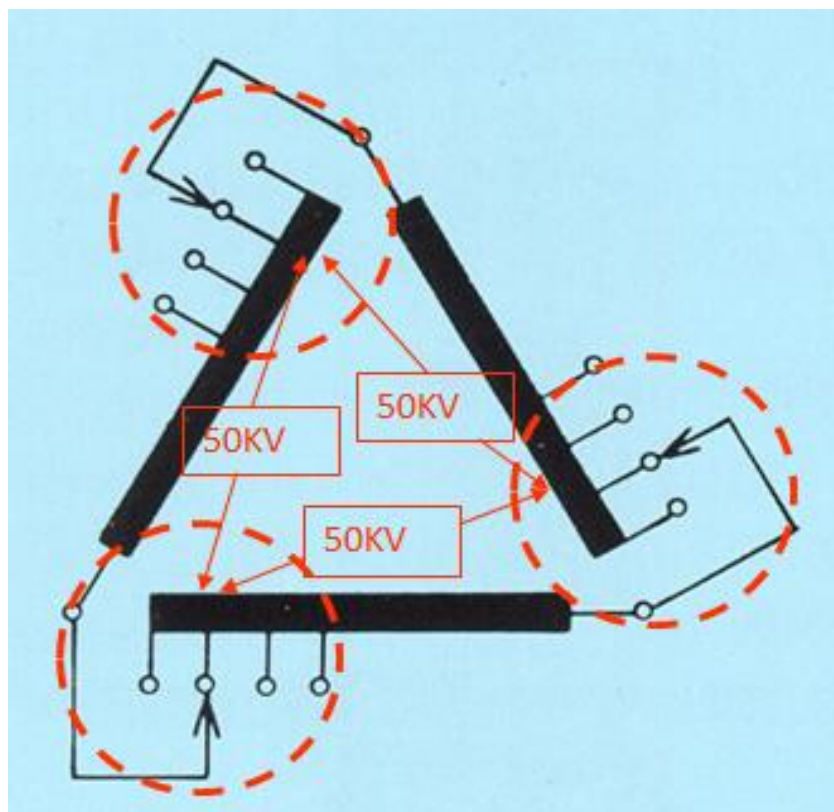


Figure 2.9. Schematic diagram of delta-connected tap changers [6].

The switch in delta-connected tap changers is placed on the winding ends. Delta connected tap changers must insulate for the whole line to line voltage. In addition, the voltage difference between the phases of delta connected tap changers equals the line voltage ( $V_{p-p} = V_{line} = 50 \text{ kV}$ ), as seen in Figure 2.9. The voltage difference between phases in delta connected tap changers is higher than in star-

## 2 OLTC Technologies and Major Electrical Defects

connected tap changers. Delta connected tap changers have to cope with higher electrical stresses and are, therefore more prone to insulation defects than star-connected tap changers.

The difficulty of the high electrical stress between contacts of different phases can be solved by optionally using 3 single phase switches instead of one three phase switch. Another solution is presented in Figure 2.10. The winding ends of two phases are coupled and the switch is shared by the two phases. The combination of a two phase switch with a single phase switch relieves the tension between two phases.

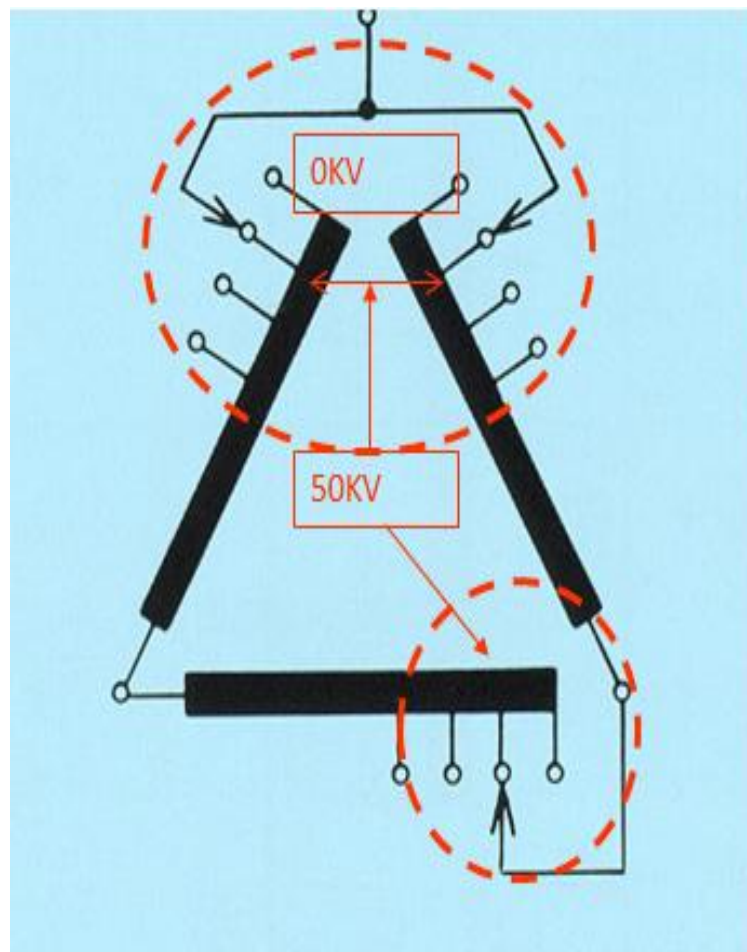


Figure 2.10. Combination of a two phase and a single phase tap changer [6].

The switch can also be located halfway through the windings instead of the winding ends. This configuration is presented in Figure 2.11.



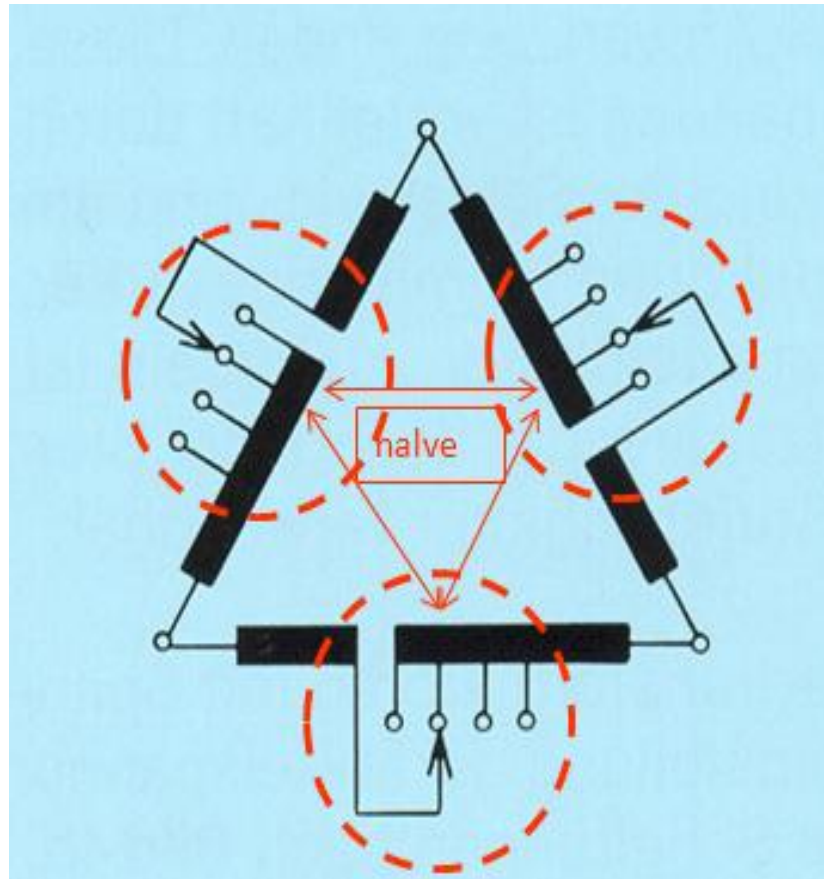


Figure 2.11. Switch located halfway through the windings [6].

The voltage difference between the phases in this configuration is reduced. In that way, the electrical stress is lower than the case where the switch is connected to the winding ends. In this configuration, three single phase tap changers can also be used but the cost of the system is substantially increased.

### 2.3 Insulation defects

The relatively high failure rate of tap changers [7] strengthens the need to understand the mechanisms that lead to failure. The main degradation mechanisms of tap changers are presented in Figure 2.12. The degradation mechanisms (electrical, mechanical, thermal and chemical) can ultimately lead to tap changer failure. This research project focuses on insulation degradation mechanisms which are highlighted in Figure 2.12. More specifically, insulation defects which cause the appearance of partial discharge activity will be examined and detected by means of electrical detection methods. Other types of defects such as mechanical can be detected with other methods. Vibrational analysis is an important tool used to identify the mechanical defects that could hamper the operation of the tap changer.

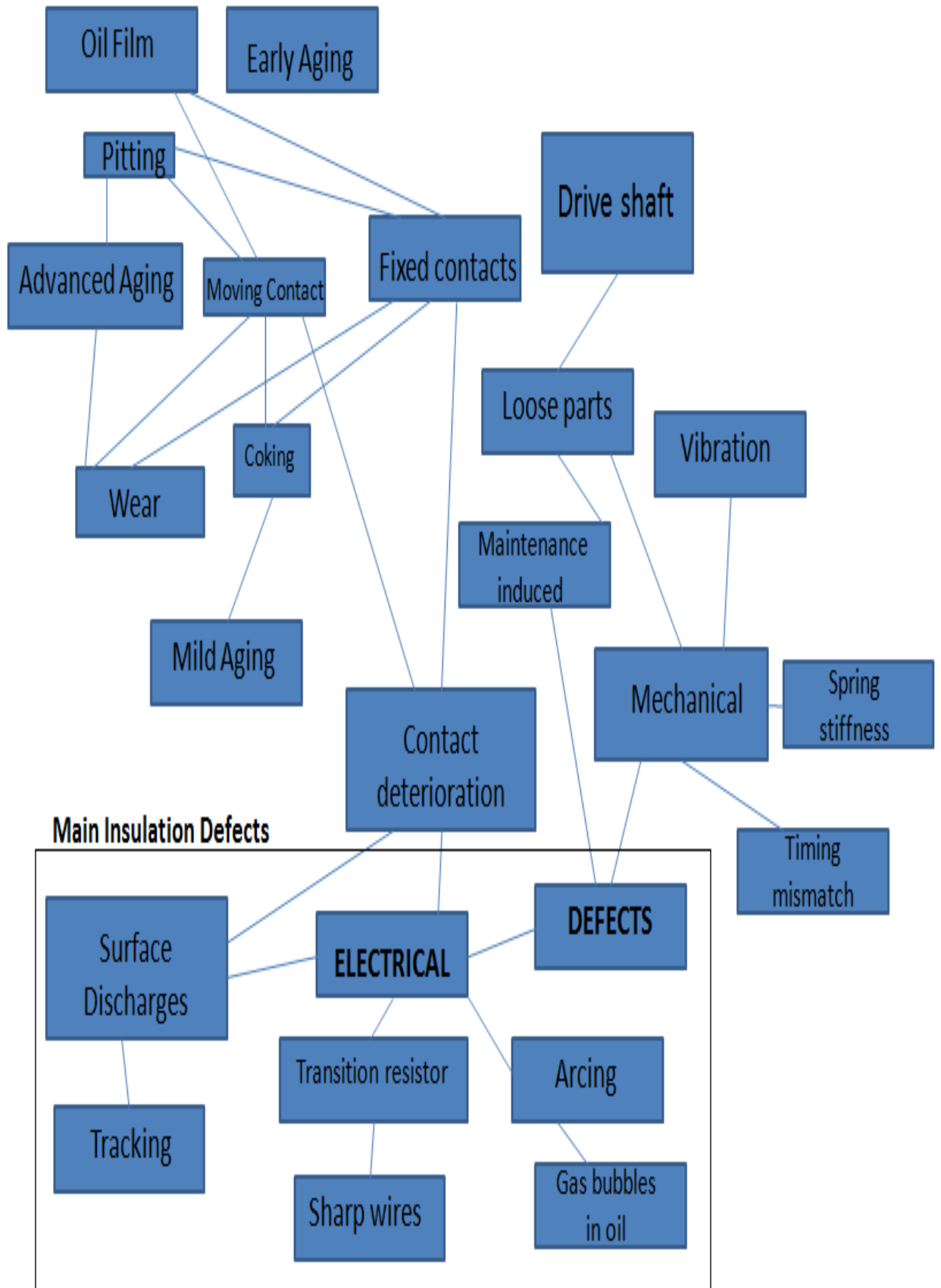


Figure 2.12. Main degradation mechanisms in OLTCs.

### 2.3.1 Gas bubbles in oil

The OLTC must transfer the load current from one tap position to another without interrupting it. The transition process is performed in 150-200 milliseconds. The transition period between two adjacent tap positions is presented in Figure 2.13. The transition period is described in detail in Appendix A.

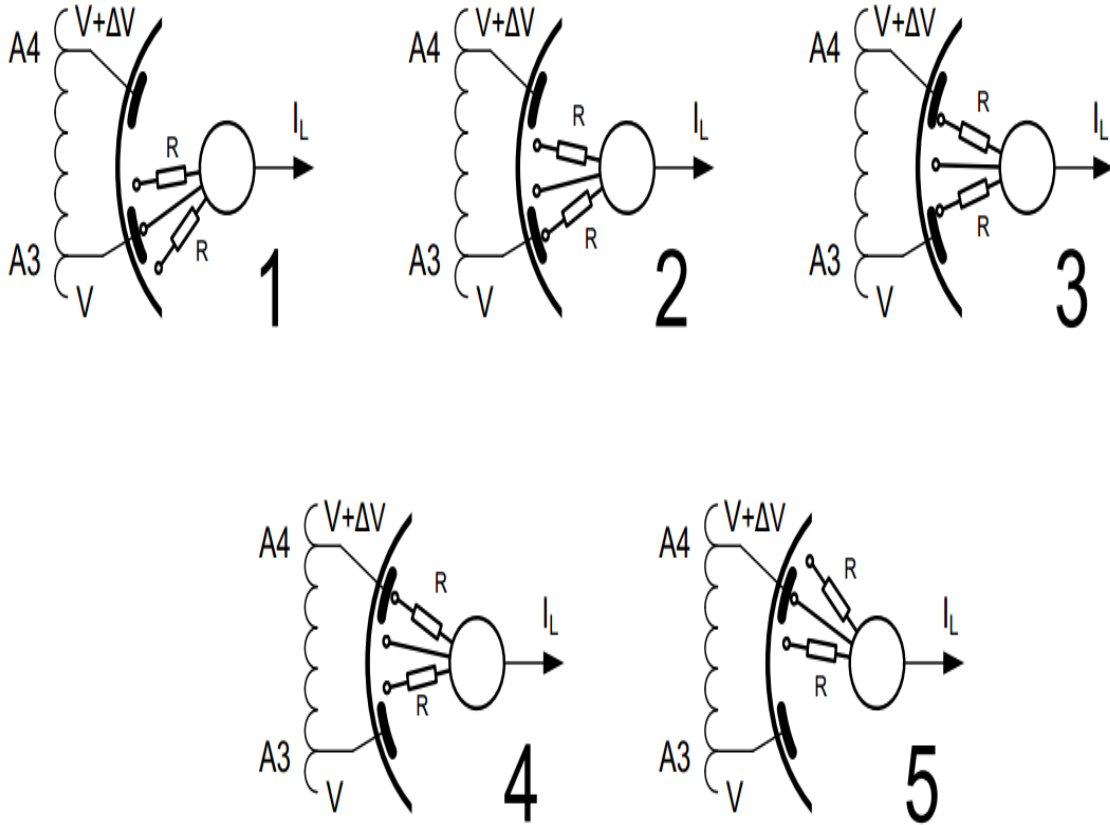


Figure 2.13. The transition process between two adjacent tap positions [5].

During this process electrical arcs are created in the insulating oil. The arcs are created between transition period 2 to 3 and transition period 3 to 4. When the bridging contact is about to touch the next tap position, an arc is created (see Figure 2.14). The arc is created because when the bridging contact touches the next tap position (contact A4 in Figure 2.13 position 3) a circulating current will start flowing as shown in Figure 2.15. In Figure 2.14 the load current flows only through one of the transition resistors.

When the transition period 2 to 3 is complete, a circulating current  $I_c$  starts flowing through the transition resistors. The circulating current is:  $I_c = \Delta V / 2R$  (see Figure 2.13 – position 3). The load current ( $I_L$ ) is then split between the two transition resistors. The circulating current and the load current at position 3 of Figure 2.13 are presented in Figure 2.15.

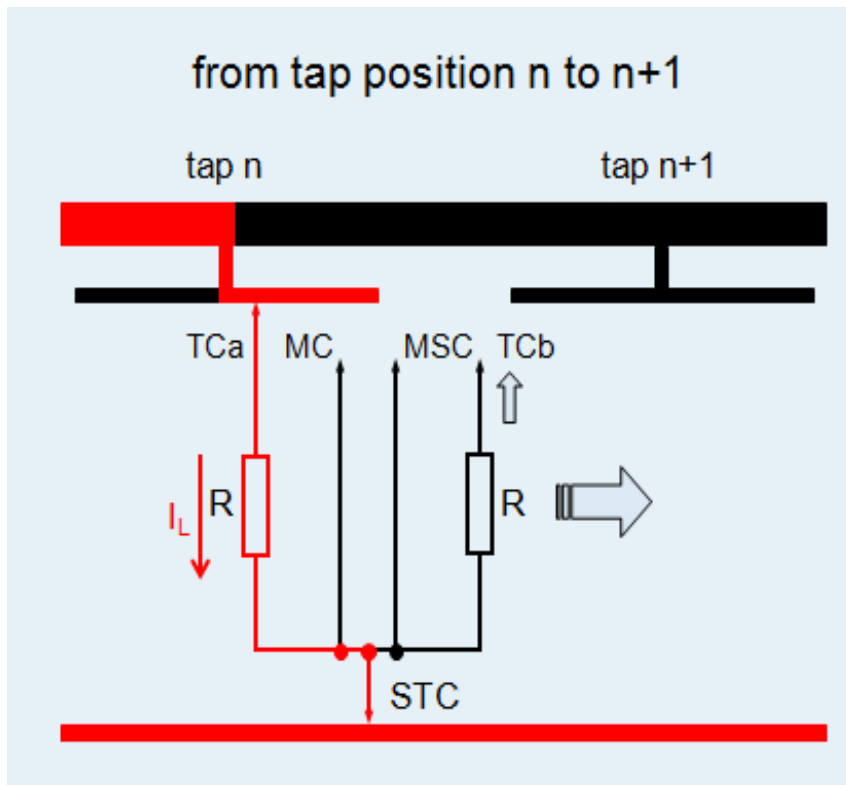


Figure 2.14. Load current through one of the transition contacts. Circulating current will be created when TCb touches the next tap position [6].

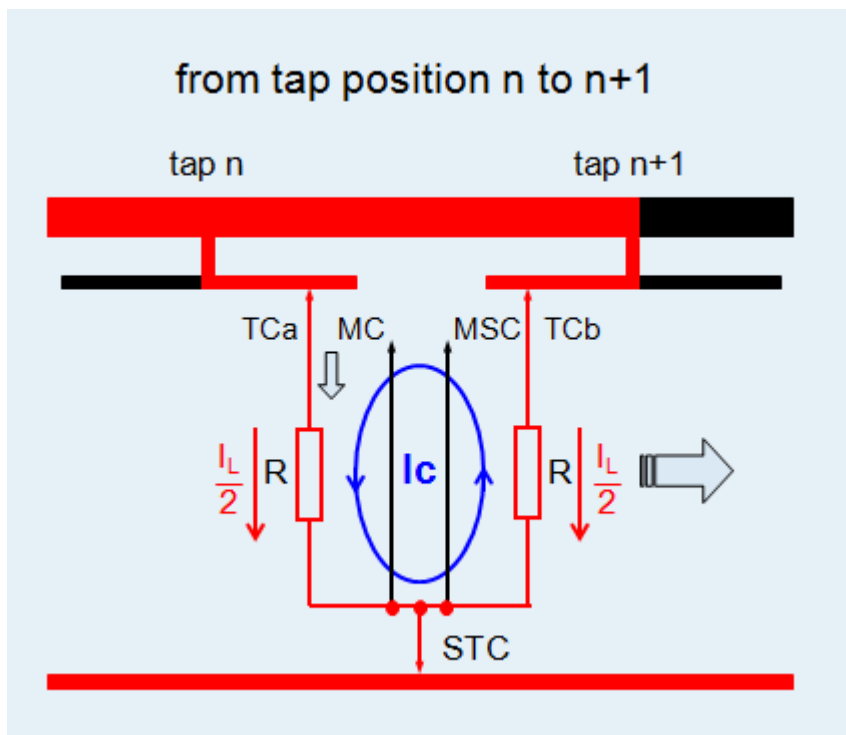


Figure 2.15. Circulating and load current [6].

An arc in the oil will be formed during the transition period 3 to 4 in Figure 2.13. When the bridging contact leaves contact A3 (see Figure 2.13 - position 4) then

a current is interrupted. The interrupted current is:  $I = \Delta V/R$ . During the interruption of the current, an electrical arc is created in the oil of the switching compartment. The load current is again flowing only through one of the transition resistors (see Figure 2.16).

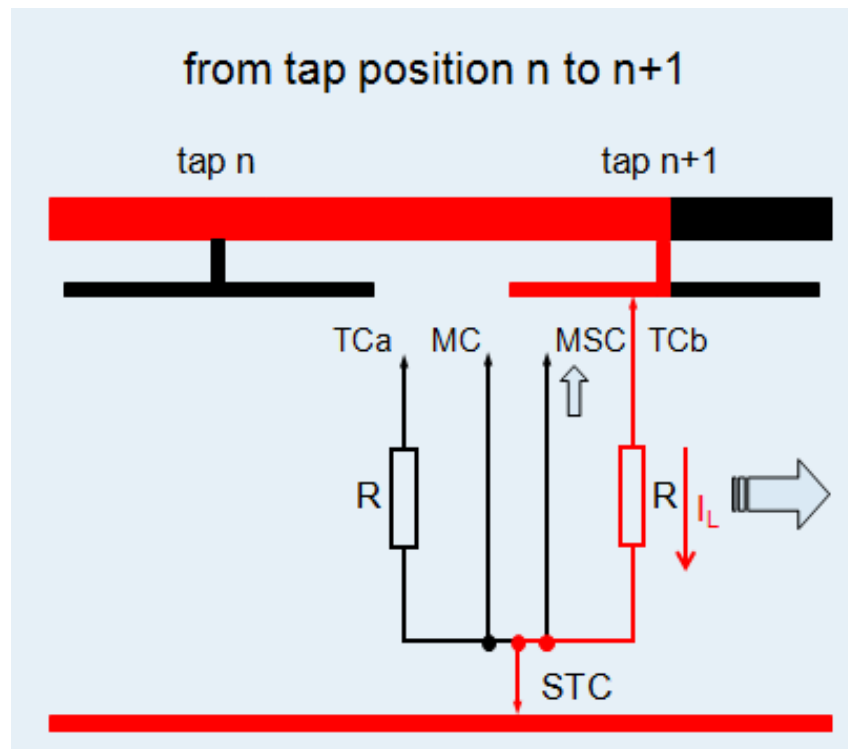


Figure 2.16. Interruption of the circulating current. Again load current flowing through one of the transition contacts [6].

The electrical arcs heat the insulating oil and as a result, gases are produced. The gas which is produced during the arcing periods will move towards the top part of the tap changer. The tap changer is equipped with a special vent in order to remove the gas that is produced during the arcing periods. Gas bubbles can be trapped between contacts of different phases. The electric field between contacts of different phases is large, for the case of delta connected tap changers (see paragraph 2.2.2). The presence of gas bubbles in areas of high electric field can cause the appearance of partial discharge activity (see chapter 5).

However, it must be noted that the presence of arcs in the insulating oil constitutes a normal operation for the tap changer. In addition, it is referred in [8] that discharges occurring in gas bubbles in oil are less severe than discharges that occur in gas bubbles which involve the hard paper insulation. Nevertheless, the presence of gas bubbles in areas of high electric field may give rise to partial discharge activity. Excessive arcing, can lead to the production of a larger quantity of gas bubbles and thus to increased partial discharge activity. Gas bubbles in the oil of the tap changer do not constitute a defect under normal operation. On the other hand, increased partial discharge activity from gas bubbles in the oil can provide

information about the arcing process. The probability of partial discharge inception in gas bubbles is presented in more detail in Chapter 4.

### **2.3.2 Sharp points in oil**

The OLTC is equipped with two transition resistors per phase which ensure the uninterrupted transfer of the load current from one tap position to another. When the contacts of the tap changer have moved to the next tap position, the current will flow through the main contact, as it is seen from Figure 2.13 (position 5). No current is flowing through the transition resistors. In an extreme case, a transition resistor could be broken. The effect of the broken transition resistor will not be noticed until the tap changer performs another voltage regulation. A broken transition resistor can lead to local electric field enhancement at the tip of the broken wire. The local high electric field can lead to partial discharge activity at the tip of the wire. By monitoring the PD activity in the tap changer sharp wires in the oil of the tap changer can be identified before leading to more severe damage of the tap changer.

### **2.3.3 Surface discharges**

The interfaces between different insulating materials constitute one of the most critical parts in high voltage equipment. In the OLTC the oil-hard paper interface presents such a critical part. Surface discharges constitute a significant degradation mechanism in composite oil-paper insulating systems [9]. Surface discharges occur along insulating interfaces when a high tangential electric field is present [9].

Conductive particles can be found in the oil of an OLTC due to the contact wear during the transition process. A part of the conductive particles can accumulate on the surface of the hard paper insulating material of the OLTC which can lead to partial discharge activity on the hard paper surface [10].

The damage of the hard paper insulation due to the partial discharge activity depends strongly on the applied voltage and time [9]. Surface discharges ultimately lead to the creation of a tracking path on the paper insulation. This happens due to the carbonization of the material and the drying of the oil at the spot where the partial discharge activity is present. Finally, a carbonized conductive path (tracking) is created which can lead to the OLTC failure (see Figure 2.17).

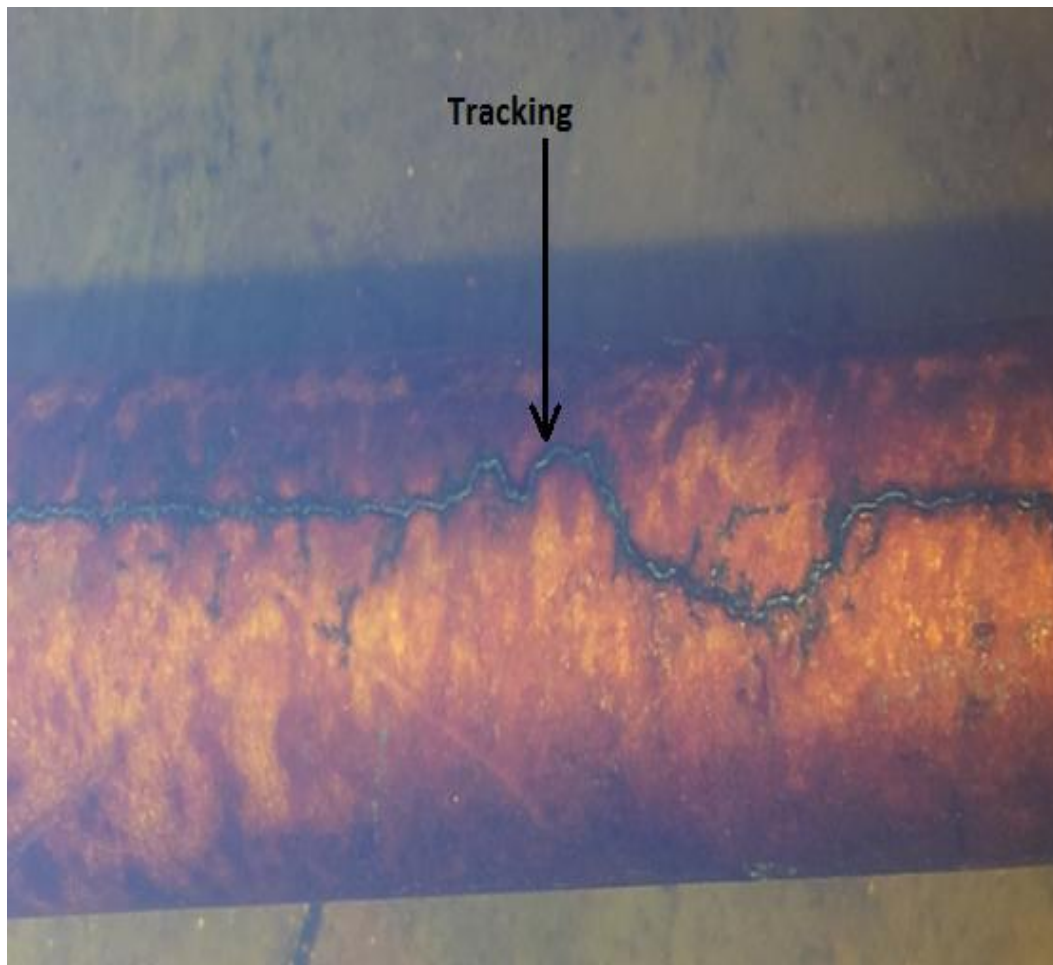


Figure 2.17. Tracking on paper insulation.

### 2.3.4 Tracking

Most organic materials that are used for electrical insulation of high voltage equipment could suffer from a deterioration process which is called tracking. Tracking occurs on the surface of solid insulation materials due to creepage discharges [11]. Discharges along the surface of a solid insulating material are the result of surface contamination. Tracking phenomena result in the formation of a carbonized conductive path over the surface of the insulation. The conductive path will be elongated over time. The propagation of the path depends on the conductivity of the carbon. After the initiation of the tracking phenomenon, the electrical properties of the insulation are permanently compromised. Ultimately, the carbonized path leads to a flashover and failure of the high voltage equipment.

A hard paper insulating cylinder is used to insulate tap changers which are placed in the same tank as the transformer (in-tank). Due to the contact wear that occurs during every operation of the tap changer, the surface can become contaminated by metallic conductive particles. As a result, the electric field that stresses the cylinder can be greatly enhanced, leading to partial discharge activity on the surface of the cylinder. Creeping discharges on the surface of the cylinder

## 2 OLTC Technologies and Major Electrical Defects

ultimately may create a permanent electrically conductive path - tracking (see Figure 2.17). The conductive path reduces the insulating properties of the material and more specifically reduces the voltage which the paper cylinder can withstand. In addition, the surface resistance of the paper is significantly reduced [12].

This change in the local surface resistance of the paper leads to local field enhancement causing partial discharge activity when the electric field is large enough to cause a local breakdown of the insulation. When the heat energy of the PD activity that takes place at the edge of the conductive path is high, then burning of the paper insulation at the spot of the discharge will occur. Therefore, the surface is further carbonized and the conductive path is elongated. Tracking is a slow process which depends on the applied voltage and time [9]. The initiation of the conductive path requires a significant amount of time. Once initiated, the conductive path will grow in length. The conductive path will be elongated and once the insulating distance between the contacts is bridged, a large short-circuit current will flow through the conductive path. This process takes place almost instantaneously. The short circuit current causes a flashover between the contacts and ultimately failure of the tap changer.

The OLTC is installed in either star-connected windings or in delta-connected windings. The electric field in tap-changers which are installed in delta-connected windings is larger than in tap changers installed in star-connected windings (see paragraphs 2.2.1 and 2.2.2). According to the experience, tracking on the hard paper cylinder insulation is a more likely insulation defect in delta-connected tap changers. On the other hand, star-connected tap changers are less prone to electrical tracking [13].



## Insulation diagnosis

In Chapter 2 the major insulation degradation mechanisms of on-load tap changers were discussed. Defects in the insulation can lead to OLTC failure. In order to minimize OLTC failures, a number of diagnostic systems have been developed. In this chapter, diagnostic systems used for the condition assessment of the electrical insulation will be described. Condition based maintenance has become a major priority in modern power systems. Monitoring and diagnostic systems are used in order to reduce the failure rate of high voltage equipment and to allow for a more reliable, safe and effective way of operating power systems. In general, there are two ways to monitor high voltage equipment: on-line monitoring and off-line diagnosis.

On-line monitoring of high voltage equipment requires sensors permanently mounted on the equipment. The monitoring sensors continuously check all the parameters that are required in order to assess the condition of the insulation. Thus, on-line monitoring systems oversee the normal and safe operation of the high voltage equipment. In addition, alarms can be activated when defects are present, according to some rules and proceedings.

On the other hand, off-line diagnosis is based on periodic measurements. The condition assessment of the OLTC can be performed by using sophisticated measuring systems. In many cases, on-line monitoring and off-line diagnostics are used together in order to assess the condition of high voltage equipment. Condition assessment diagnostic systems aim to identify defective operation of high voltage equipment at the early stage and reduce the damage caused by such defective operation. The identification of defects in high voltage equipment at early stages ensures that catastrophic and expensive consequences will be avoided [14].

Dissolved gas analysis (DGA) is a diagnostic procedure which is frequently used for transformer diagnosis. The applicability of DGA analysis can be expanded in the case of on-load tap changers. This chapter provides an overview of the DGA analysis used in power transformers and on-load tap changers.

### 3 Insulation diagnosis

Another method, which seems promising, is the detection of partial discharges (PD). Defects that deteriorate the electrical insulation and lead to aging and potential failure of high voltage equipment can be detected by monitoring the partial discharge activity. There are a number of different diagnostic systems which are capable of measuring partial discharge activity in high voltage equipment. A variety of sensors can be used to detect partial discharge activity. Acoustic sensors can be used to detect PD activity in power transformers. The acoustic sensors detect acoustic signals in the ultrasonic frequency range [20 kHz - 1 MHz] that are created by PD activity [15]. Moreover, detection of the high frequency electromagnetic signals [300 MHz – 3 GHz] caused by PD activity via ultra high frequency (UHF) antennas is used in power transformers [16].

A different type of sensor which is capable of detecting PD activity is the high frequency current transformer (HFCT). HFCT sensors used for PD measurements are connected on the grounding point of the equipment. In [17], the performance of the HFCT sensors is investigated. The advantage of the acoustic sensors and UHF antennas over the HFCT sensors is that the location of the PD source can be found inside the high voltage equipment [15–16]. In this chapter, the most significant aspects of DGA and of PD measurements by using electrical methods are presented. In addition, a description of the capabilities of the HFCT sensors is provided.

#### **3.1 Dissolved gas analysis (DGA)**

The dissolved gas analysis (DGA) is a procedure by which the condition of the insulating oil and the type of the fault that occurred in the transformer can be estimated through an analysis of the gases in the oil. To perform the DGA test an oil sample from the transformer must be taken. Depending on the values of the DGA analysis for the concentration of the different gases in the oil of the transformer, estimation about the type of the fault can be made. The main gases that can be formed in the oil depending on the type of the fault include: hydrogen ( $H_2$ ), methane ( $CH_4$ ), ethylene ( $C_2H_4$ ), acetylene ( $C_2H_2$ ), carbon dioxide ( $CO_2$ ) and carbon monoxide ( $CO$ ) [18]. DGA can be applied to on-load tap changers since the energy produced by arcing or PD activity can trigger chemical reactions.

DGA can be performed in oil from the arcing switch compartment [19] or in oil from the coarse switch compartment. The gases that are produced depend on the temperature of the oil at the location of the fault as presented in [19]. The dependence of the gas concentration with the temperature is presented in Figure 3.1. The determination of the type of the fault is based on the gas ratios, as presented in Table 3.1.

### 3 Insulation diagnosis

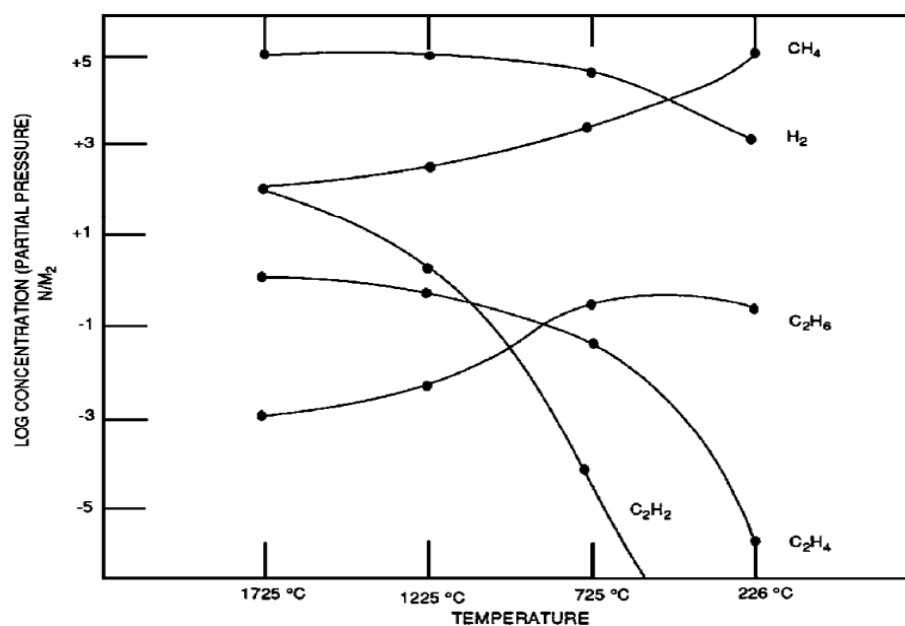


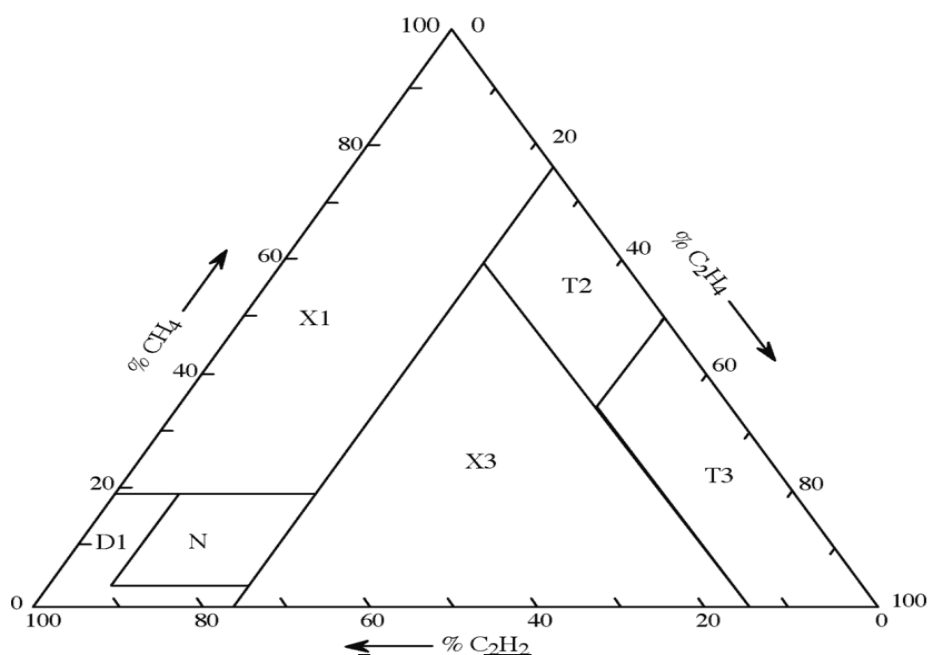
Figure 3.1. Gas concentration in oil for different fault temperatures [20].

Table 3.1. Gas formation in transformer oil-  
Gas ratios depend on the temperature at the location of the fault [21].

Key gases	Characteristic fault
H <sub>2</sub>	Partial Discharge
C <sub>2</sub> H <sub>6</sub>	Thermal fault <300°C
C <sub>2</sub> H <sub>4</sub>	Thermal fault 300 to < 700°C
C <sub>2</sub> H <sub>2</sub> , C <sub>2</sub> H <sub>4</sub>	Thermal fault > 700°C
C <sub>2</sub> H <sub>2</sub> , H <sub>2</sub>	Discharge of energy

DGA can be used in on-load tap changers as well. The oil from the arcing switch can be used to assess the switching operation of which the tap changer. In [22], an example of DGA analysis in an OLTC in the case of coking or overheating is presented. In [19], the gas concentrations in the oil are used in order to identify the type of defect in on-load tap changers. The type of defect is identified by comparing the gas ratios in the OLTC as shown in Figure 3.2.

### 3 Insulation diagnosis



Zone	Identification	Recommended actions
N	Normal operation	
T3	Severe thermal fault T3 ( $T > 700$ °C), heavy coking.	Change the oil. Inspect the LTC for coking of contacts
T2	Severe thermal fault T2 ( $300 < T < 700$ °C), coking	
X3	Fault T3 or T2 in progress, usually with light coking or increased resistance of contacts. Or, severe arcing D2	Test or inspect the LTC for signs of light coking or resistance of contacts, or of severe arcing
D1	Irregular arcing D1 (outside zone N)	Inspect the LTC for small signs of arcing
X1	Irregular arcing D1 or thermal fault in progress	Area still under investigation

Figure 3.2. Duval's triangle: The source of the fault can be identified by comparing gas ratios [19].

DGA offers a method for on-line diagnosis of on-load tap changers. However, there are some disadvantages in the application of this method as on-line diagnosis. DGA analysis is inadequate to provide information about the change over switch when the switch uses the same insulating oil as the transformer. In addition, it is rather difficult to locate the position of the defect inside the OLTC. DGA analysis offers information mainly about overheating faults. The quality of the hard paper insulation of the OLTC cannot be assessed.

Moreover, DGA analysis must cope with the fact that leakage of oil from the arcing switch to the main tank makes the analysis even more demanding. Nevertheless, DGA can be used as an additional diagnosis of the OLTC condition. The oil samples can be processed in the laboratory, but devices which can process the oil samples on-site are also available [23].

### 3.2 PD measurements by electrical methods

A new approach to assess the condition of the insulation of on-load tap changers can be based on PD monitoring. PD activity can provide valuable information about defects in the tap changer. In chapter 2 the main electrical defects that can be found in an OLTC have been discussed. Partial discharge activity can occur due to defects in the insulation materials. A PD monitoring system relies on proper sensing of the PD activity, removal of the external background noise and identification of the PD source. PD monitoring systems are currently used in most of the high voltage equipment. Standards, such as IEC 60270, have been established to provide detailed explanations about PD measurements and calibration proceedings.

#### 3.2.1 IEC 60270 test circuit

The basic circuit for PD measurements proposed by IEC 60270 is presented in Figure 3.3.

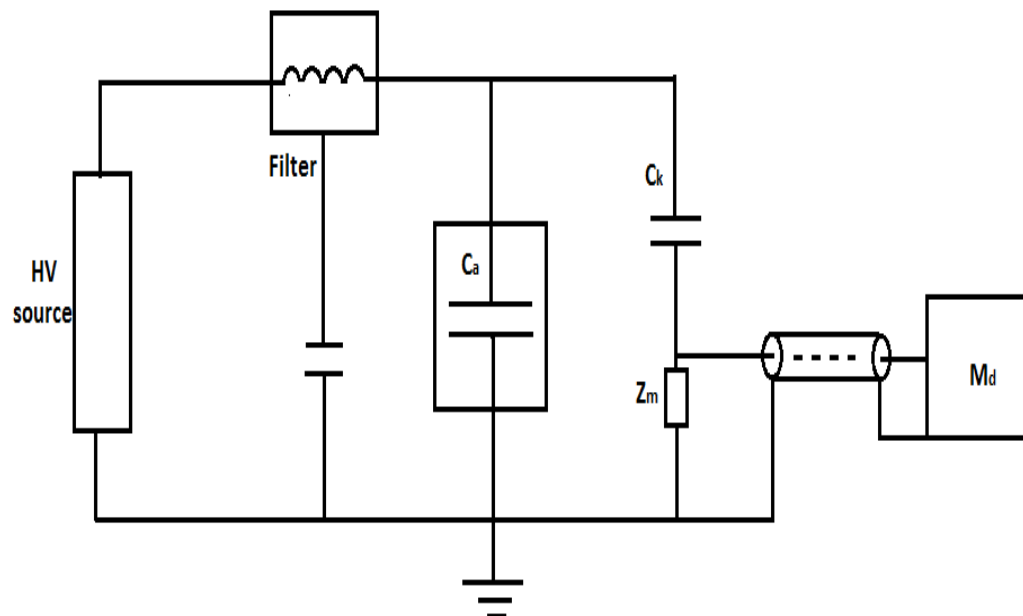


Figure 3.3. Basic PD test circuit.

In the basic PD test circuit of Figure 3.3, the noise blocking filter is used to reduce the electromagnetic noise coming from the high voltage source. In addition, it prevents the PD signal from travelling through the high voltage transformer [24]. The test object is presented as a capacitance  $C_a$ . The coupling capacitor is connected in series with the measuring impedance  $Z_m$ . At the measuring impedance, voltage pulses are formed which are then amplified and displayed in an oscilloscope and then analyzed by a discharge analyzer. The measuring impedance can also be connected in series with the grounding point of the test object as presented in Figure 3.4.

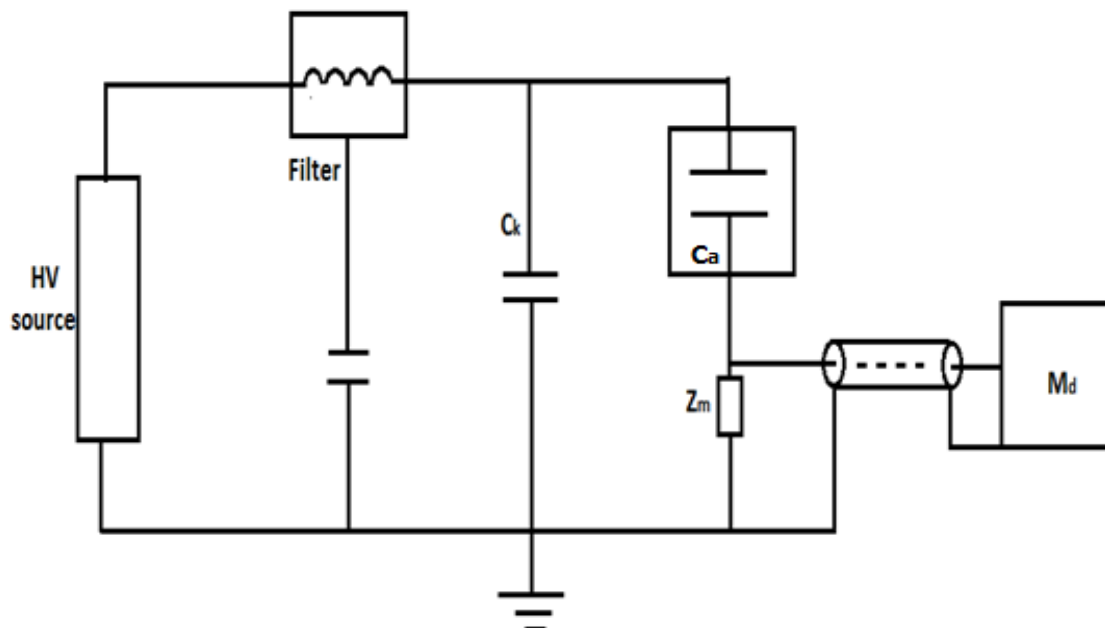


Figure 3.4. Basic PD test circuit- $Z_m$  in series with the test object.

The sensitivity of the PD detection system can be increased when the measuring impedance  $Z_m$  is connected in series with the test object. The major disadvantage of this circuit is that a current flowing through the test object is also flowing through the measuring impedance  $Z_m$ . If the current is large enough – case of breakdown of the test object- then the measuring impedance could be damaged [25].

The coupling capacitor provides a closed path for the discharge pulse current. Then the signal detected at the measuring impedance is displayed on the measuring device  $M_d$ . The coupling capacitor, as well as the high voltage transformer, must be PD free at the highest test voltage. In addition the test circuit must be of low inductance in order to transmit the PD signal without any unwanted oscillations. Finally, the capacitance of the coupling capacitor  $C_k$  must be of the same order as the capacitance of the test object. In general, the ratio of  $C_k/C_a > 0.1$  must be fulfilled in order to get a high sensitivity of the measuring system [24].

### 3.2.2 Calibration

The measuring system is calibrated with a step generator in series with a small capacitor, as presented in Figure 3.5. The generator injects a pulse  $q_{cal}=b\Delta V$  into the test object. A signal of fixed magnitude is injected and the recording instruments are calibrated. The calibrating pulse must be injected directly into the test object.

### 3 Insulation diagnosis

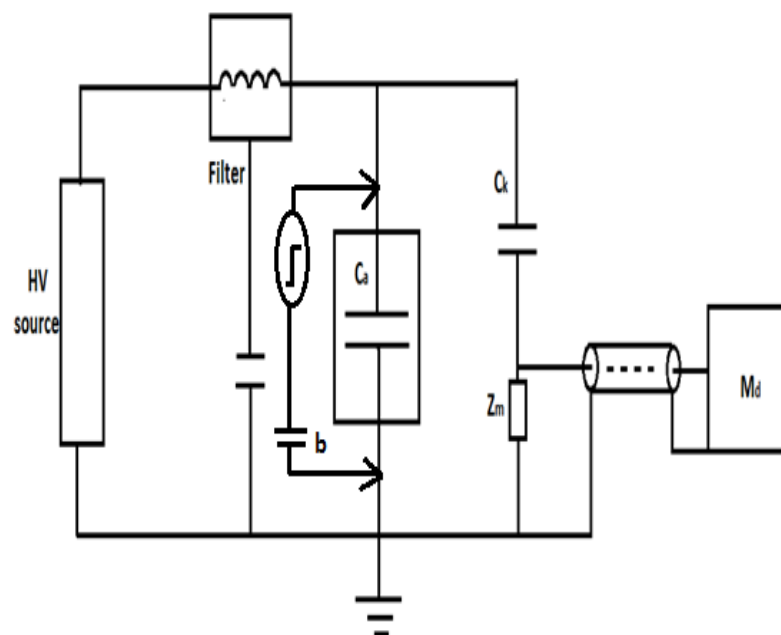


Figure 3.5. Calibrator connected across the test object.

The correct calibration of the measuring system is very essential, especially when the magnitude of the discharge is of importance. The calibrator is connected across the test object and a calibration pulse is injected to the test object. The calibration pulse is then picked up by the PD detector. The picked up signal is measured in millivolts. The charge in pC can then be calculated by integrating the calibration pulse. The calibration of PD measuring systems which use HFCT sensors is very essential in order to get the correct magnitude of the discharge.

During the experiments of this research project, the sensor that was used to detect PD activity was the HFCT sensor. HFCT sensors with two different frequency bandwidths were used. The properties of the HFCT sensors are described in Table 3.2. To test the response of the sensors to a calibration pulse, both sensors were connected to a Tektronix oscilloscope and the set up of Figure 3.6 was devised.

Table 3.2 Properties of the HFCT sensors.

Sensor	Detection bandwidth
HFCT-L	30 kHz to 30 MHz
HFCT-H	1 MHz to 60 MHz

### 3 Insulation diagnosis

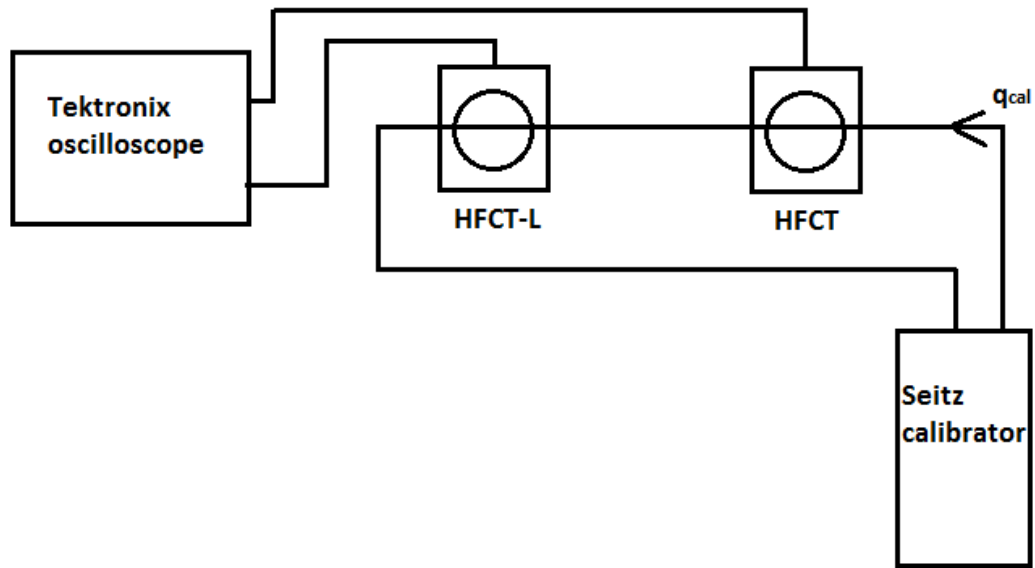


Figure 3.6. The set up to test the HFCT sensors.

A Seitz calibrator was used to inject a pulse through the HFCT sensors as shown in Figure 3.6. The response of the sensors was displayed on the oscilloscope. The data from the HFCT sensors was acquired from the oscilloscope and was plotted in Matlab. Then the integral of the pulses was calculated. The pulse shape and the integral of the pulses are shown in Figures 3.7 and 3.8.

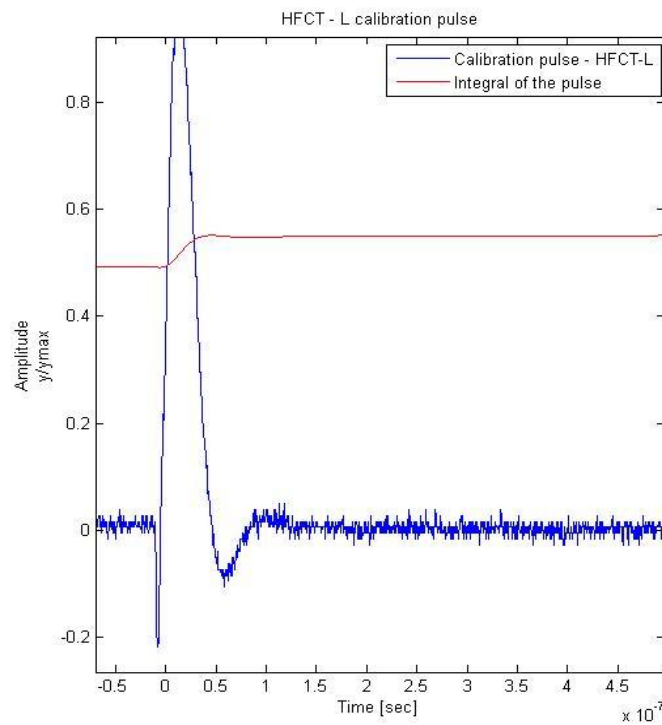


Figure 3.7. Pulse shape and integral of the pulse (HFCT-L)



### 3 Insulation diagnosis

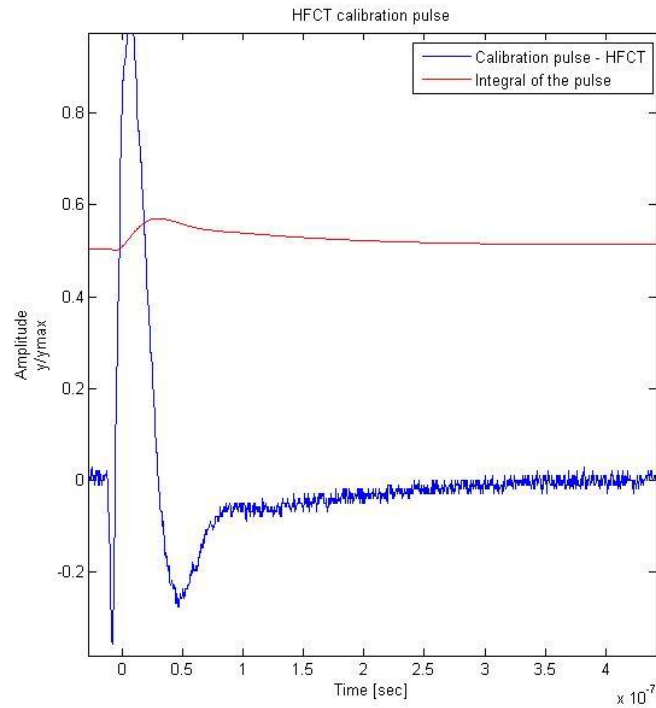


Figure 3.8. Pulse shape and integral of the pulse (HFCT-H)

The FFT of the pulses from the HFCT sensors was also calculated. The FFT was plotted in Matlab and is presented in Figures 3.9 and 3.10.

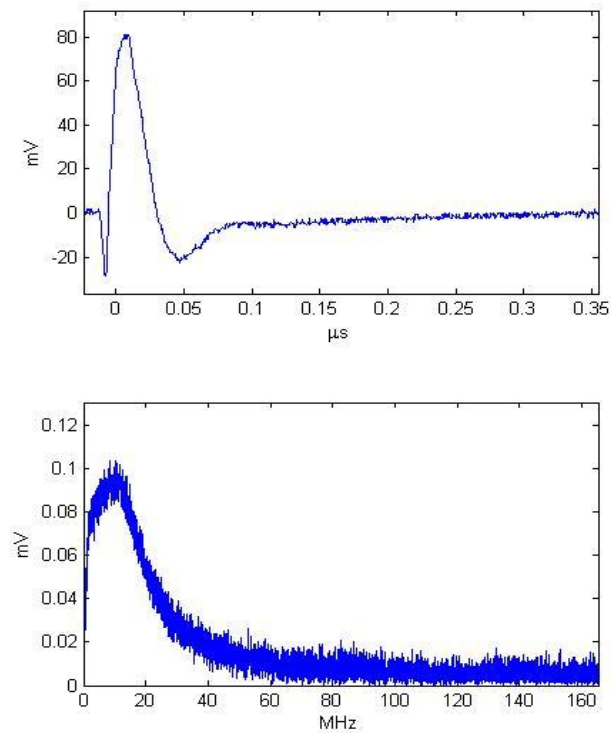


Figure 3.9. FFT of the pulse (HFCT-H).

### 3 Insulation diagnosis

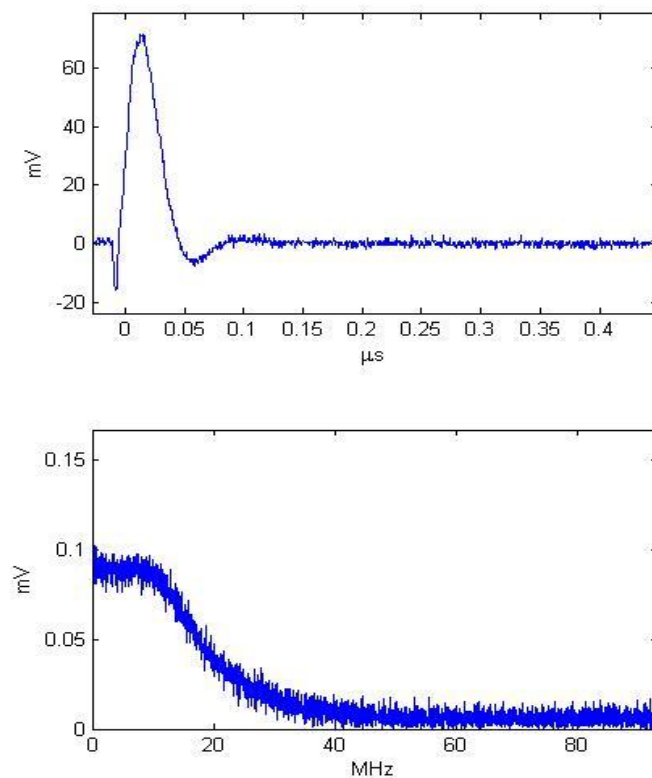


Figure 3.10. FFT of the pulse (HFCT-L).

The FFT of the pulses obtained by the two HFCT sensors are significantly different. The FFT of the pulse from the HFCT-H sensor drops fast to zero when compared to the FFT of the HFCT-L sensor. The frequency range in the FFT depends on the bandwidth of the sensor. The FFT of the pulse of Figure 3.9 starts approximately at 1 MHz and becomes zero at approximately 60 MHz which corresponds to the bandwidth of the HFCT-H sensor. On the other hand, the FFT of Figure 3.10 becomes zero at approximately 30 MHz.

An important observation can be drawn by Figure 3.8 and Figure 3.9. The integral of the pulse obtained by the HFCT-L sensor does not become zero after a large period of time when compared to the integral of the pulse obtained by the HFCT-H sensor. This means that the calibration will only be successful for the HFCT-L sensor and not for the HFCT-H sensor. As a result, the discharge magnitude will be correctly measured only when using the HFCT-L sensor. The discharge magnitude will not be measured correctly when using the HFCT-H sensor due to the fast drop of the integral to zero.

In the next experiment, a calibration pulse was injected to a test object as presented in Figure 3.11.

### 3 Insulation diagnosis

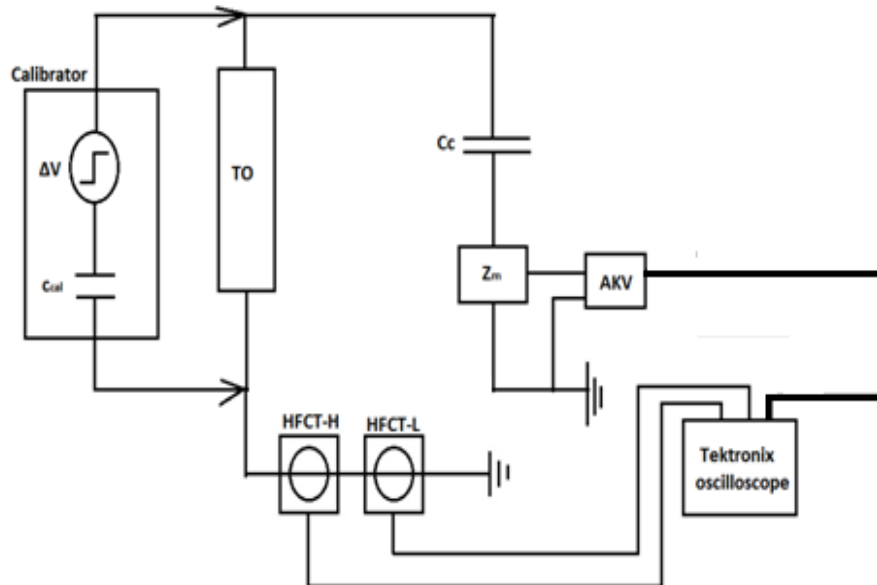


Figure 3.11. Injecting a calibration pulse through a test object.

The set up of Figure 3.11 consists of a test object (TO), the coupling capacitor ( $C_c$ ) with measuring impedance ( $Z_m$ ), a synchronizing unit (AKV) and an oscilloscope (Tektronix). The synchronizing unit also provides the output signal from the measuring impedance  $Z_m$ . The HFCT sensors and the output of the measuring impedance  $Z_m$  were connected to the oscilloscope. The calibrator that was used to inject the pulse to the circuit was a Seitz PD calibrator. The signals that were obtained by the oscilloscope are shown in Figure 3.12.

The integral of the signals is an essential parameter which determines whether the calibration process can be successfully performed or not. If the integral drops to zero fast then the calibration cannot be performed. Figure 3.12, presents the normalized integral of the three signals that were obtained by the different HFCT sensors and the output of the measuring impedance (Haefely).

### 3 Insulation diagnosis

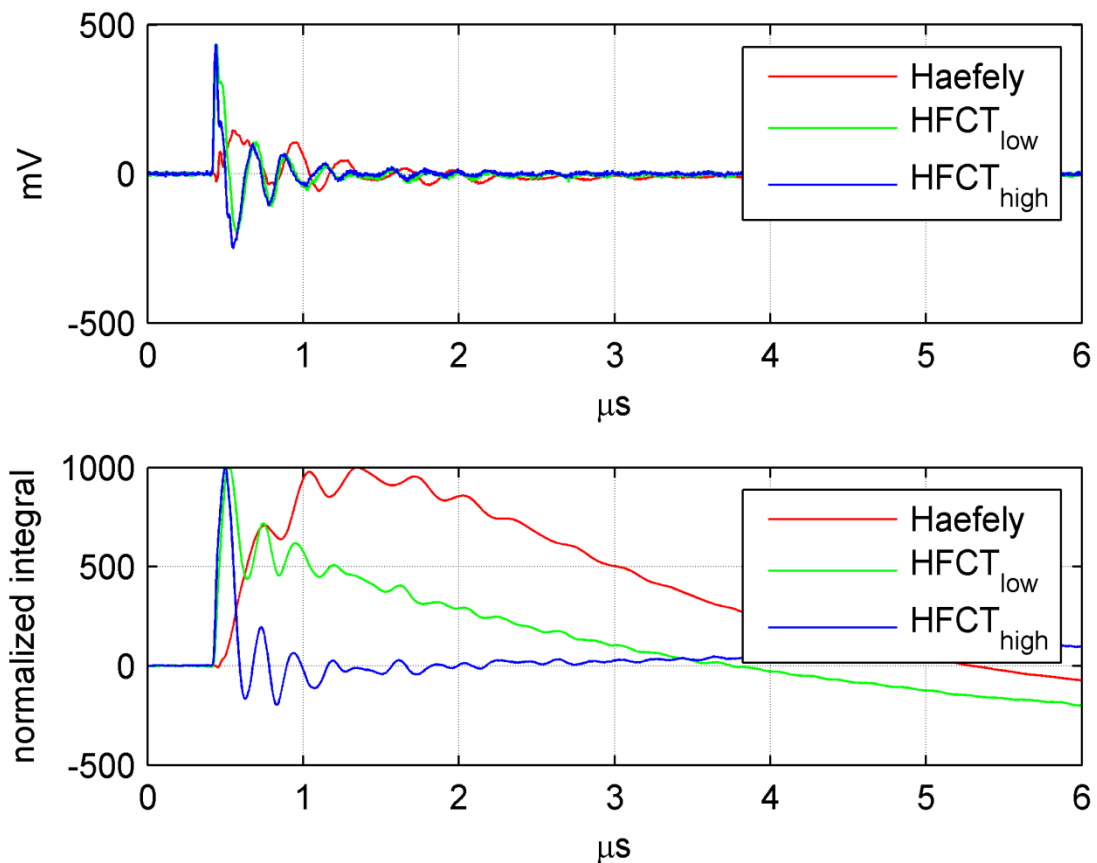


Figure 3.12. Obtained calibration signals.

The signals from the two HFCT sensors display minor dissimilarities. The small differences in the signals are due to the different frequency bandwidths. The signals that were obtained from the HFCT sensors differ from the signal obtained by the output of the measuring impedance  $Z_m$ . The frequency of the signal obtained by the measuring impedance is different and the amplitude of the signal is substantially smaller than the amplitude of the signals obtained from the HFCT sensors. The oscillations in the signals are created because of the inductance of the set up and the inductance introduced by the measuring impedance and the calibrator.

From Figure 3.12 it can also be observed that the integral of the signal which is obtained by the output of the measuring impedance displays the best response. The integral falls to zero after the integrals of the two other signals. From Figure 3.12 it is concluded that calibration can be achieved for the signals obtained by the output of the measuring impedance and HFCT-L sensor. The integral of the signal obtained by the HFCT-H sensor goes fast to zero. The calibration process when using this sensor is not reliable.

### 3.2.3 Partial discharge patterns

The recognition of the different PD sources that may hamper the operation of high voltage equipment is very important. A procedure to recognize PD sources is presented in Figure 3.13.

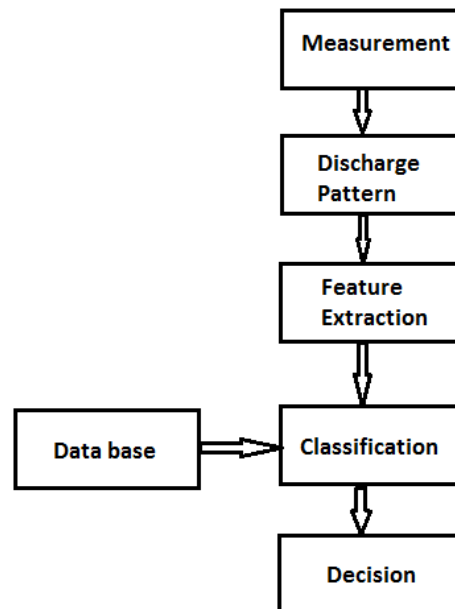


Figure 3.13. Recognition process [26].

The recognition of PD consists of three important steps: The measurement of the PD activity by means of electrical methods which leads to the creation of a discharge pattern, *the feature extraction* from the discharge pattern and *the classification*. There is a variety of patterns which can be used to recognize the PD source.

One of the patterns that can be used in PD recognition is the phase resolved PD pattern. The phase resolved PD pattern relates the amplitude of the measured PD pulses to their phase, in respect to the applied sinusoidal voltage wave (see chapter 4). In general, PD patterns describe the relationship between the number of the discharge pulses, the magnitude of the discharge pulses and the phase of the discharge pulses.

Before the classification of the PD source, the discharge activity can be described by a set of features. These sets of features can be used to compare different PD sources. The accuracy of the recognition process depends on the determination of the features that represent the discharge source. Under A.C voltage the different features are typically extracted by the phase resolved pattern. For the process of PD recognition different distributions can be used. Examples of the different distributions that can be used for recognition are presented in Figure 3.14. The distributions of Figure 3.14 are typically extracted by the phase resolved PD pattern under A.C voltage.

### 3 Insulation diagnosis

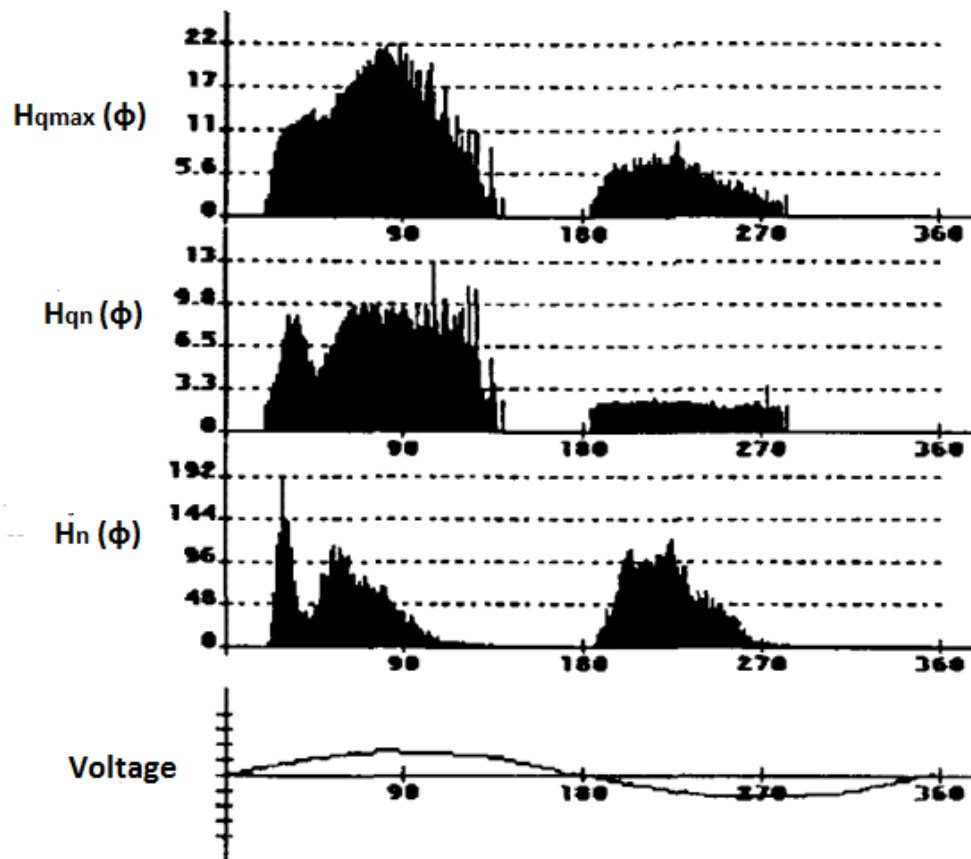


Figure 3.14. Different PD distributions [27].

The first distribution of Figure 3.14, relates the maximum amplitude of the discharge pulses to the phase of the PD occurrence ( $H_{qmax}(\phi)$ ).  $H_{qn}(\phi)$  relates the mean value of the pulse magnitude to the phase of the Pd occurrence and the  $H_n(\phi)$  is the pulse count distribution which displays the number of pulses in relation to the phase of the pulse occurrence. The different distributions are then described by a number of statistical parameters [27].

The most important statistical parameters are the *skewness* and the *kurtosis* of the distributions. The skewness actually describes the asymmetry of the distribution with respect to the normal distribution. If the distribution is symmetric then  $Sk=0$ . If the distribution is asymmetric to the left,  $Sk>0$ , and if the distribution is asymmetric to the right,  $Sk<0$ . The kurtosis represents the sharpness of the distribution with respect to the normal distribution. For a distribution with the same sharpness as the normal distribution,  $Ku=0$ . If the distribution is sharper than the normal,  $Ku>0$  and if it is flatter,  $Ku<0$ . Finally, describing the distributions by statistical parameters leads to the calculation of different features which are used for PD recognition. Each feature represents a '*fingerprint*' of the PD and is used to recognize different PD sources.

### 3.3 Summary

In this chapter an overview of the DGA analysis was presented. DGA analysis is a useful and convenient diagnostic tool used in power transformers. The availability of the DGA analysis can be expanded in OLTC as well. Reliable information can be extracted by DGA regarding the quality of the insulation.

In addition, the most important features of PD measurements by means of electrical detection and the most important parameters for PD recognition were discussed. The calibration process is a very important process when dealing with PD measurements. It was shown in this chapter that the different types of sensors that are used in PD measurements give a different response to the calibration signals. When using HFCT sensors the frequency bandwidth of the sensor is essential to the calibration process. The lower cut off frequency is very important. It was shown in this chapter that the HFCT sensor with 30 kHz lower cut off frequency can be correctly calibrated by finding the integral of the calibration pulse. HFCT sensors with higher cut off frequencies cannot be calibrated in a proper way because the integral of the pulse drops to zero very fast. This means that the calculated charge of the pulse is approximately zero.

Therefore, when dealing with PD measurements by electrical methods, the calibration process is very essential in order to obtain reliable results regarding the magnitude of the partial discharges.

# 4

## Small-scale experiments: Part 1

A three-phase, selector switch type OLTC was transported to the high voltage lab for testing. A thorough examination of the OLTC revealed the position where an OLTC is maximally stressed. The maximum step voltage of an OLTC was found to be 5 kV. The distance between adjacent tap positions in the three-phase OLTC was measured to be 220 mm. On the other hand, the voltage difference between adjacent contacts of different phases is much larger than the step voltage (also refer to chapter 2) and the distance between adjacent contacts of different phases (90 mm) is smaller than the distance between adjacent tap positions. As a result, it was concluded that an OLTC is maximally stressed between adjacent contacts of different phases.

Therefore, a small scale set up was built in such a way that it would simulate as close as possible the conditions inside an on-load tap changer. The small scale set up was designed to simulate the conditions present between adjacent contacts of different phases. Insulation defects are more probable to lead to problems when they are located between contacts of different phases where the OLTC is more stressed by the electric field. The small scale set up is a first step for testing the PD activity that can be observed in an OLTC. Small scale set ups are used because of the flexibility they provide. The defects can be easily introduced and removed and the test conditions can be easily reproduced [8]. On the other hand, the exact operating conditions are difficult to be simulated. Nevertheless, small scale experiments constitute the first essential step for testing high voltage equipment.

In the first part of this chapter, the equipment that was used for the PD measurements is presented. Then the insulation defects that were presented in chapter 2 are introduced to the small scale set up and the PD activity originating from each different defect is measured.



## 4.1 PD detectors and additional equipment

The detection systems, as well as the sensors and all the equipment that were used in the experiments are presented in Table 4.1.

Table 4.1. Equipment used in the experiments.

PD detector	Sensor	Additional equipment
PDBasell Haefely type 561	HFCT (High Frequency Current Transformer)	a) Capacitive Divider (1nF) b) High voltage transformer (230V/150kV)

Two different PD detectors have been used in this research project. In accordance with the IEC 60270 standards and recommendations and in the 115 – 440 kHz frequency range the detectors that have been used are:

- 1) The *analogue Haefely 561* type PD detector (conventional method)
- 2) The *digital PDBasell* of *TechImp Spa*

### 4.1.1 PD detectors

#### Haefely 561 type PD detector



Figure 4.1. Haefely 561 PD detector.

In Figure 4.1 the analogue PD detector type 561 of Haefely is presented. The detector works in accordance with the IEC 60270 specifications. The discharge pulses are displayed on the screen of the detector superposed on an ellipse that represents the sinusoidal test voltage as presented in Figure 4.2.

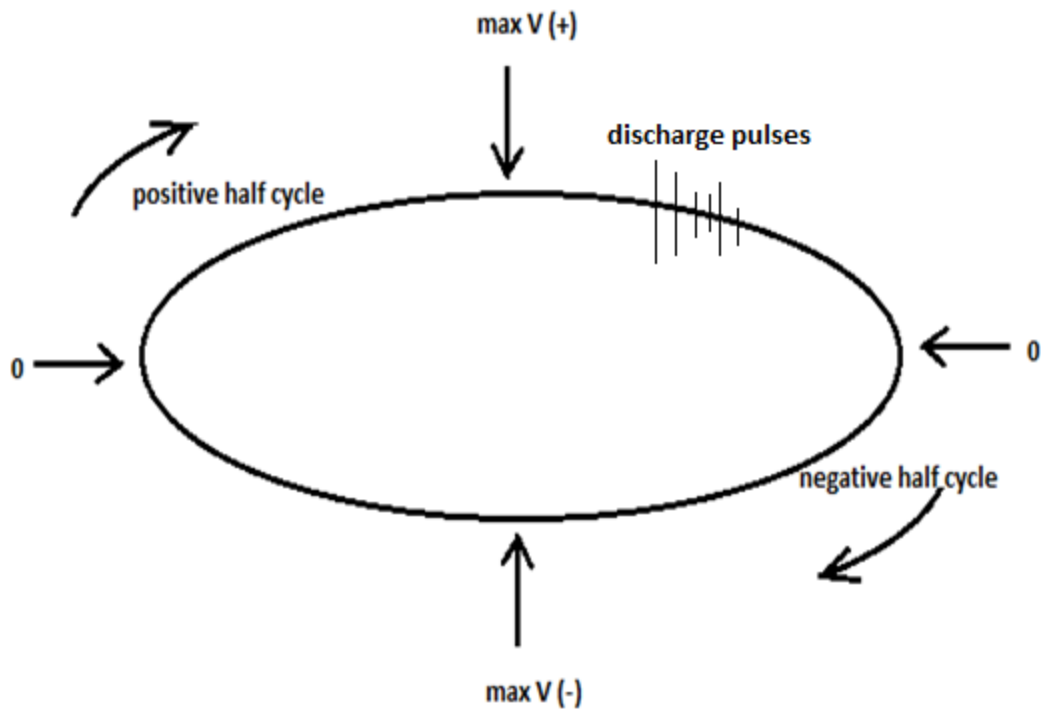


Figure 4.2. Display screen of Haefely 561 PD detector.

In Figure 4.2, the positive and the negative half cycle of the test voltage can be observed. In addition, Figure 4.2 presents the maximum value and the zero crossings of the test voltage. The PD detector also displays the apparent charge of the discharge. A calibration of the whole system as presented in Figure 3.3 is required. A measuring impedance  $Z_m$  is also connected in series with a coupling capacitor  $C_c$  as presented in Figure 3.3. The pulses which are formed by the measuring impedance are then displayed on the screen of the detector. The data cannot be stored and extracted from the detector. For that reason further processing of the data is not possible with the conventional PD detector.

On the other hand, the digital detector of TechImp Spa - PDBasell - provides the possibility of analyzing and processing the acquired data. The two detectors were used simultaneously. The conventional PD detector was used as a verification of the results that were obtained by PDBasell. The analysis of the PD patterns is based on the results obtained by PDBasell.

### TechImp PDBasell



Figure 4.3. Digital detection unit - PDBase II.

Figure 4.3 presents the PD detection system (PDBasell) which is manufactured by *TechImp Spa*. PDBasell provides the user with different acquisition modes. The difference in the acquisition modes is the frequency bandwidth of the acquisition. The different acquisition modes are:

- 1) W.B (Wide Band): The range of frequency acquisition is from 16 kHz to 48 MHz.
- 2) W.B + HPF (High Pass Filter): is the wide band plus a 2.5 MHz high pass embedded filter. The range of frequency acquisition is from 2.5 MHz to 48 MHz.
- 3) IEC 60270: is the IEC standard bandwidth. The range of frequency acquisition is from 115 to 440 kHz. In Appendix B, the different features of the IEC acquisition mode are discussed in more detail.

A very essential feature which is provided by the PD detector is the phase resolved PD (PRPD) pattern of the pulses. An example of the PRPD provided by the PD detector is shown in Figure 4.4.

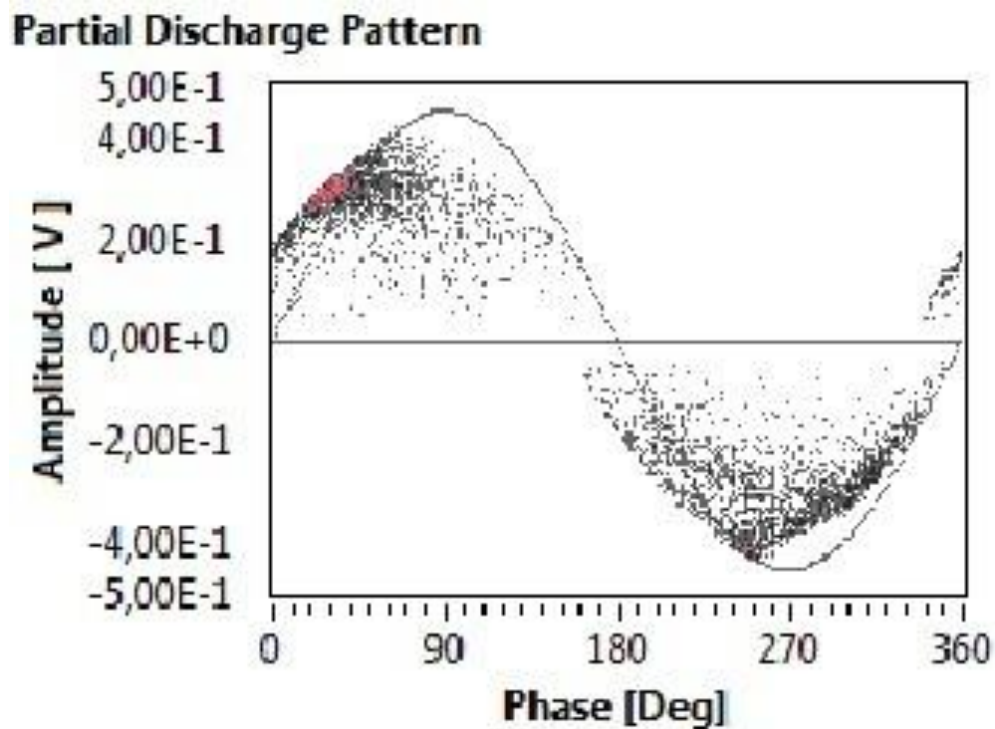


Figure 4.4. The PRPD pattern of the pulses as provided by PDBasell.

The PRPD pattern relates the amplitude of the acquired pulses with their phase with respect to the synchronization voltage. The amplitude of the PD pulse can be displayed in pC if a calibration is possible and has been performed or in V if the calibration cannot be performed (see chapter 3). As an example, the amplitude in Figure 4.4 is given in mV. In other words, the PRPD pattern shows in which part of the sinusoidal waveform of the voltage the PD pulses were created. The PRPD pattern is used to classify the different PD sources. Moreover, the PRPD pattern is used to discriminate between the PD pulses and the background noise.

The PD pulses can also be presented in three other ways as shown in Figure 4.5. The different ways in which PD pulses are presented consist of: the pulse waveform, the pulse spectrum and the classification map.

*The waveform graph* displays the shape of the PD pulse in the time domain. *The spectrum graph* displays the power spectrum of the PD pulse in the frequency domain.

#### 4 Small-scale experiments: Part 1

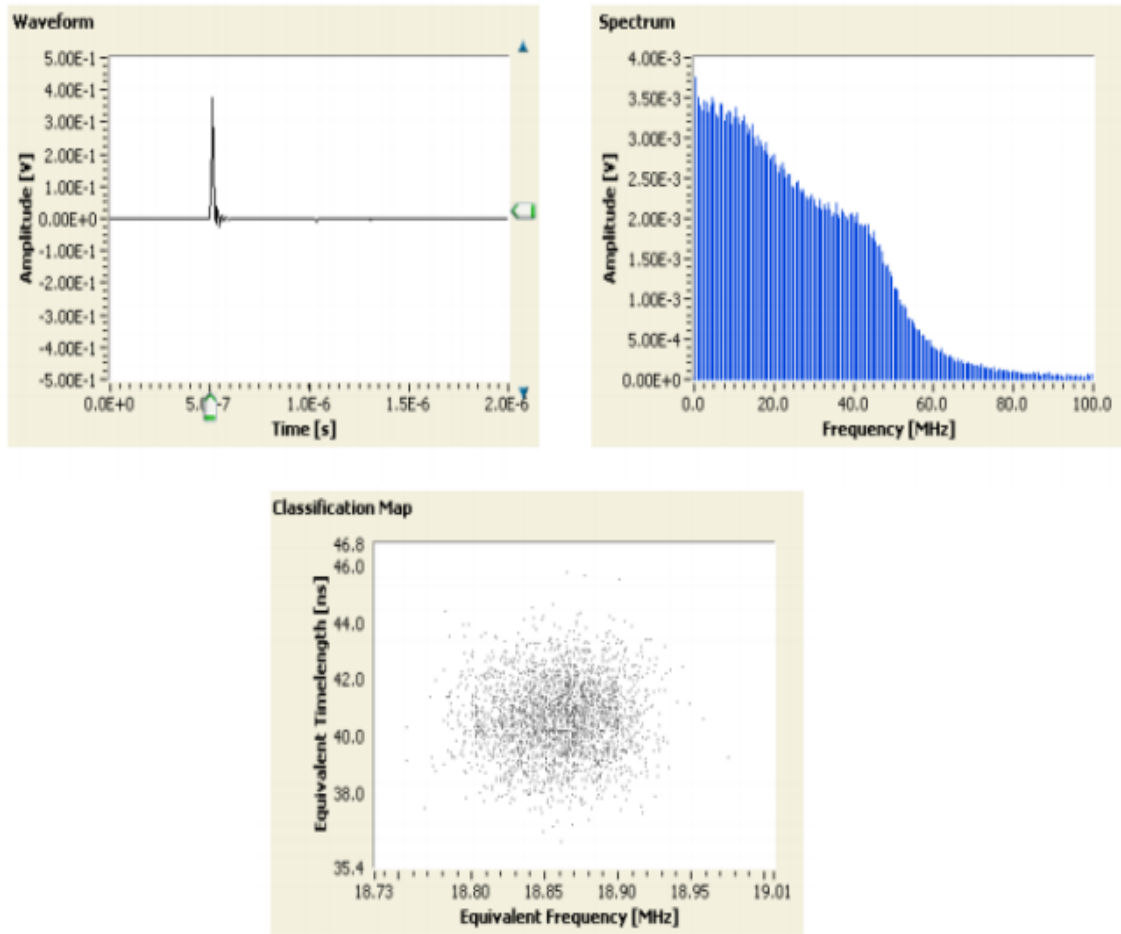


Figure 4.5. Different visualizations of the PD pulses.

The *classification map* shows the acquired pulses classified by their *equivalent timelength* and the *equivalent frequency*. These two parameters are relevant to the pulses waveform. Each point into the classification map corresponds to a single point in the PRPD pattern graph of the pulses. A single PD pulse is acquired in a number of samples  $K$ . If  $s_i(t_i)$  is a sample which is detected at the time  $t_i$ , then the position of the signal in time or the center of gravity of the energy of the signal or time-barycentre,  $t_0$  is,

$$t_0 = \frac{\sum_0^K t_i \cdot s_i(t_i)^2}{\sum_0^K s_i(t_i)^2}$$

the *equivalent timelength (variance)* of the PD pulse is defined as,

$$T^2 = \frac{\sum_0^K (t_i - t_0)^2 \cdot s_i(t_i)^2}{\sum_0^K s_i(t_i)^2}$$

If  $X(f_i)$  are the frequency components of the PD pulse after applying the FFT transform, then the equivalent bandwidth can be calculated by,

$$W^2 = \frac{\sum_0^K f_i^2 |X_i(f_i)|^2}{\sum_0^K |X_i(f_i)|^2}$$

The parameters  $T^2$  and  $W^2$  can fully represent a PD signal in a  $T^2, W^2$  plane with a simple and fast procedure. PD pulses with similar shapes can be grouped in well defined areas in the  $T^2, W^2$  plane. The different groups that contain PD pulses with similar characteristics are called clusters. This procedure causes a loss of information regarding the shape of the PD pulse. The procedure adopted in PDBasell is a good compromise between the complexity of the required computations and the real-time demands [28].

The sensors that were used to detect the PD pulses are the *high frequency current transformers* (HFCT). The HFCT sensor is coupled around the ground connection of the test object. The frequency bandwidths of detection for different HFCT sensors are presented in Table 4.2. The capabilities of the sensors were discussed thoroughly in Chapter 3 where it was shown that only the HFCT-L sensor can be correctly calibrated. For that reason, calibration was only performed in the HFCT-L sensor. Finally the HFCT-L sensor was used with IEC 60270 detection mode and HFCT sensor with WB detection mode.

Table 4.2 The sensors that were used in the experiments.

Sensor	Detection bandwidth	Detection mode in PDBasell
HFCT-L	30 kHz to 30 MHz	IEC 60270
HFCT	1 MHz to 60 MHz	Wide band (W.B)

## 4.2 Experiments on the small scale set up

The stator of the tap changer consists of a hard paper insulating material where the fixed contacts are mounted and it is placed in oil. The rotor of the tap changer is made of the same hard paper insulating material. The moving contacts are mounted on the rotor of the OLTC. The small scale set up which was built to simulate the conditions that are present inside a tap changer is presented in Figure 4.6. The small scale set up simulates the exact distance between adjacent contacts of different phases. The distance between the contacts shown in Figure 4.6 is 90 mm. In addition, an insulation sample which resembles the hard paper insulation of the OLTC was used. The material shown in Figure 4.6 is pertinax. The small scale set up simulates a part of the stator of an OLTC as shown in Figure 4.7.

#### 4 Small-scale experiments: Part 1

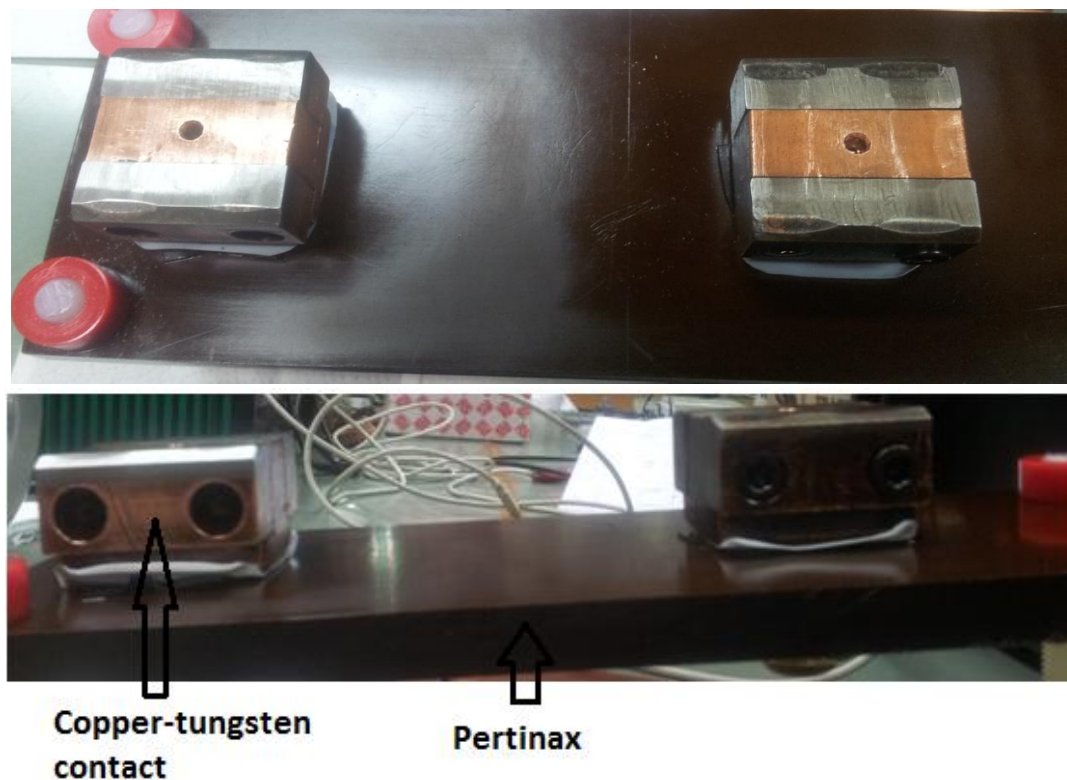


Figure 4.6. Simulation of the distance between adjacent contacts of different phases by using a small scale set up.

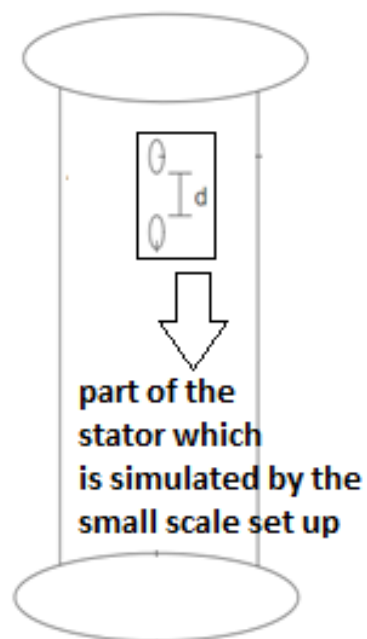


Figure 4.7. Part of the stator which is simulated by the small scale set up.

The small scale set up presented in Figure 4.6 consists of:

- 1) Two copper and tungsten contacts which were obtained from a small single phase tap changer. One of the contacts is connected to the high voltage and the other contact is grounded.
- 2) A piece of hard paper insulating material (pertinax).



#### 4 Small-scale experiments: Part 1

The configuration is placed in a glass container which is filled with transformer oil as shown in Figure 4.8.



Figure 4.8. The small scale set up put inside transformer oil.

The type of oil is Shell Diala B. The maximum applied voltage is 60kV. Increasing the voltage above 60 kV led to the appearance of internal discharges from the high voltage transformer.

The major suspected sources of partial discharge activity inside a tap changer include: 1) *the gas bubbles* that are created during the arcing periods and 2) *tracking* on the paper insulation. Tracking on the paper insulation of the tap changer is most likely to be observed in delta connected tap changers (see Chapter 2). Tracking on the paper cylinder can lead to a flashover between the contacts and therefore, can cause failure of the tap changer.

Under extreme conditions there is a rare scenario where a transition resistor is broken. In that case a sharp wire could result in local high electric field (see chapter 2). This scenario will also be examined. In the experiments that are presented in this chapter, the defects that were investigated are:

- a) *Corona discharges* in oil. This test corresponds to the unlikely phenomenon of a broken transition resistor.
- b) *Surface discharges* on the paper insulation. Surface discharges can be created due to the accumulation of conductive particles at the paper insulation of the tap changer.



## 4 Small-scale experiments: Part 1

- c) PD activity originating from *tracking defects*. Tracking is the result of excessive surface discharges occurring on the surface of the paper insulating cylinder of the tap changer.
- d) PD activity in *gas bubbles* which are produced during the arcing periods.

This part of the chapter focuses on the simulation of the PD activity occurring in an OLTC by using a small scale model of the OLTC. The different defects that may cause PD activity in the OLTC are presented.

### 4.2.1 Calibration

The next step in the experimental procedure is the calibration of the measuring circuit. The calibrator that was used in the experiments was the PD calibrator type 451 manufactured by Haefely. The calibrator is presented in Figure 4.9.

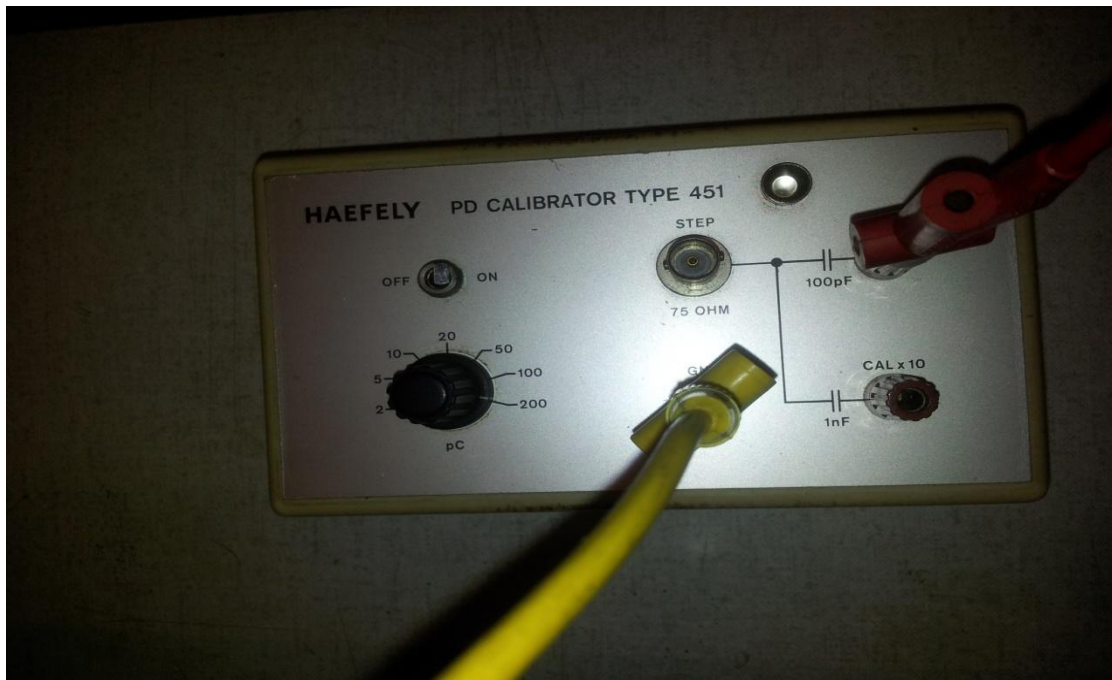


Figure 4.9. The calibrator of Haefely.

The calibrator is connected across the test object as shown in Figure 4.10. The pulse is injected between the contact which is connected to the high voltage and the contact which is connected to the ground.

The pulse of the calibrator as obtained by using a Tektronix oscilloscope is shown in Figure 4.11. The amplitude of the calibration pulse is 200pC. The software then uses the calibration pulse to convert the amplitude from mV to pC using the integral of the pulse. The detection modes that were used in the experiments were the wideband (WB) detection mode and IEC60270 detection mode. The bandwidth of the WB detection mode is from 16 kHz to 48MHz and the bandwidth of the IEC60270 detection mode is from 110 to 440 kHz. The sensors used in the

## 4 Small-scale experiments: Part 1

experiments were the HFCT sensors. From the two sensors only the HFCT-L sensor was calibrated (see chapter 3).

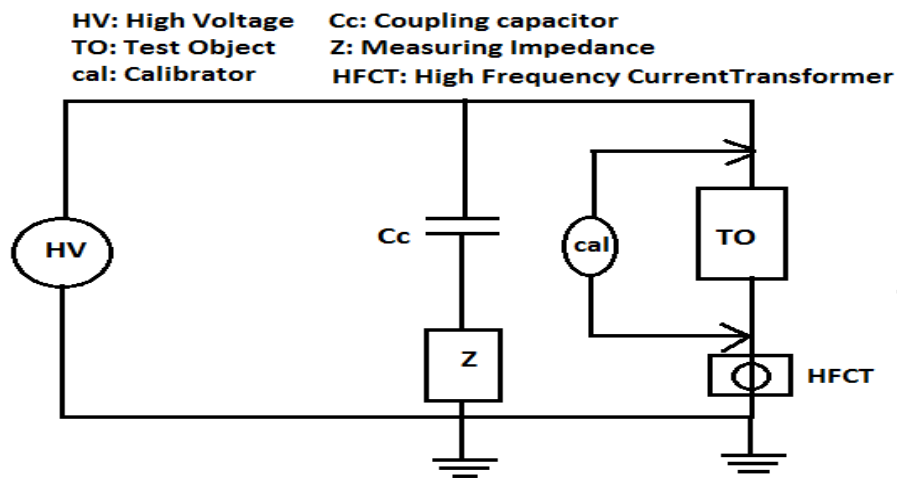


Figure 4.10. Connection of the calibrator across the test object.

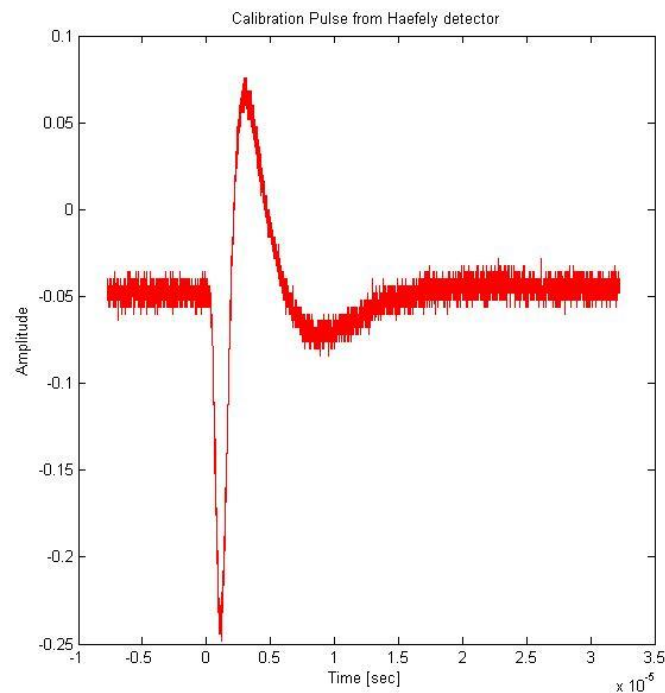


Figure 4.11. The calibration pulse.

### 4.2.2 PD measurements

The first experiment was performed without introducing any defects into the test set up. The purpose of this experiment was to investigate if there were any unwanted PD sources in the small scale set up and eventually to eliminate any unwanted PD sources. The voltage was increased up to 55kV. The acquisition of the pulses revealed the presence of only the background noise. The acquisition of the pulses at a voltage level of 45kV and 50kV are presented in Figure 4.12 and Figure 4.13 respectively.

#### 4 Small-scale experiments: Part 1

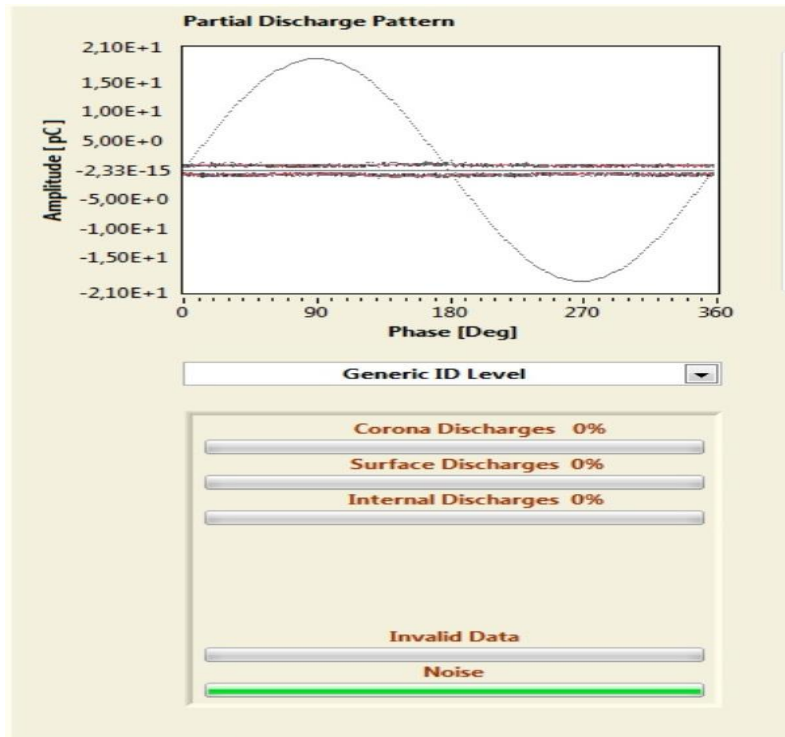


Figure 4.12. Background noise at 45kV.

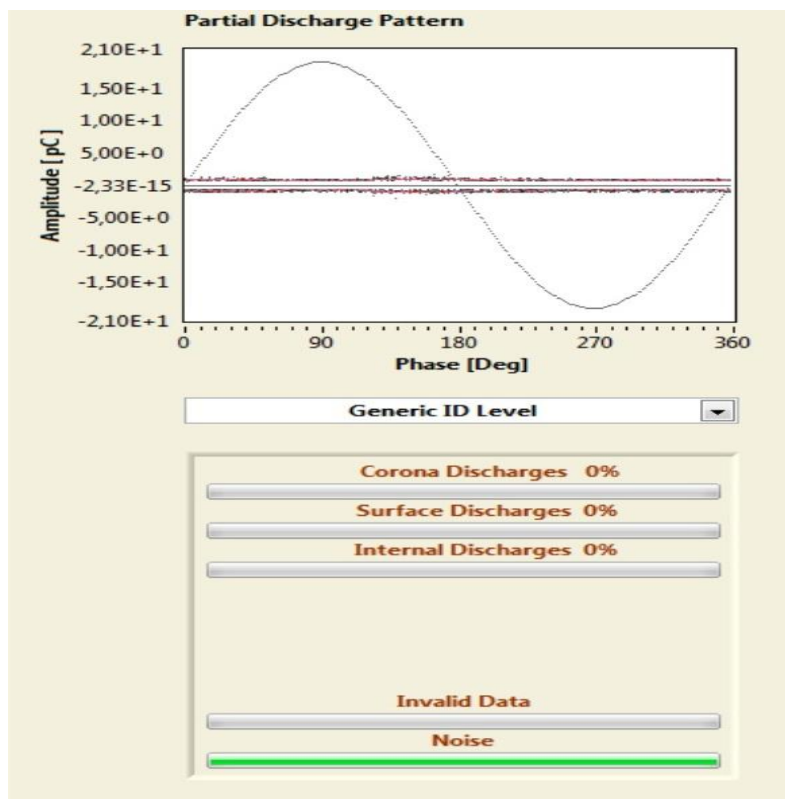


Figure 4.13. Background noise at 50kV.

As we can observe from Figure 4.12 and Figure 4.13 the small scale set up is PD free up to a voltage level of 50kV. The peak level was set to 21pC (see Figures 5.12, 5.13) and to 48pC at both voltage levels and the trigger level was set at 3pC, but no discharge activity was measured. At 60kV some discharges were observed.

#### 4 Small-scale experiments: Part 1

The discharges that were measured originated from the high voltage transformer that was used in the experiments.

##### 4.2.2.1 Corona discharges in oil

The second experiment focuses on corona discharges in oil. The schematic diagram of the test set up is presented in Figure 4.14. In Figure 4.15 the point to plane set up is presented.

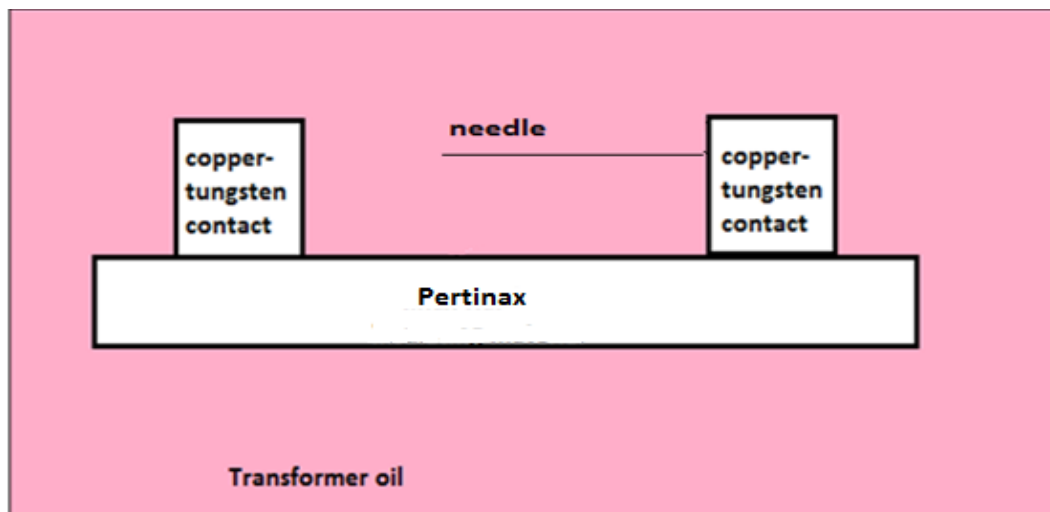


Figure 4.14. Schematic diagram of the set up.

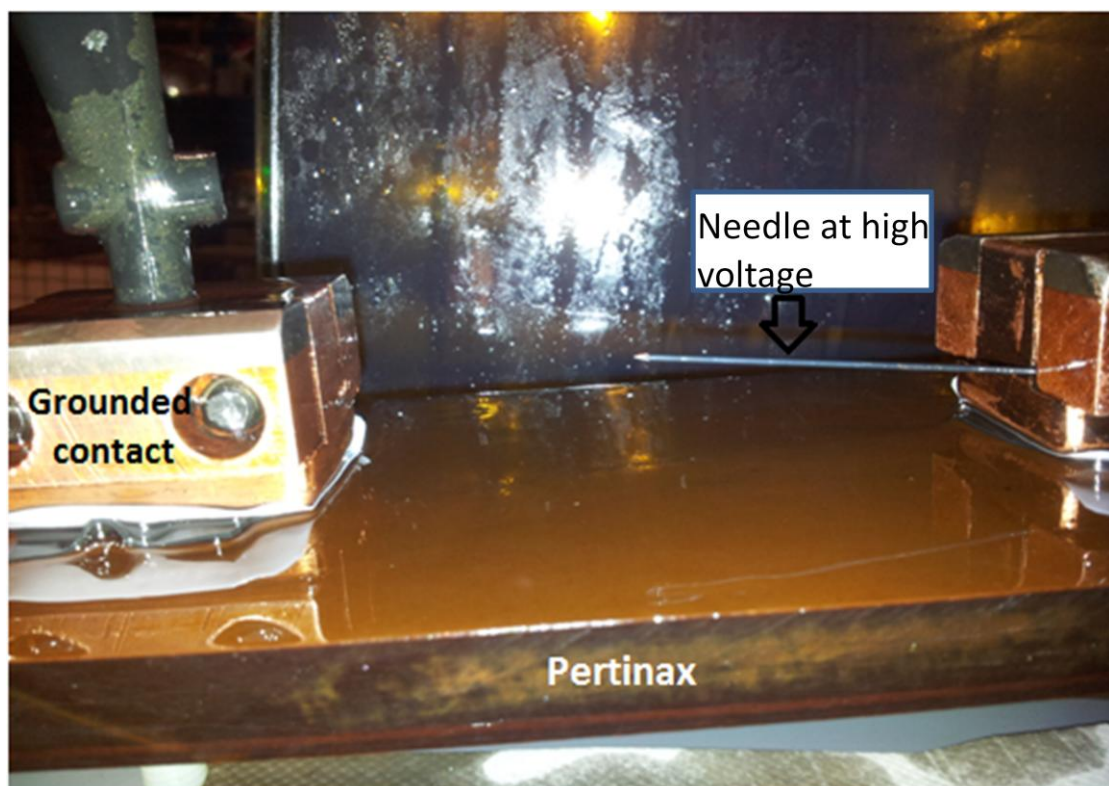


Figure 4.15. The set up to create corona in oil.

The needle is placed on the high voltage connected contact. The radius of the tip is 50 $\mu$ m and the distance from the tip of the needle to the grounded contact is

#### 4 Small-scale experiments: Part 1

30mm. The results of this experiment are presented in Table 4.3. The inception voltage was 36kV.

Table 4.3. Results of the experiment.

Detection Mode	Voltage [kV]	N/s Repetition Rate	Qmean [pC]	Number of pulses	Acquisition time
IEC	39	0.014	450	17	20 minutes
IEC	45	0.106	800	123	20 minutes
IEC	50	0.174	1000	208	20 minutes

From Table 4.3 we can observe that the repetition rate of the corona discharges in oil is very slow. We can also observe that the repetition rate increases with increasing applied voltage which is a characteristic of corona discharges. The PRPD patterns of the corona discharges in oil at 39kV, 45kV and 50kV are presented in Figures 4.16, 4.17 and 4.18 respectively.

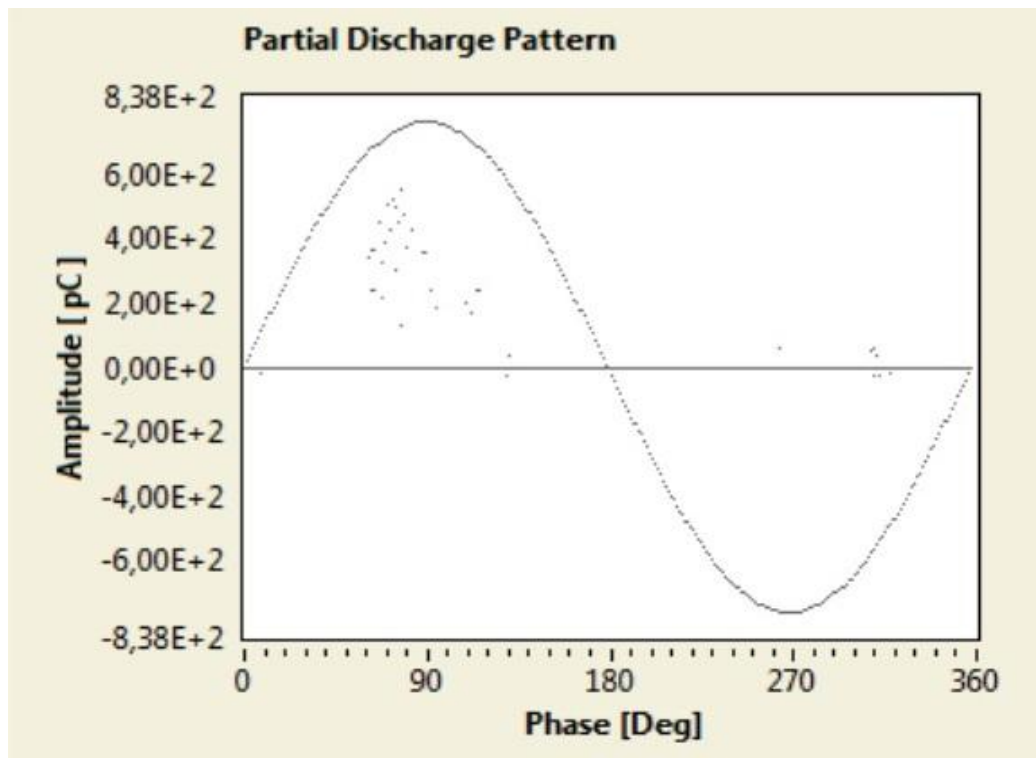


Figure 4.16. The PRPD pattern at 39kV.

4 Small-scale experiments: Part 1

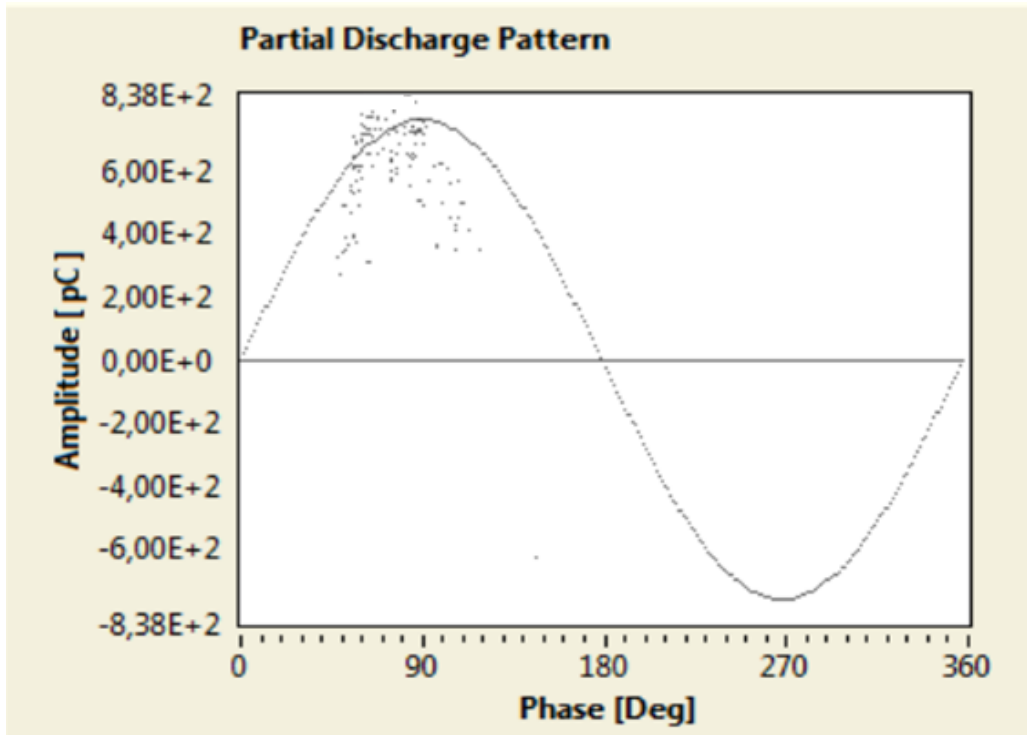


Figure 4.17. The PRPD pattern at 45kV.

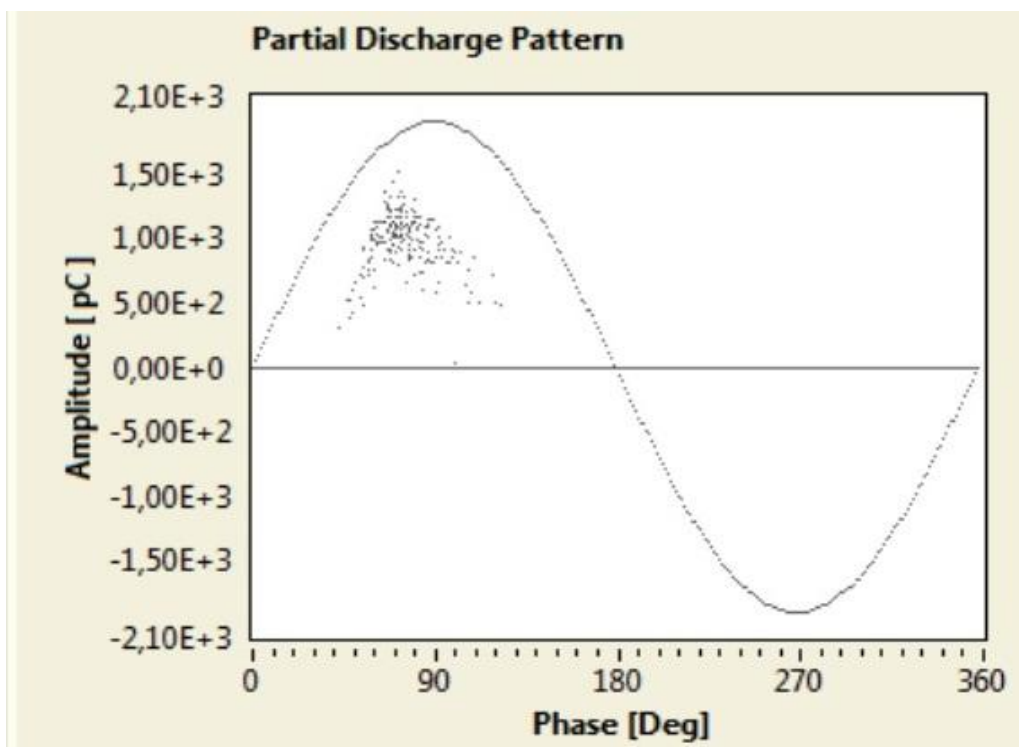


Figure 4.18. The PRPD pattern at 50kV.



#### 4 Small-scale experiments: Part 1

Figure 4.19 presents the shape of the PD pulse obtained by using the IEC detection mode.

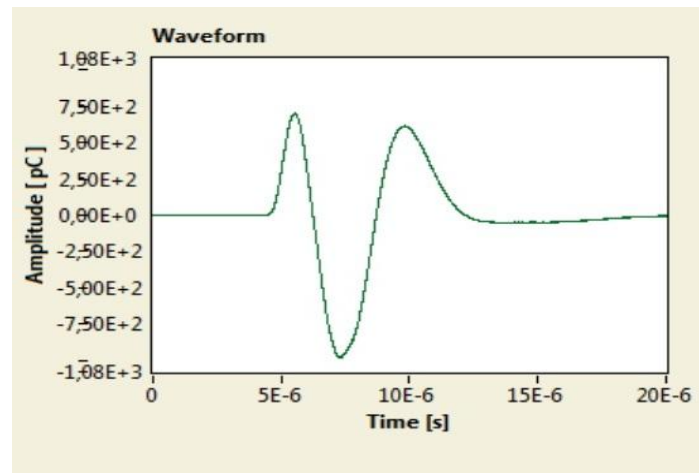


Figure 4.19. The shape of the PD pulse (IEC).

The pattern that is observed in Figures 4.16, 4.17 and 4.18 represent corona discharges in oil. The pattern is positioned close to the peak of the applied voltage. The small phase shift from the peak of the applied voltage could be explained by the presence of charge around the tip of the needle. The presence of charge could alter the electric field at the tip of the needle, causing the appearance of corona discharges before the voltage peaks. The magnitudes of the discharges increase with increasing voltage. The mean values of the PD magnitudes range from 450 pC to 950 pC. The PD pulses of Figures 4.16 to 4.18 do not display a large scatter of PD magnitudes. For example, in Figure 4.18 the magnitudes of the majority of the PD pulses are in a range from 950 pC to 1050 pC. Moreover, the repetition rate of the PD pulses increases with increasing voltage. This specific behavior of the PD pulses could be attributed to corona discharges in oil [29]. Figure 4.19 represents the shape of a positive PD pulse. A PD pulse is characterized as positive or negative by the first observed peak of the pulse which is in this case positive. The identification of the PD source as obtained by PDBasell is presented in Figure 4.20.

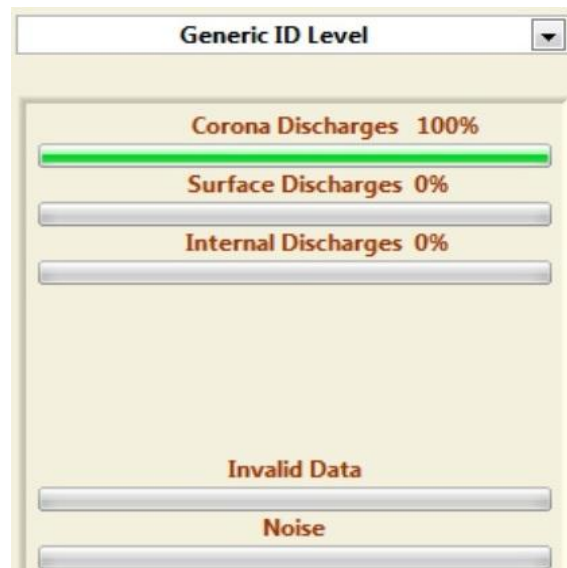


Figure 4.20. Identification of the PD source.

#### 4.2.2.2 Surface discharges in oil

During the next experiment, surface discharges in oil were investigated. In order to create the surface discharges a sharp needle was used. The radius of the tip of the needle was  $50\mu\text{m}$ . The needle was initially at high voltage and then at ground potential and the point where the needle touched the paper insulation differs from experiment to experiment (see Figure 4.22). The needle always touched the paper insulation at an acute angle. In that way, a strong tangential electric field was created at the surface of the paper insulating material (pentinax).

##### Experiment 1

In the first experiment the needle was attached to the contact which was connected to the high voltage. The set up used to create surface discharges is presented in Figure 4.21. The schematic diagram of the set up is presented in Figure 4.22.

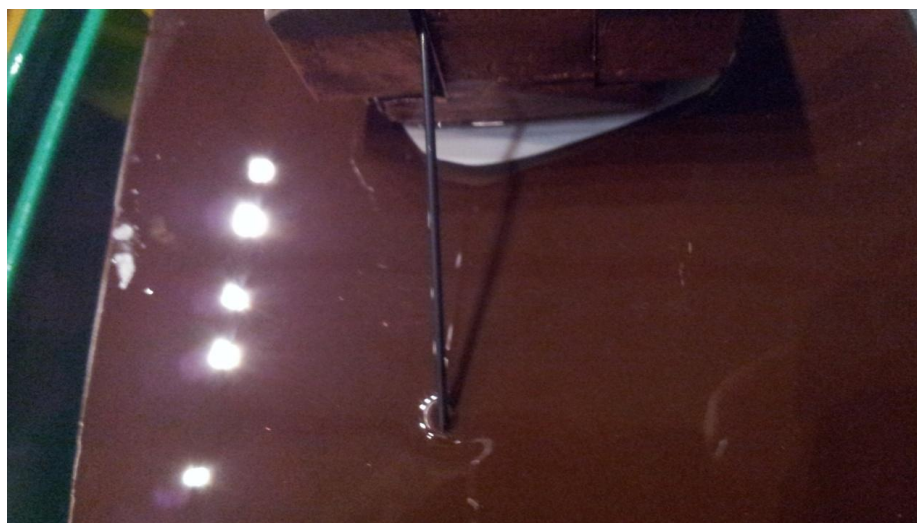


Figure 4.21. The set up to create surface discharges.



#### 4 Small-scale experiments: Part 1

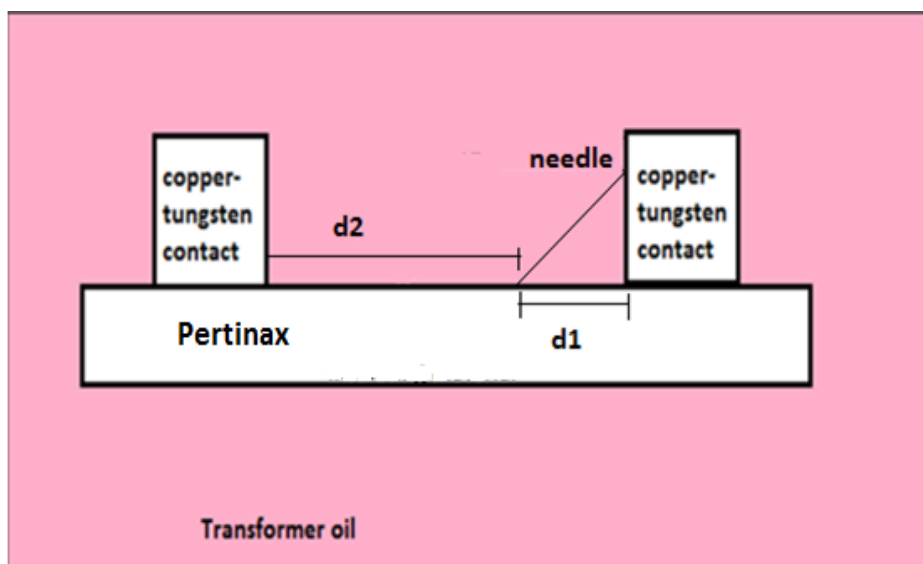


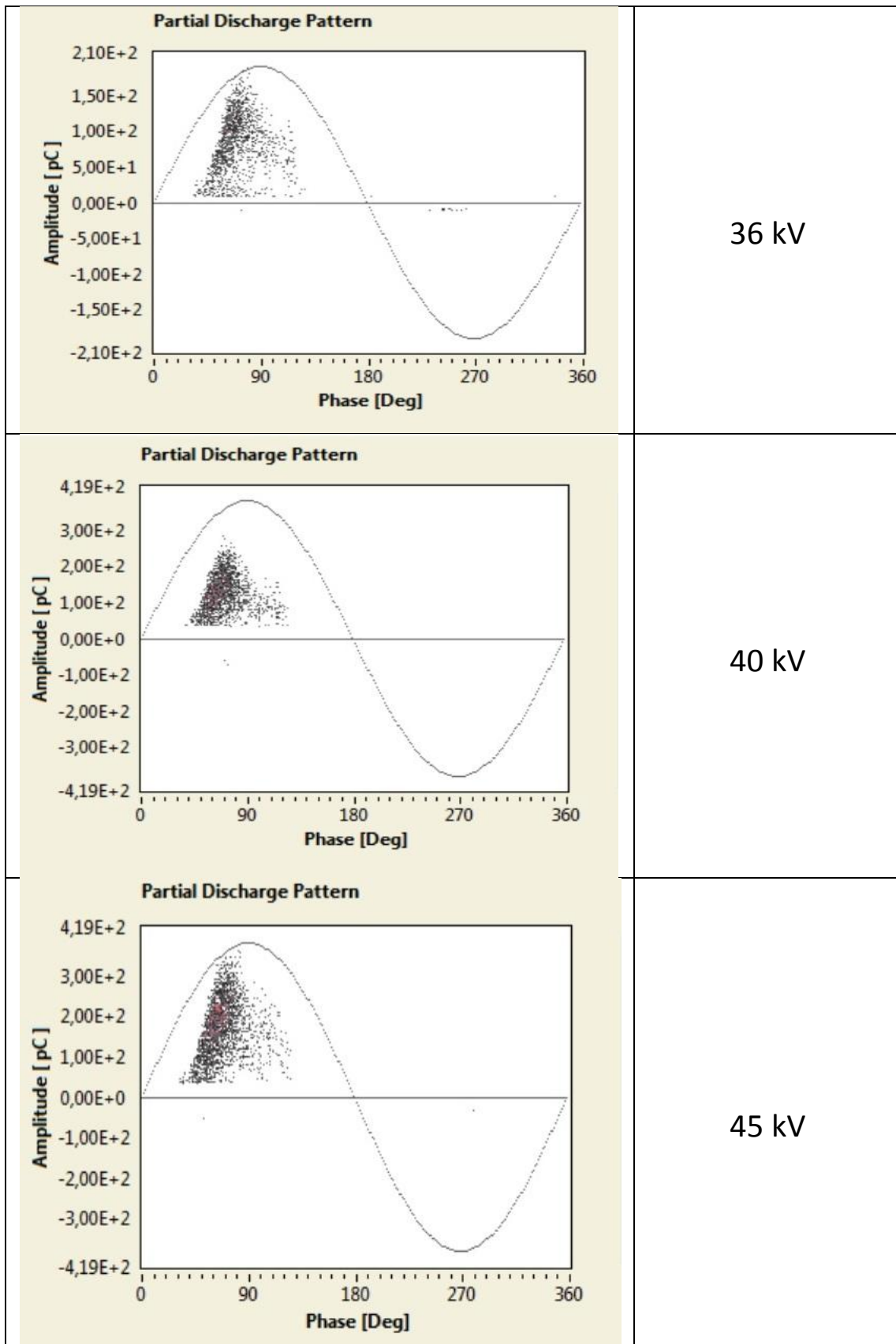
Figure 4.22. Schematic diagram of the set up.

In Figure 4.22, the distance  $d_1$  is 20mm and the distance  $d_2$  is 70mm. The first PD pulses were observed at approximately 28 kV. The repetition rate was very slow at the inception voltage. The acquisition time was set to 20 minutes. At 28kV only 5 pulses were measured. The voltage was slowly increased until a higher repetition rate was achieved. The repetition rate increased with increasing voltage. At 32 kV, 600 pulses were measured in the acquisition time of 20 minutes. The first acquisition which gave a solid pattern of the discharges was at 36 kV. The results of this experiment starting at 36 kV are presented in more detail in Table 4.4. The PRPD patterns of the pulses at the different voltage levels are presented in Figure 4.23 and the shape of a PD pulse as obtained by IEC 60270 acquisition mode is presented in Figure 4.24.

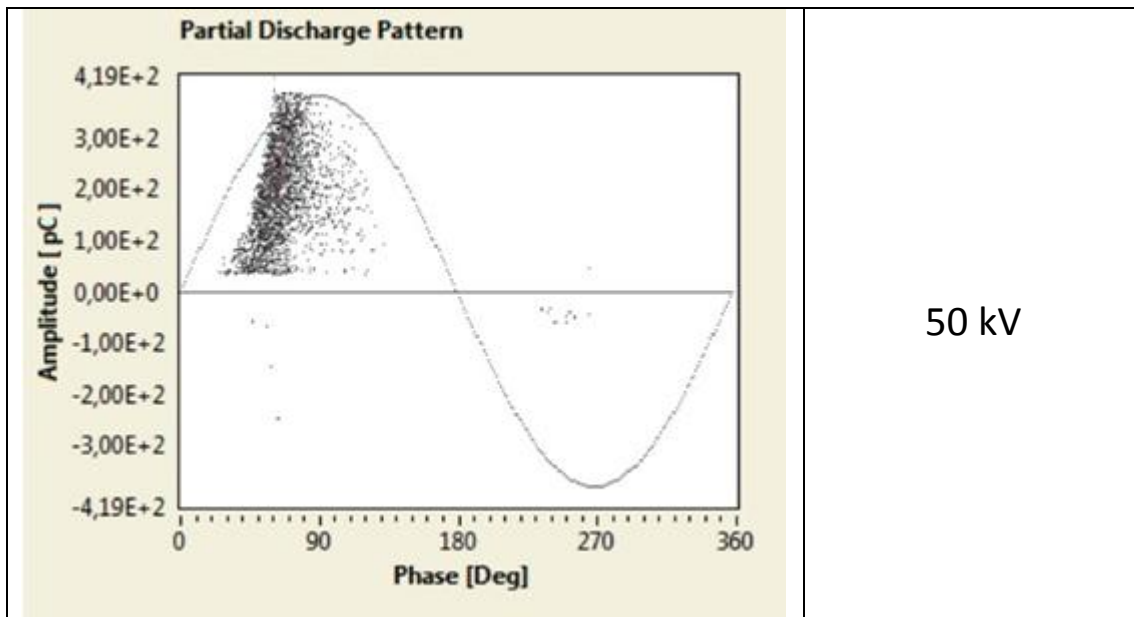
Table 4.4. Results of the experiment.

Detection mode	Repetition rate N/s Negative half-period	Repetition rate N/s Positive half-period	Voltage [kV]	Q [pC] Positive half-period	Q [pC] Negative half-period	Number of pulses Positive half-period	Number of pulses Negative half-period	Acquisition time
IEC	0.009	1.205	36	188	8	1445	11	20minutes
IEC	0.002	1.621	40	282	69	1938	2	20minutes
IEC	0.002	2.082	45	360	49	2497	2	20minutes
IEc	0.021	3.443	50	416	246	2982	18	20minutes

4 Small-scale experiments: Part 1



#### 4 Small-scale experiments: Part 1



50 kV

Figure 4.23. The PRPD pattern of the PD pulses.

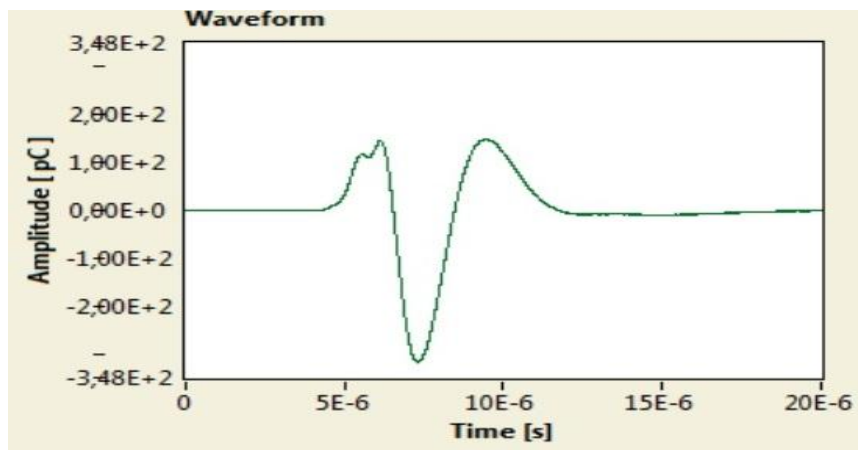


Figure 4.24. The shape of the PD pulse.

From Table 4.4, we can observe that the repetition rate of the surface discharges in oil was very low. Moreover, we can notice that the magnitude of the discharges is increasing when the voltage is increased. In addition, the surface discharges appear in the positive half period. Only a very small number of discharges can be observed in the negative half period. Figure 4.23, presents the PRPD pattern of the pulses. In this case, the PD pulses show a greater differentiation of their magnitudes. The magnitudes of the PD pulses display a large scatter which is characteristic for surface discharges [30]. In addition, the pattern is not positioned around the peak of the voltage but the majority of the pulses are placed between  $40^{\circ}$  and  $80^{\circ}$  of the applied voltage. In Figure 4.24, the shape of a positive PD pulse as obtained by the IEC 60270 detection mode is presented. The shape of the pulse is the one provided by the PD detector after applying filters. Figure 4.25 presents the trending of the PD activity over time and applied voltage. More specifically, in Figure 4.25, the repetition rate of the discharges and the magnitude of the PD activity for

#### 4 Small-scale experiments: Part 1

the applied voltage levels are presented. The values of the repetition rate and the PD magnitude for the applied voltage levels are presented in Table 4.5.

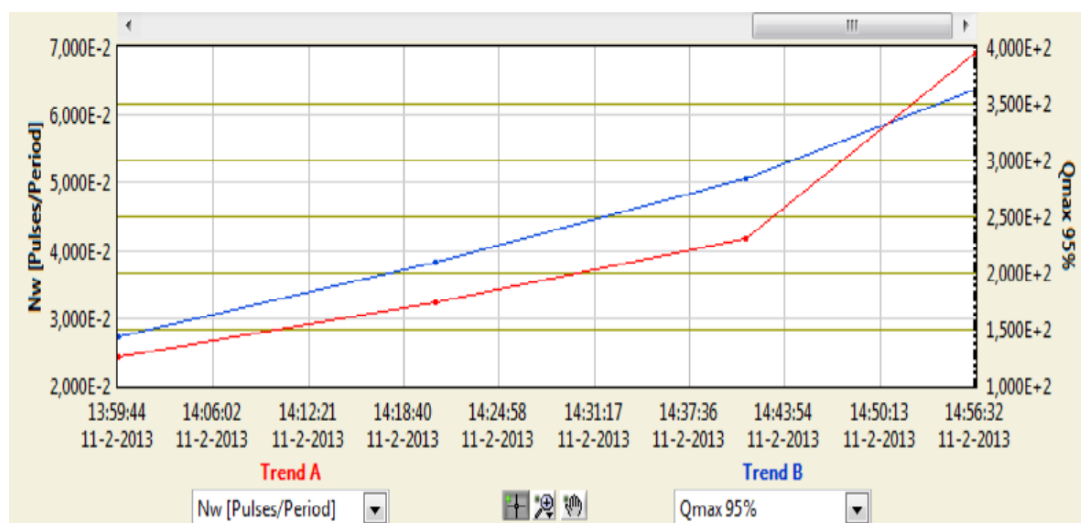


Figure 4.25. The trending of the PD activity.

Table 4.5. Repetition rate and PD magnitude over the applied voltage.

Voltage [kV]	Repetition rate [Pulses/Period]	PD magnitude Qmax 95% [pC]
36	0.024	144
40	0.032	209
45	0.041	284
50	0.070	363

The repetition rate is increasing with increasing voltage as shown by the red line of Figure 4.25. The repetition rate starts from 0.024 pulses/period and increases up to 0.070 pulses/period. In addition, the magnitude of the discharges [Qmax 95%] also increases with increasing voltage. The magnitude of the discharges starts from 144 pC at 36 kV and reaches 363 pC at 50 kV (blue line in Figure 4.25). These facts in combination with the large scatter of the PD magnitudes contribute to the classification of the PD source as surface discharges.

#### Experiment 2

The position of the needle is different in the next experiment. The needle is still attached at the contact connected to the high voltage but now the distance of the point where the needle touches the paper insulation from the grounded contact is 40mm (d2=40mm). The inception voltage of the discharges in this case is 26 kV. The results of this experiment are presented in Table 4.6.

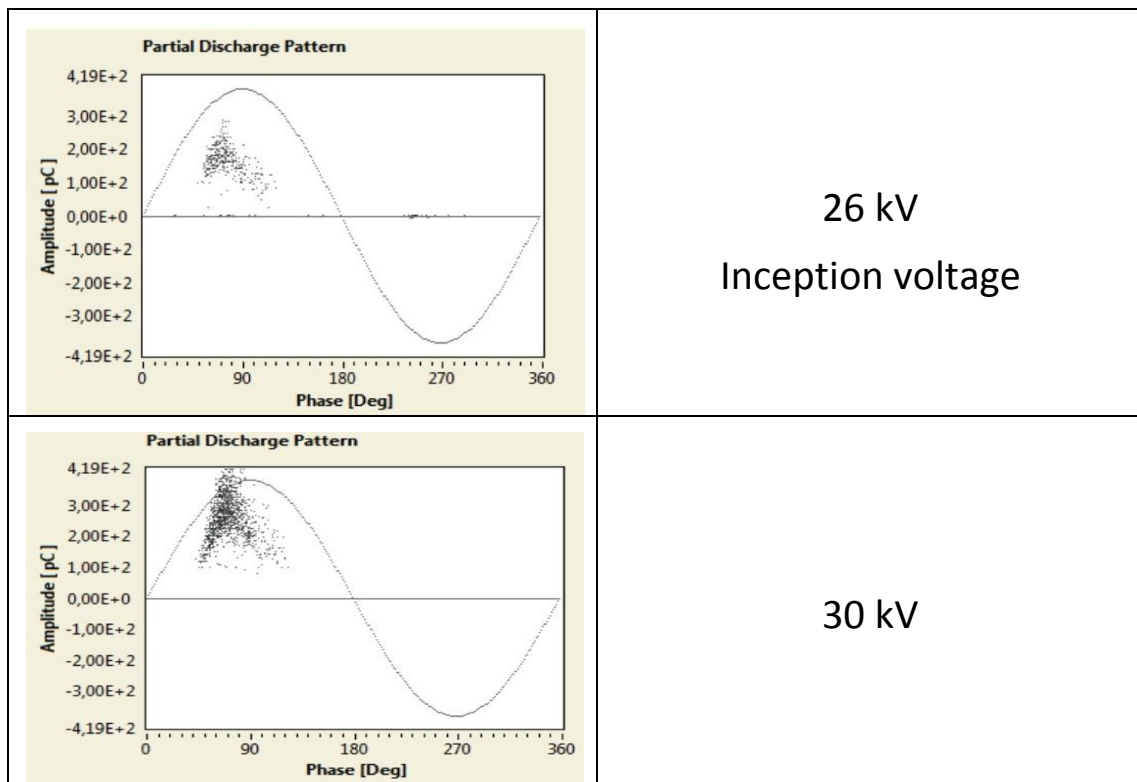
#### 4 Small-scale experiments: Part 1

Table 4.6. Results of the experiment.

Detection mode	Repetition rate N/s Negative half-period	Repetition rate N/s Positive half-period	Voltage [kV]	Q [pC] Positive half-period	Q [pC] Negative half-period	Number of pulses Positive half-period	Number of pulses Negative half-period	Acquisition time
IEC	-	0.319	26	288	-	412	-	20minutes
IEC	-	1.105	30	416	-	1324	-	20minutes
IEC	-	3.5	36	832	-	4230	-	20minutes
IEC	0.834	9.611	40	1179	66	4598	402	20minutes

Figure 4.26 presents the PRPD pattern of the discharge pulses for the different voltage levels. In this case we can also observe that the majority of the discharges occur in the positive half period of the voltage. Moreover, the repetition rate as well as the magnitude of the discharges increases with increasing voltage. When the voltage is increased further, the number of pulses measured in the negative half period of the voltage increases. The point where the needle touches the surface of the paper insulation is now closer to the grounded contact while the needle remains attached to the contact which is connected to the high voltage.

The trending of the PD pulses through the whole period of applying voltage to the test set up is presented in Figure 4.27. Figure 4.27 specifically presents the repetition rate (Pulses/Period) and the magnitude of the PD pulses (Qmax 95%) over the applied voltage.



#### 4 Small-scale experiments: Part 1

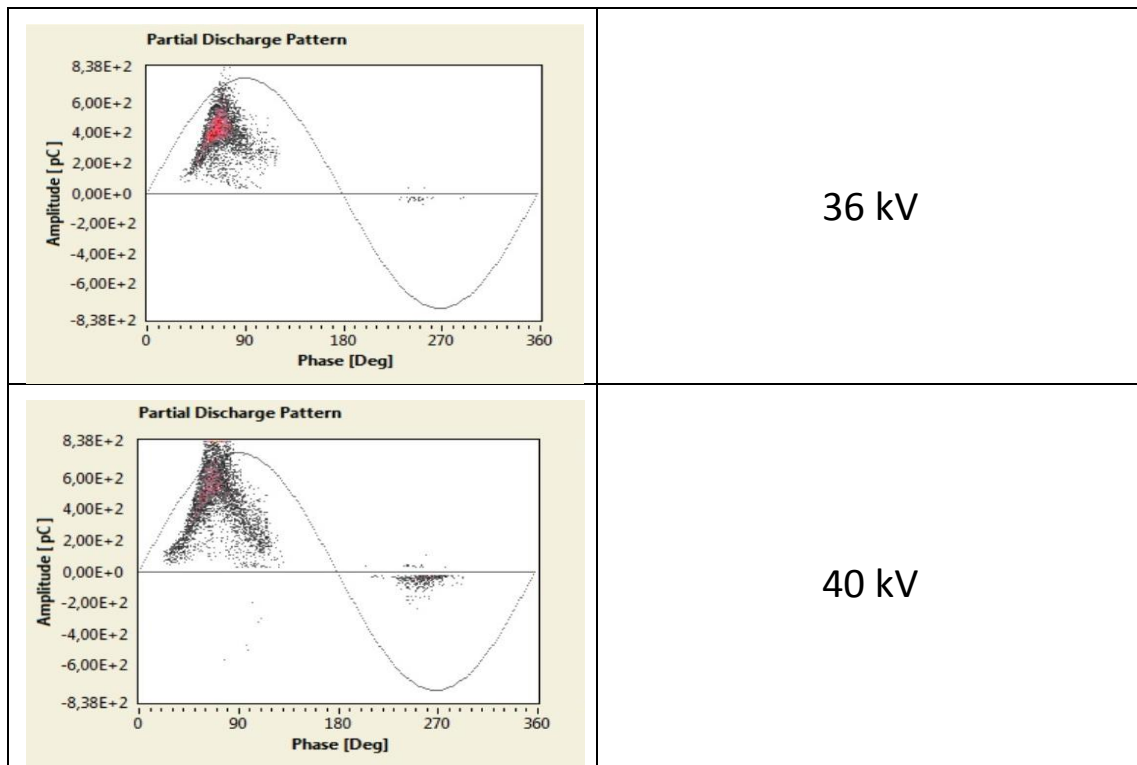


Figure 4.26. The PRPD pattern of the discharge pulses.



Figure 4.27. The trending of the PD pulses over time and applied voltage.

The repetition rate of the discharges increases with increasing voltage. The repetition rate at 26 kV is 0.00688 pulses/period and at 40 kV the repetition rate becomes 0.209 pulses/period. The magnitude of the discharges  $Q_{\max 95\%}$  starts from 233 pC at 26 kV and reaches 780 pC at 40 kV (1.5 times the inception voltage). The values of the repetition rate and the PD magnitude over the applied voltage are presented in Table 4.7.

#### 4 Small-scale experiments: Part 1

Table 4.7. Repetition rate and PD magnitude over the applied voltage.

Voltage [kV]	Repetition rate [Pulses/Period]	PD magnitude $Q_{max}$ 95% [pC]
26	0.00688	233
30	0.022	374
36	0.070	597
40	0.209	780

The trending of the PD pulses presented in Figure 4.27 and Table 4.7, show that the repetition rate increases with increasing voltage. In addition, the PD pulses display a large scatter in their magnitudes. The large scatter in the magnitudes of the PD pulses, as well as the increase in repetition rate and PD magnitude with increasing voltage is a characteristic behavior of surface discharges [29].

#### **Experiment 3**

In the next experiment the needle was attached to the grounded contact. As mentioned before, the radius of the tip of the needle is  $50\mu\text{m}$ , the distance of the point where the needle touched the paper insulating material from the contact which was connected to the high voltage is  $40\text{mm}$  ( $d_1=40\text{mm}$ ) and the distance from the grounded contact is  $50\text{mm}$  ( $d_2=50\text{mm}$ ) as shown in Figure 4.28.

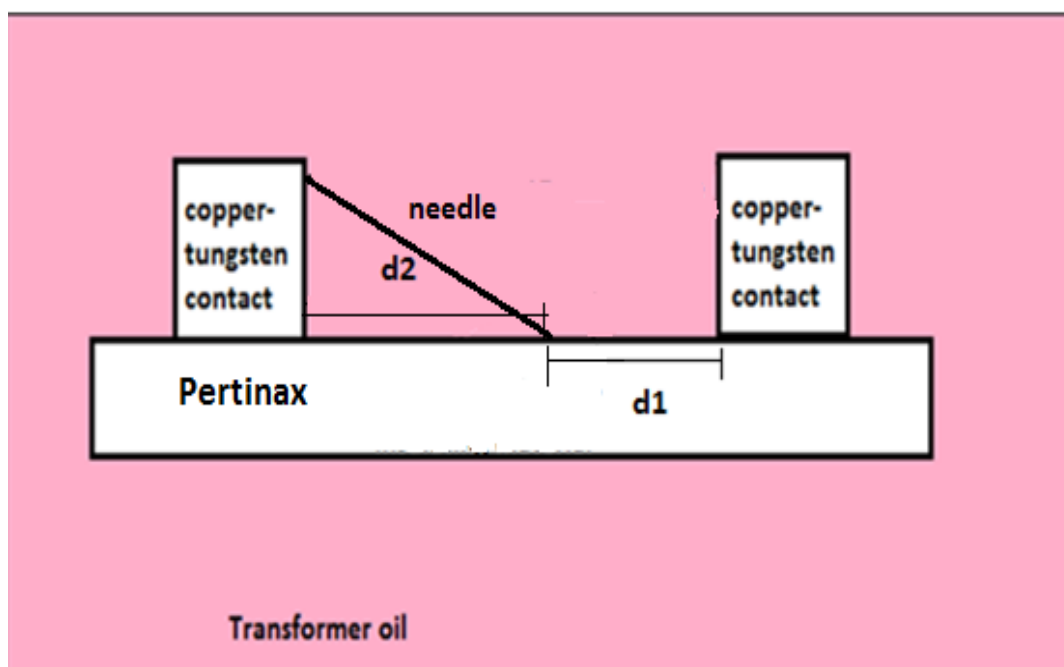


Figure 4.28. Needle connected to the grounded contact.

The results of this experiment are summarized in Table 4.8. The first PD activity appeared at  $36\text{kV}$ . The repetition rate of the discharges was extremely low. After 20 minutes of acquisition only 20 pulses were measured (1 pulse/minute). The voltage was increased to  $40\text{kV}$  but the repetition rate was still very low. In order to

#### 4 Small-scale experiments: Part 1

get a higher repetition rate and a solid PRPD pattern, the voltage was increased to 45kV. The PRPD pattern of the partial discharge pulses is presented in Figure 4.29.

Table 4.8. Results of the experiment.

Detection mode	Repetition rate N/s Positive half-period	Repetition rate N/s Negative half-period	Voltage [kV]	Q [pC] Positive half-period	Q [pC] Negative half-period	Number of pulses Positive half-period	Number of pulses Negative half-period	Acquisition time
IEC	0.044	0.963	45	45	208	53	1155	20minutes
IEC	0.061	1.075	50	51	496	73	1287	20minutes

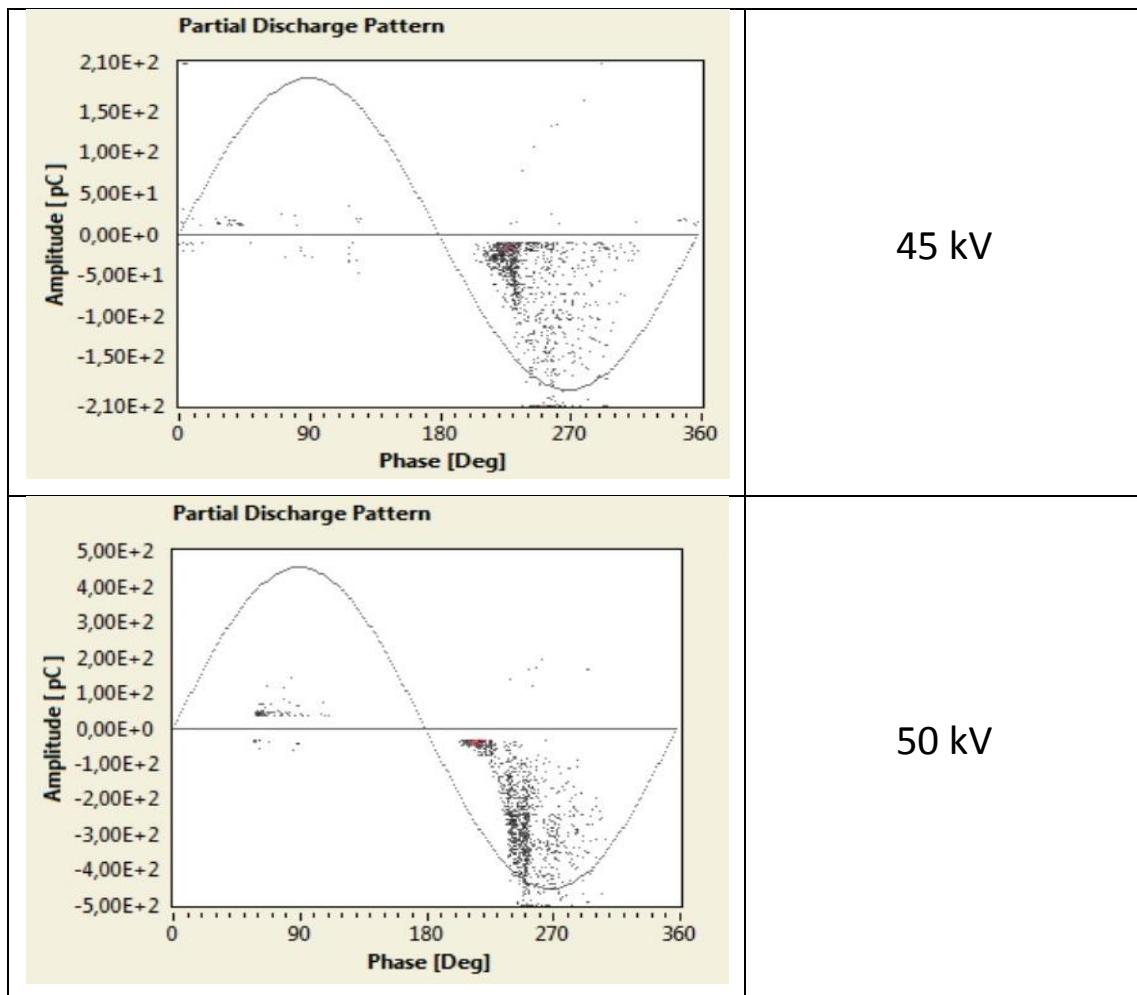


Figure 4.29. PRPD pattern of the PD pulses (IEC).

The voltage was increased up to 45 kV in order to get a good repetition rate and acquire a significant amount of PD pulses. In addition, more discharges at the positive half period are present when the voltage is increased to 50 kV. The PD pulses show again a large scatter regarding their PD magnitudes. The pattern is



#### 4 Small-scale experiments: Part 1

located between  $220^\circ$  and  $300^\circ$ . The shape of a negative PD pulse as obtained by using the IEC detection mode is presented in Figure 4.30. Figure 4.31 presents the trending of the PD pulses over time and applied voltage. In the same way as in the previous experiments, the magnitude of the discharges increases with increasing voltage. The repetition rate also increases slightly. The values of the repetition rate and the magnitude of the discharges are presented in Table 4.9.

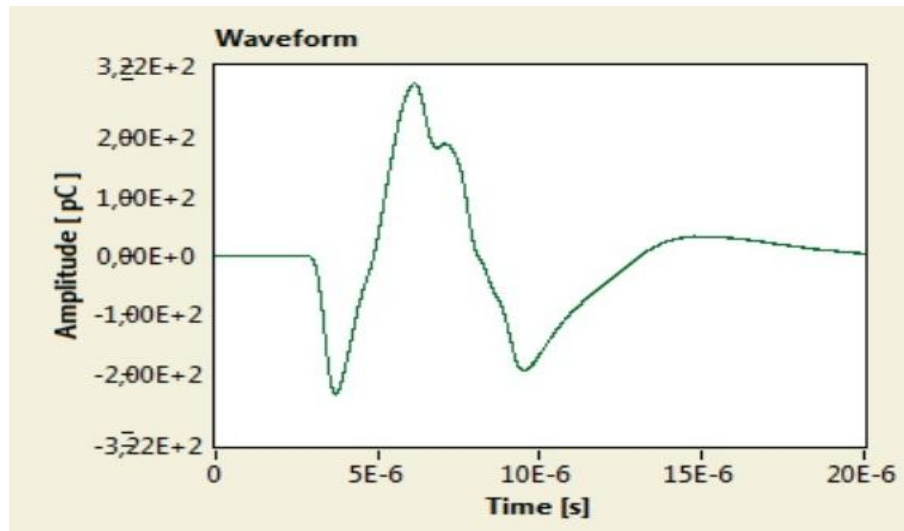


Figure 4.30. The shape of the PD pulse.



Figure 4.31. The trending of the PD pulses over time and applied voltage.

Table 4.9. Repetition rate and PD magnitude overtime and applied voltage.

Voltage [kV]	Repetition rate [Pulses/Period]	PD magnitude Qmax 95% [pC]
45	0.020	209
50	0.023	440

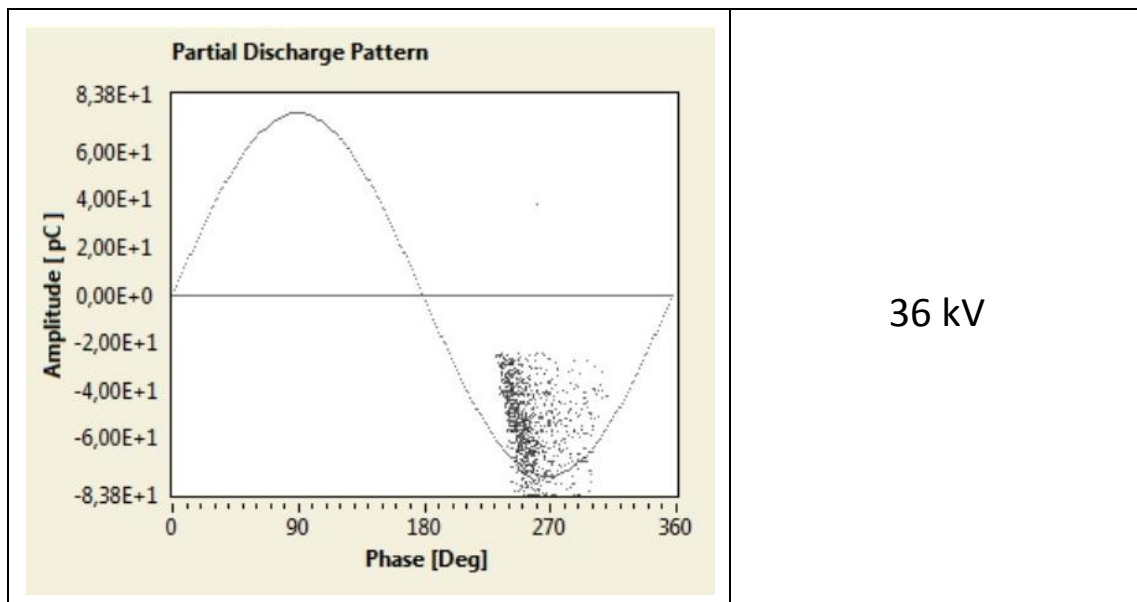
**Experiment 4**

In the next experiment the position of the needle was changed. The distance of the point where the needle touched the paper insulation from the contact which was connected to the high voltage is 60mm (d1=60mm) and the distance from the grounded contact is 30mm (d2=30mm). The first PD pulses were observed at 29 kV.

The repetition rate was again very low, for that reason the voltage was increased in order to increase the repetition rate and to get a larger number of PD pulses. The acquisition of PD pulses was performed at 36 kV because at that voltage level the number of PD pulses increased significantly compared to the number of pulses at 29 kV. The results that were obtained in this experiment are summarized in Table 4.10, the PRPD pattern of the obtained pulses as obtained by the IEC 60270 acquisition mode is presented in Figure 4.32 and the shape of a negative PD pulse in IEC 60270 acquisition mode is presented in Figure 4.33.

Table 4.10. Results of the experiment.

Detection mode	Repetition rate N/s Positive half-period	Repetition rate N/s Negative half-period	Voltage [kV]	Q [pC] Positive half-period	Q [pC] Negative half-period	Number of pulses Positive half-period	Number of pulses Negative half-period	Acquisition time
IEC	-	0.913	36	-	83	-	1090	20minutes
IEC	-	0.918	40	-	136	-	1100	20minutes
IEC	-	1.227	45	-	208	-	1471	20minutes



#### 4 Small-scale experiments: Part 1

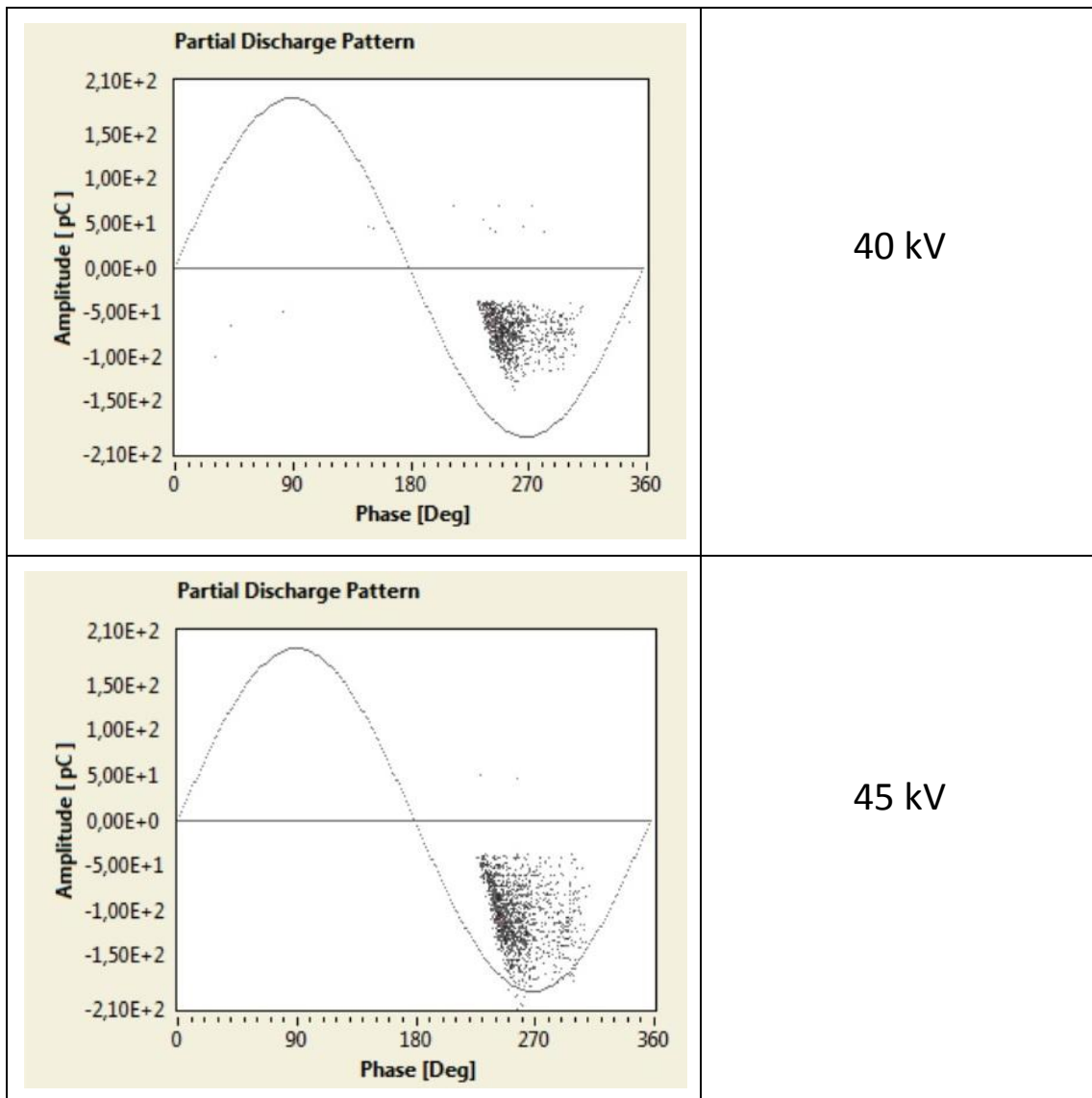


Figure 4.32. PRPD pattern of the PD pulses (IEC).

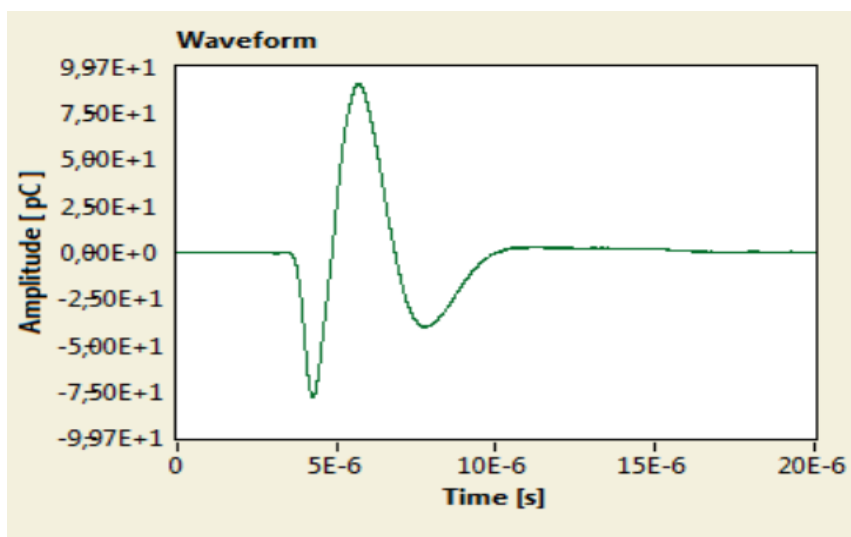


Figure 4.33. The shape of the PD pulse.

### 4.2.2.3 Tracking on the paper insulation

The on-load tap changer (OLTC) can be connected either in star or in delta. The voltage level a tap changer must withstand is higher for delta-connected tap changers than for star-connected tap changers (see Chapter 2). In delta-connected tap changers, according to the experience, the most important defect is the tracking on the paper insulation of the tap changer. This is because delta-connected tap changers must insulate for the whole line-to-line voltage, as explained in Chapter 2. The metallic particles that can accumulate on the paper insulation of the tap changer can cause the appearance of surface discharges. In the case of delta-connected tap changers, where the tap changer is stressed by higher electric fields, surface discharges can occur more easily. In the previous paragraph, the PRPD patterns of surface discharges were discussed. Surface discharges can create black carbon spots on the surface of the paper insulating material. The carbon spots can be elongated and a conductive path can be formed (see Chapter 2).

Partial discharges occur at the edge of this path due to the strong field enhancement. The discharges lead to the elongation of the carbonized path. This phenomenon is called tracking. Tracking depends on the applied voltage but also on time. After a long period of time, the conductive path could bridge a large part of the insulating distance between two contacts and cause a flashover. This can lead to the failure of the tap changer and the power transformer. For star-connected tap changers this phenomenon is rare because the electric field between contacts of different phases is small. This is because star-connected tap changers must insulate only for a part of the line-to-neutral voltage, as presented in Chapter 2.

In this part of the research project, the creation of a tracking defect on a paper insulation sample was attempted. In order to create the defect on the surface of a paper sample the set up which is presented in Figure 4.34 was built. The set up consists of:

- a) A high voltage transformer
- b) A  $1\text{k}\Omega$  resistance connected in series with the paper sample
- c) A needle at high voltage which was touching the surface of the paper sample at an acute angle.

#### 4 Small-scale experiments: Part 1

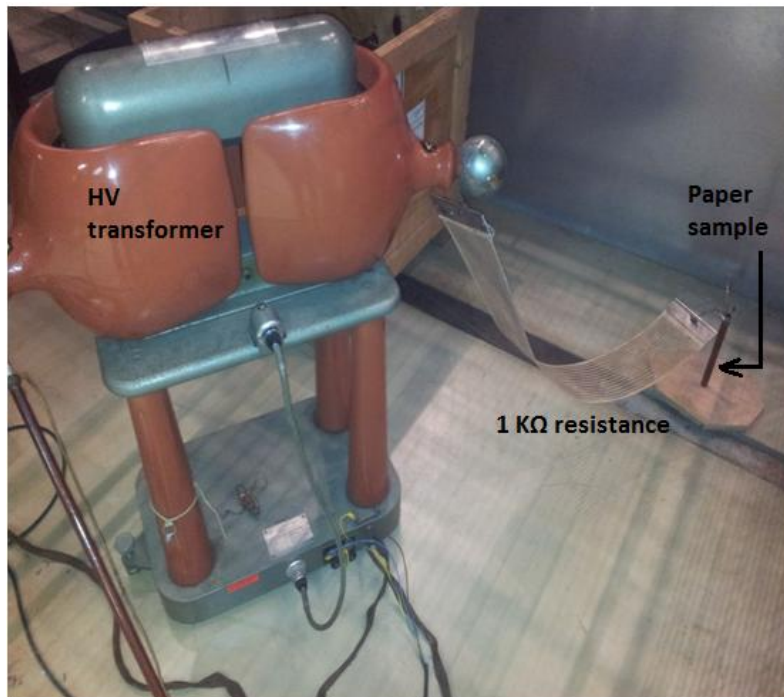


Figure 4.34. The set up for the creation of tracking.

The transformer used in this experiment can provide up to 100 kV AC. The paper sample and the needle touching the surface are shown in Figure 4.35. The voltage that was applied was approximately 28 kV. The process was sped up by scratching the surface and by frequently spraying the paper sample with salt water. Contamination of the surface with water and salt is known to lead to surface discharges and ultimately to tracking over the surface of solid insulating material [11]. In Figure 4.36, the carbonized conductive path that was created on the surface of the paper sample can be observed.

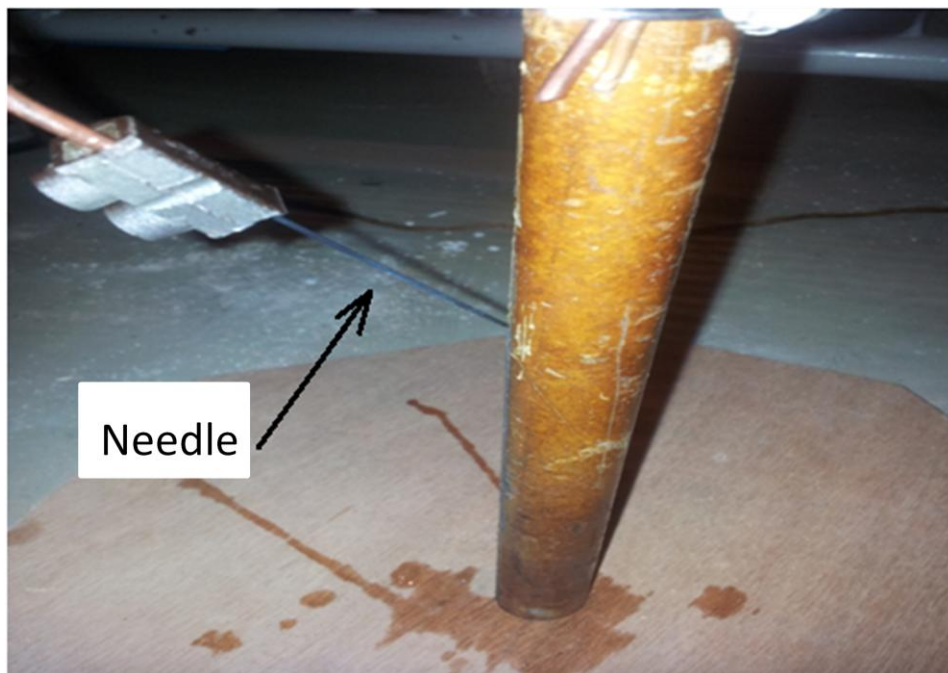


Figure 4.35. Paper sample and sharp needle touching at an angle.



#### 4 Small-scale experiments: Part 1

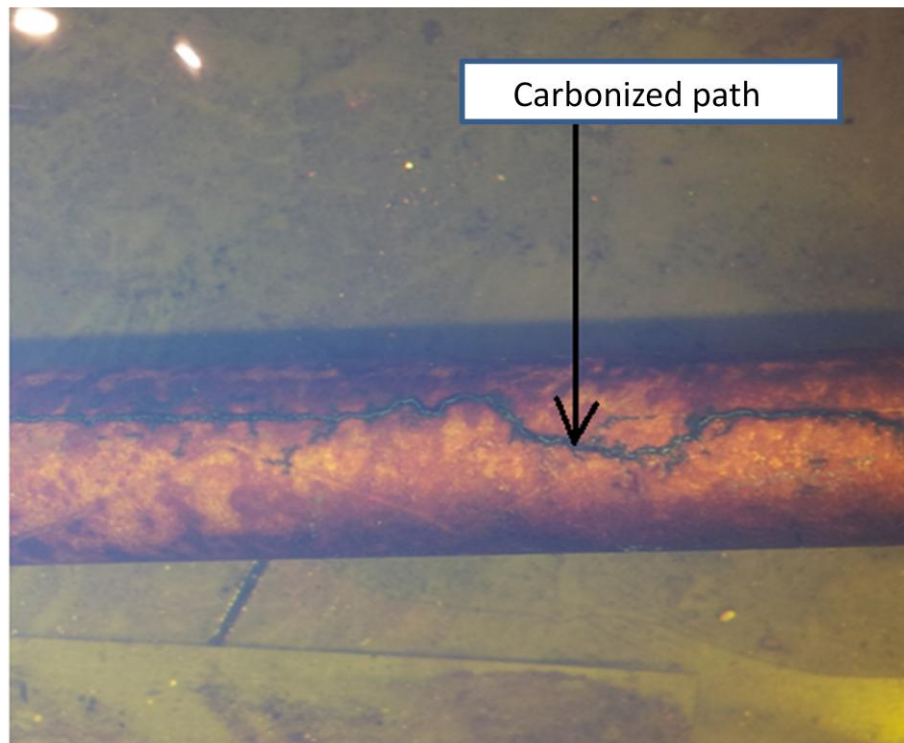


Figure 4.36. Carbonized path created on the surface of the paper sample.

The paper sample with the carbonized path was immersed in oil and via two ring electrodes a voltage was applied between the two sides of the paper tube, as presented in Figure 4.37.

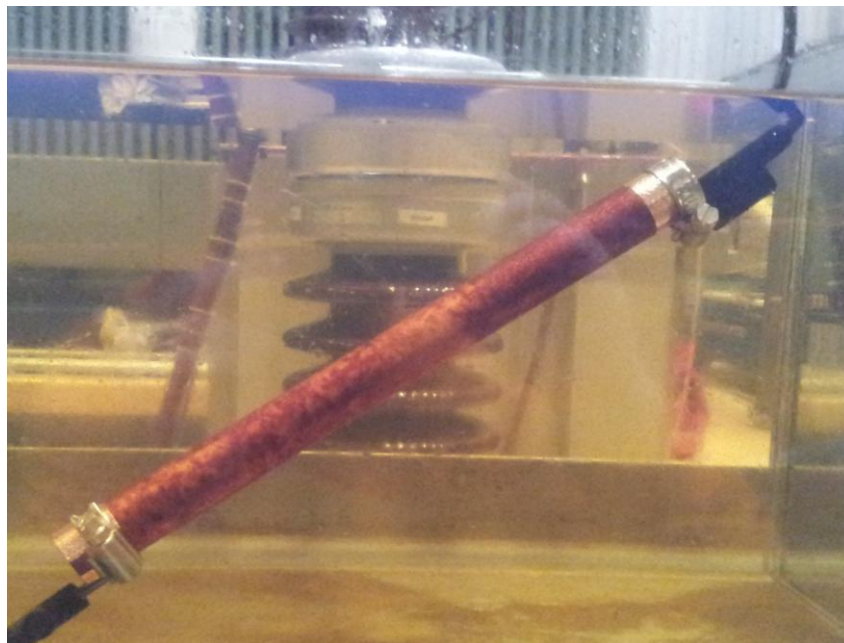


Figure 4.37. Testing the paper sample for PD activity.

The inception voltage of the PD activity was 14 kV. The PRPD pattern of the PD pulses for different voltage levels are presented in Figure 4.38.

#### 4 Small-scale experiments: Part 1

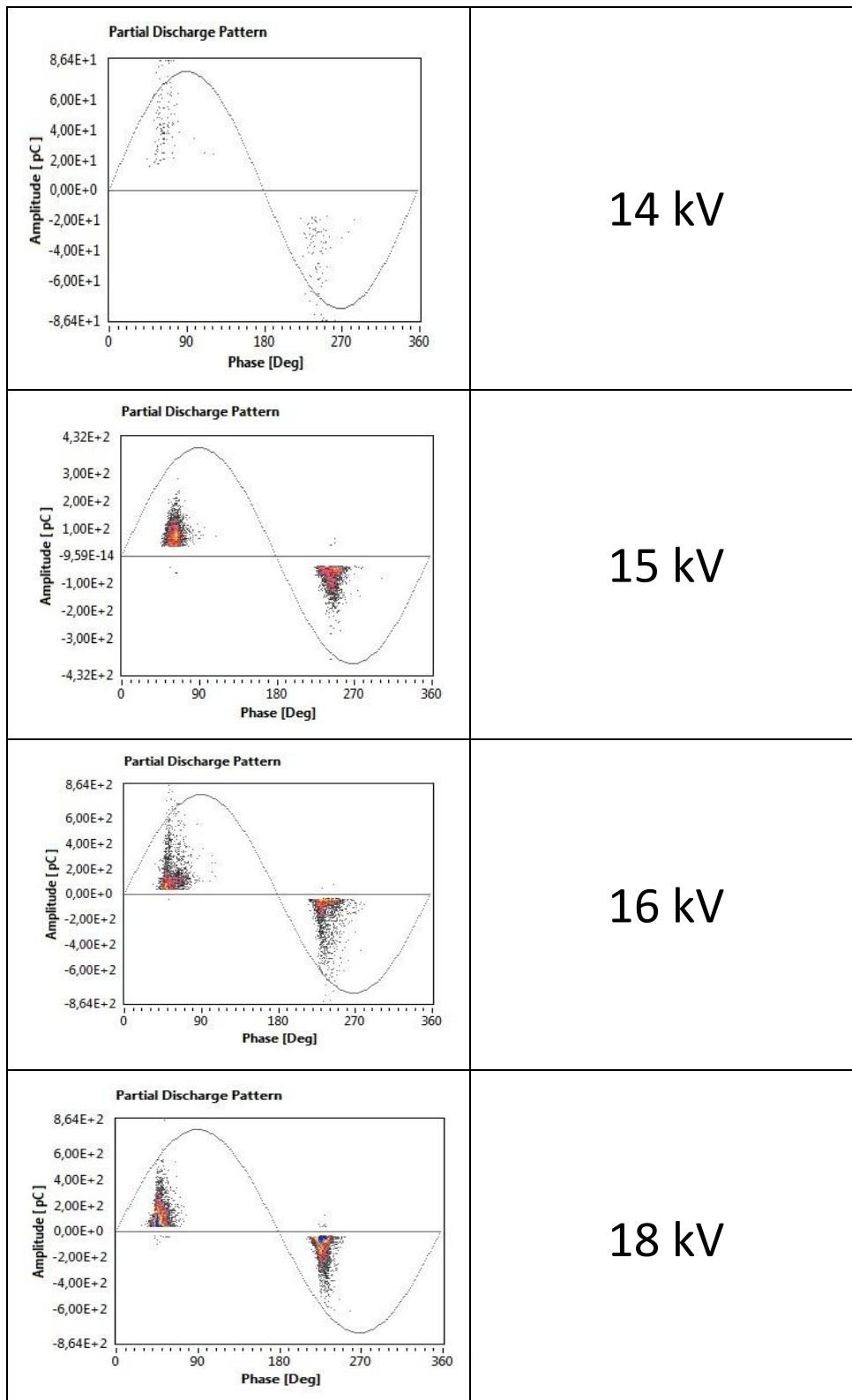


Figure 4.38. The PRPD pattern of the pulses.

The patterns of Figure 4.38 are symmetrical and located between  $30^{\circ}$  and  $60^{\circ}$  in the positive cycle of the voltage and between  $120^{\circ}$  and  $150^{\circ}$  in the negative cycle of the voltage. As expected, the pattern of the PD pulses that occur due to the

#### 4 Small-scale experiments: Part 1

tracking defect on the surface of the paper sample is similar to a pattern created by surface discharges.

The pattern of the PD pulses could depend on the shape and the conductivity of the path. Different patterns can be created by conductive or semi-conductive carbon paths. In addition the shape of the carbonized path could lead to different obtained patterns of the PD pulses. In this experiment, the path that was formed on the paper sample was straight without any branches. This could mean that the discharges originated from only one spot of the path. The trending of the PD activity over time and applied voltage is presented in Figure 4.39. The red line of Figure 4.39 corresponds to the repetition rate and the blue line corresponds to the PD magnitude. The values of the repetition rate and PD magnitude for the different voltage levels are presented in Table 4.11.

During the experiment, for a test voltage of 18 kV, it was observed that the discharges stopped after some time. Then the PD activity reappeared. In addition, the repetition rate and the magnitude of the discharges dropped as shown in Figure 4.39 and Table 4.11.



Figure 4.39. Trending of the PD pulses.

Table 4.11. Repetition rate and PD magnitude over the applied voltage.

Voltage [kV]	Repetition rate [Pulses/Period]	PD magnitude Qmax 95% [pC]
14	0.004	90
15	1	147
16	10	413
18	6	280



### 4.2.2.4 Gas bubbles in oil

During the operation of the tap changer, electrical arcs are created and extinguished in the insulating oil as described in chapter 2. As a result, gas bubbles are formed in the oil. The tap changer is equipped with a special vent which removes the gas from the tap changer. Nevertheless, gas bubbles can be found between the contacts of different phases where the electric field is larger. Gas bubbles in high electric fields can lead to PD activity. In this part of the research project, the probability of PD activity in gas bubbles present in the oil of the tap changer is investigated. To simulate the effect of gas bubbles in the oil of the tap changer, the test cell of Figure 4.40 was used.

The purpose of this experiment is to present the PRPD patterns that can be expected when gas bubbles that are formed in the oil of the OLTC are found in areas of high electric field. A test cell was used because the dimensions of the gas bubble are known and well defined. The change of the PRPD pattern in respect to the applied voltage can be well observed in this case because the bubble is trapped in the epoxy resin and cannot escape as is the case in oil. In addition, if a spherical gas bubble is considered then the permittivity of the material does not considerably affect the enhancement factor (see [33]). The small difference in the enhancement factor caused by oil and by epoxy resin would only affect the inception voltage of the discharges. The small change in the inception voltage between gas bubbles in oil and the bubble in the epoxy resin used in this experiment is not significant because as mentioned before, the purpose of the experiment is to present possible PRPD patterns that can be obtained when measuring PD activity in gas bubbles in the oil of the OLTC. For all the above mentioned reasons, the test cell of Figure 4.40 satisfies and complies with the purposes of this experiment.



Figure 4.40. Gas bubble in epoxy resin.

The test cell was placed in oil to avoid unwanted surface discharges on the outside part of the epoxy and or other types of unwanted discharges, such as corona discharges in air. The PRPD patterns of the pulses are presented in Figure 4.41. The patterns of Figure 4.41 were obtained by using the IEC 60270 detection mode. The PRPD patterns, as well as the classification map of the pulses, as obtained by using the WB detection mode are presented in Figure 4.42.

#### 4 Small-scale experiments: Part 1

Because of the large magnitude of the discharges (see Figure 4.41) and the fact that the system was not calibrated in the WB detection mode, saturation of the PD detector when using the WB detection mode appeared during the measurements. To solve this problem the connection of the HFCT sensor to the PD detector was done using two attenuators. The amplitude of the signal was thus decreased by a hundred times (see Figure 4.42).

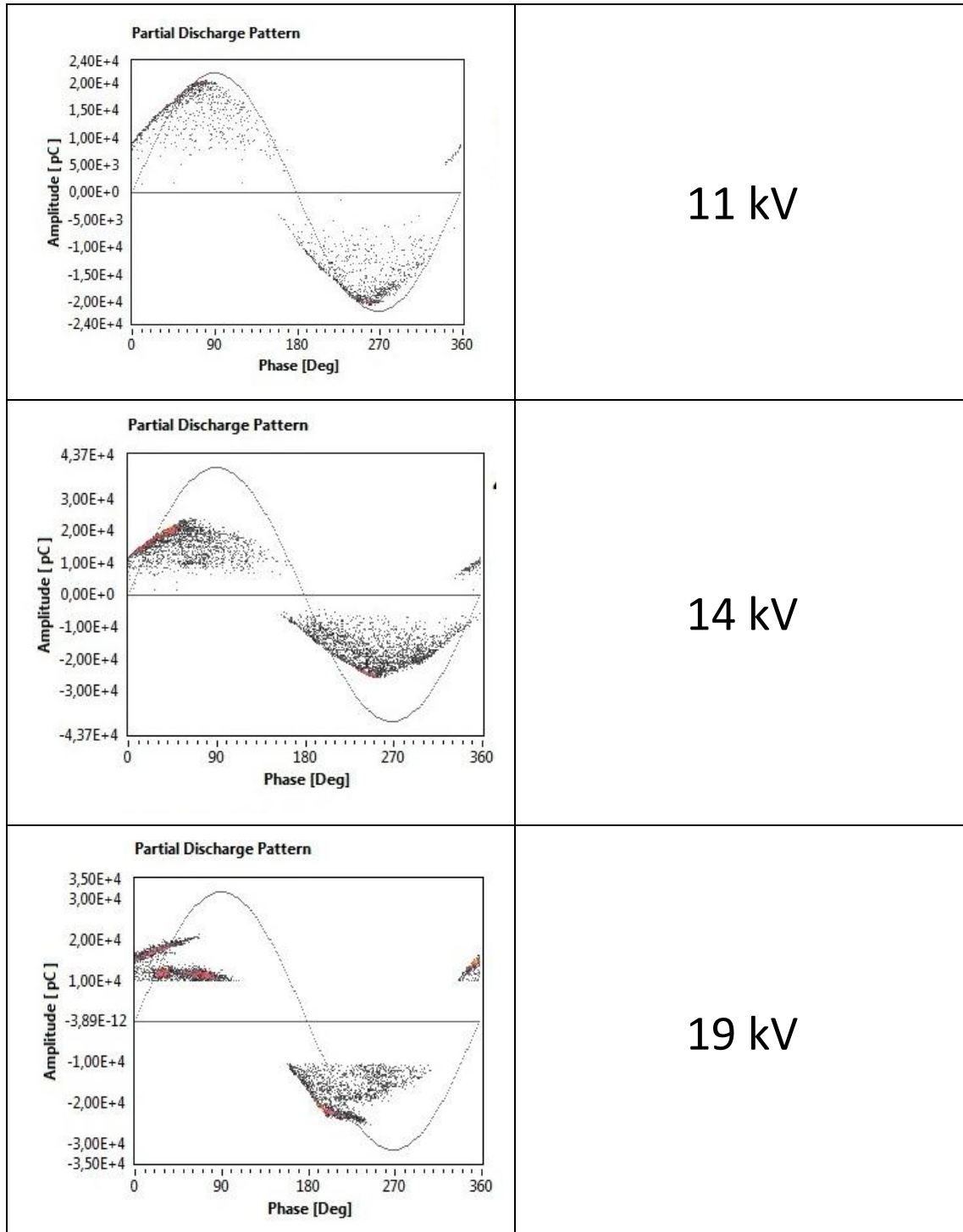


Figure 4.41. The PRPD patterns of the pulses obtained for different voltage levels in IEC detection mode.

#### 4 Small-scale experiments: Part 1

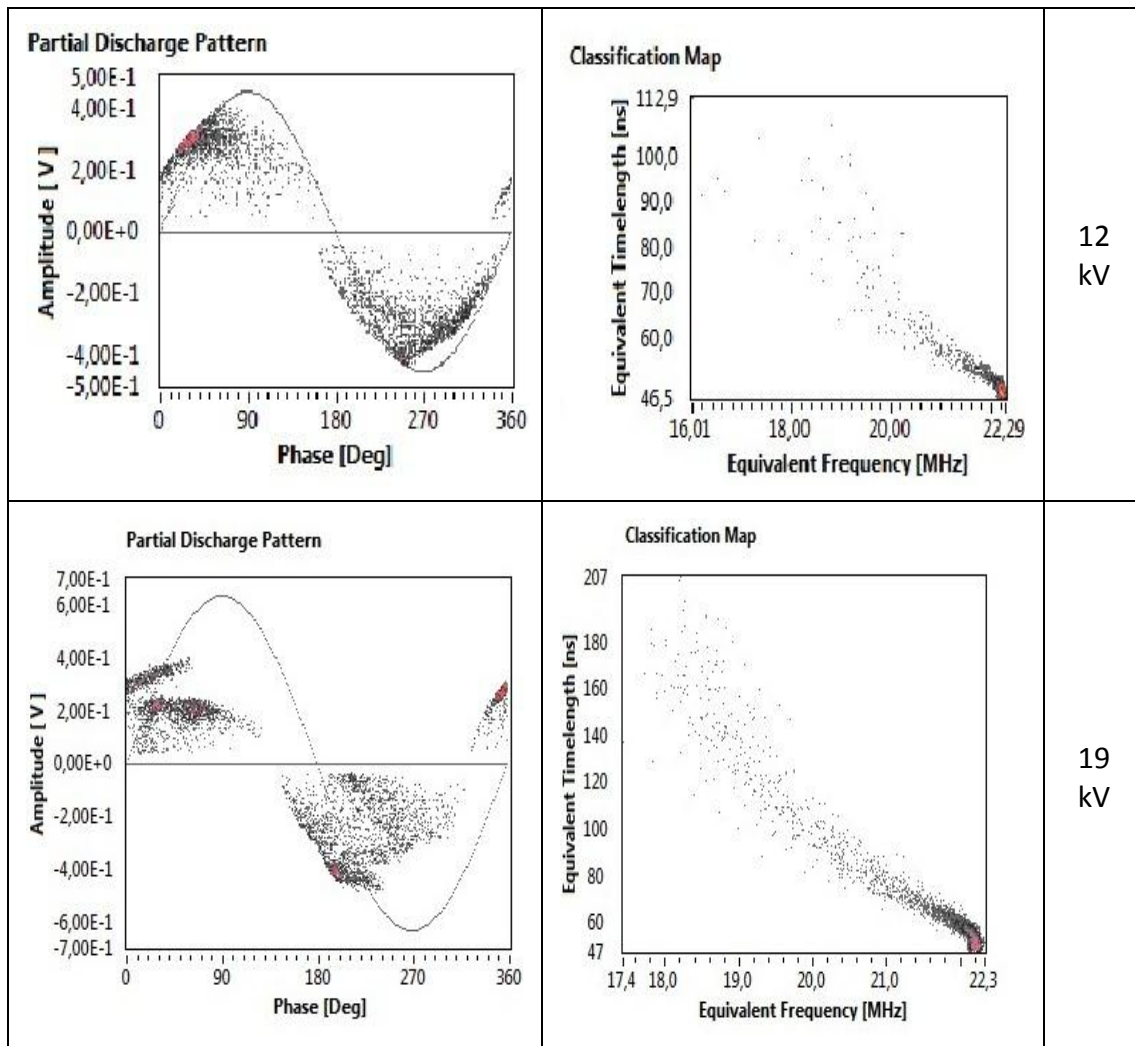


Figure 4.42. The PRPD pattern of the pulses obtained for different voltage levels in WB detection mode and the obtained classification (TF) maps of the pulses.

The patterns presented in Figure 4.41 and 4.42 are symmetrical in the positive and negative cycle of the applied voltage. In addition, the PRDP pattern also follows the sinusoidal voltage shape as it is also described in [31]. The pattern extends almost through the whole period of the voltage. The position of the void with respect to the electrodes affects the PRPD pattern and the PD activity as stated in [32]. The gas bubble is placed exactly at the middle between the two electrodes. The symmetrical behavior of the PRPD pattern is expected due to the position of the gas bubble in respect to the electrodes as explained in [31]. In [32] the effect of the position of the gas bubble in respect to the electrodes and the effect of the electrode configuration on the PRPD patterns is thoroughly presented. The trending of the PD pulses over time and applied voltage is presented in Figure 4.43 and Table 4.12 presents the exact values of the repetition rate and the PD magnitude for the different voltage levels.

#### 4 Small-scale experiments: Part 1

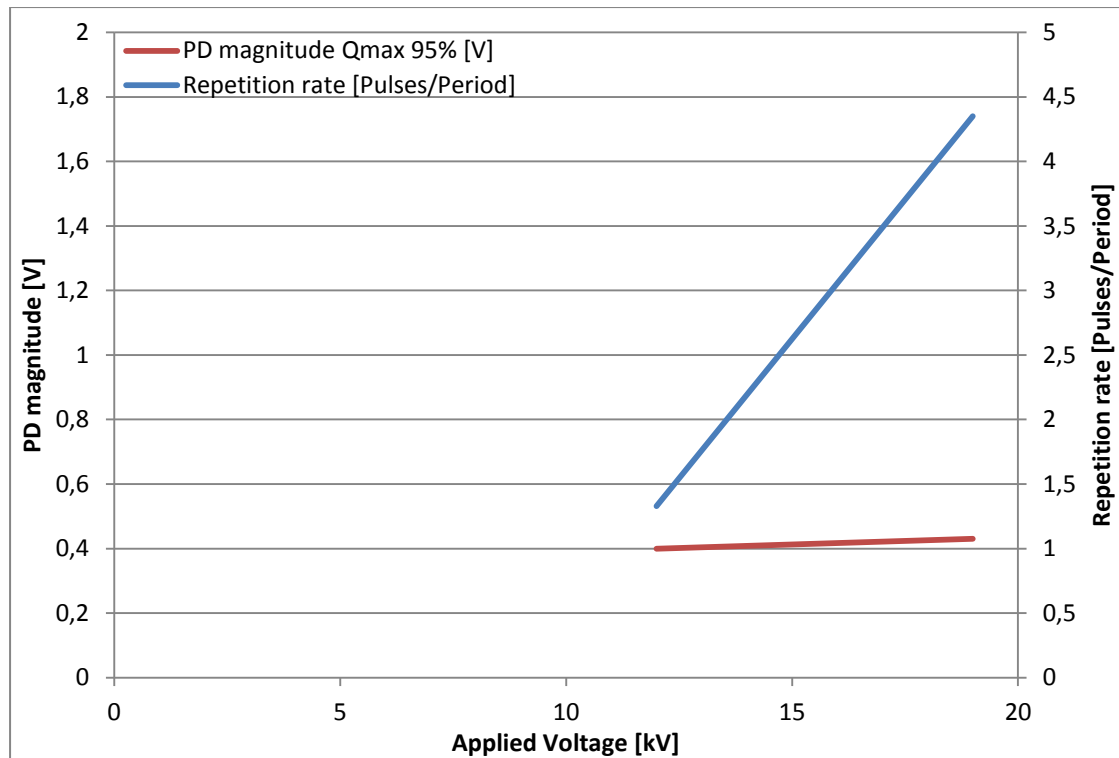


Figure 4.43. The trending of the PD pulses over the applied voltage.

Table 4.12. Repetition rate and PD magnitude for different voltage levels.

Voltage [kV]	Repetition rate [Pulses/Period]	PD magnitude Qmax 95% [mV]
12	1.33	400
19	4.35	430

The increase in the voltage level leads only to an increase in the repetition rate as shown in Figure 4.43 and Table 4.12. The magnitude of the discharges remains almost the same. This can be explained by the behavior of the discharge in the gas bubble. The gas bubble has a specific volume which ultimately determines the magnitude of the discharge. As a result, the magnitude of the discharges is not affected by the increase in voltage. Increasing the voltage and thus the electric field inside the gas bubble only affects the repetition rate of the discharges. The identification of the PD source as obtained by PDBasell is presented in Figure 4.44. The PD detector correctly classifies the source as internal discharges.

#### 4 Small-scale experiments: Part 1

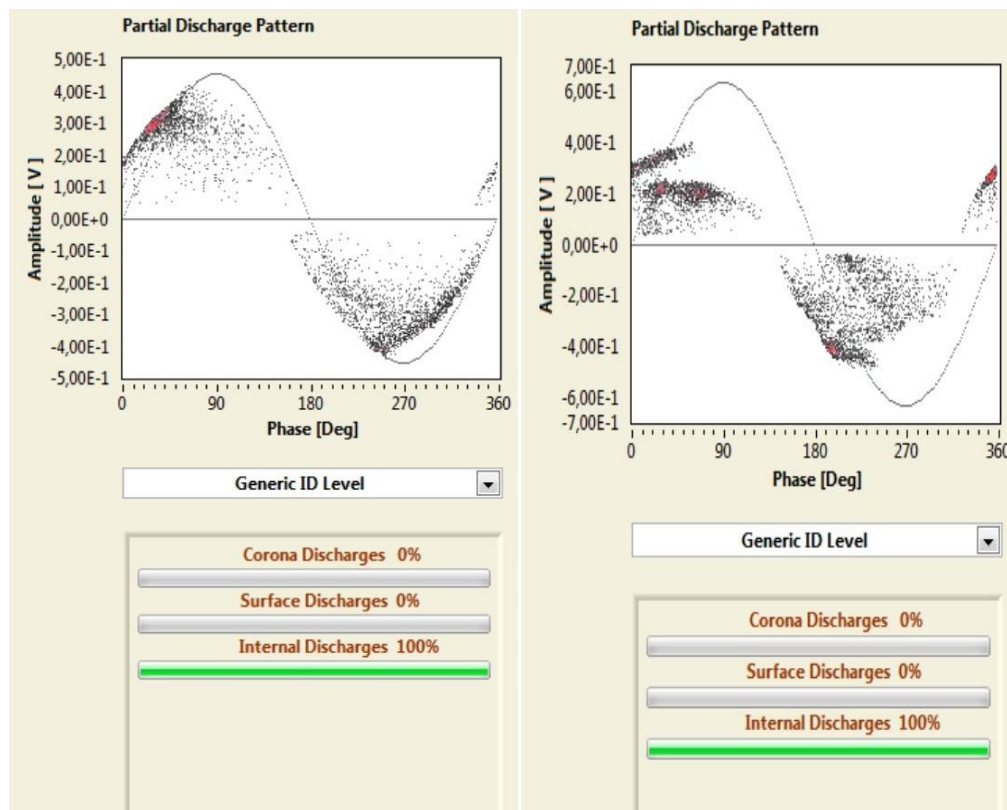


Figure 4.44. Identification of the PD source.

On the other hand, as stated in [8], PD activity in gas bubble in oil is less severe than PD activity which involves the paper insulation. A gas bubble present in the paper insulation can lead to faster degradation of the insulation. Gas bubbles in the paper insulation can initiate treeing mechanisms which can cause larger damage to the insulation. The formation of gas bubbles in the insulating oil of an OLTC is not an abnormality when the tap changer is under normal operating conditions. Gas bubbles in the oil of the OLTC cannot be considered as a defect. Nevertheless, increased PD activity caused by gas bubbles in oil could be used to provide information about the arcing process. Increased PD activity originating from gas bubbles in the oil could mean extended arcing periods during the transition from one tap position to another. To investigate the probability of PD inception in gas bubbles in the oil of the tap changer, the minimum electric field that is required to cause PD activity in a spherical gas bubble must be calculated.

A spherical gas bubble consisting of air is considered inside the oil of the tap changer. The permittivity of the oil is  $\epsilon=2.5$  and the permittivity of air is  $\epsilon_0=1$ . The spherical gas bubble is located in an area where the electric field is  $\mathbf{E}$ . The electric field inside the spherical gas bubble will be:

$$\mathbf{E}_{\text{sph}} = \frac{3\epsilon}{1+2\epsilon} \mathbf{E} \quad , \quad [33]$$

## 4 Small-scale experiments: Part 1

where  $\beta = \frac{3\varepsilon}{1+2\varepsilon}$  is the enhancement factor. The electric field inside the spherical gas bubble will be  $E_{sph} = 1.25 \times E$ . If the size of the bubble is 1 mm diameter and the pressure of the gas is 1 bar and by taking that the breakdown strength of air for the assumed dimensions and pressure of the bubble according to the modified Paschen curve is approximately 3.2 kV/mm, then the field that is required to initiate discharge activity in the gas bubble is  $E = 3.2/1.25 = 2.56 \text{ kV/mm}$ . In that case PD activity originating from the spherical gas bubble could be initiated.

The required field strength to cause PD activity in a gas bubble of 1mm diameter is therefore 2.56 kV/mm. In addition, it must also be mentioned that the initiation of PD activity in a gas bubble requires the presence of a starting electron. The appearance of the starting electron is a random process which requires a significant amount of time. This process can take from seconds to almost an hour. Assuming that a spherical gas bubble of 1 mm diameter can be found in a high field region where the requirement  $E = 2.56 \text{ kV/mm}$  is fulfilled. The gas bubble should remain in this area for a significant amount of time in order to measure some PD activity inside the gas bubble. Gas bubbles in the oil of the tap changer are quickly removed via a special ventilation system. For the above mentioned reasons, it can be concluded that PD activity in gas bubbles in the oil would hardly be measured. Even if some activity in gas bubbles is measured, it would not be easily feasible to assess the arcing process occurring in the selector switch of the tap changer because the gases that are produced during arcing periods are removed from the OLTC. A comparison between PD activity appearing in gas bubbles created during normal arcing and PD activity appearing in gas bubbles created during excessive arcing cannot be easily performed.

### 4.3 Summary

The small scale experiments can provide valuable information about the PD activity that can be measured in a tap changer. In this chapter, the major defects that could lead to the appearance of PD activity were investigated. This chapter focused on simulating the major defects that can lead to PD activity in an OLTC. From the experiments that were conducted in a small scale set up, the most essential results are:

- 1) Corona discharges could appear in the tap changer in the extreme case of a broken resistor. PD activity could arise from sharp wires in the insulating oil of the OLTC. The results of the small scale experiments suggest that sharp wires in oil could more likely cause the appearance of PD activity in delta-connected tap changers where the voltage levels between contacts of different phases are large. In star-connected tap changers the electric field is not sufficient to lead to PD activity originating from sharp wires in

#### 4 Small-scale experiments: Part 1

the insulating oil because the voltage between different contacts of the OLTC is not large.

- 2) Gas bubbles in the oil do not constitute a defective operation of the tap changer. In the small scale experiments the behavior of the PD activity originating from gas bubbles in the oil was presented. From the small scale experiments, it is observed that the electric field strength in the tap changer is not high enough to cause the appearance of PD activity in spherical gas bubbles of 1mm diameter in star-connected tap changers ( $E \ll 2.56 \text{ kV/mm}$ ). In delta-connected tap changers PD activity in spherical gas bubbles of 1mm diameter could appear only if the gas bubble could be trapped for a significant amount of time in an area where the electric field is  $E > 2.56 \text{ kV/mm}$ . Even then the measured PD activity could not be used to assess the arcing process occurring in the selector switch of the OLTC.
- 3) Discharges occurring on the surface of the paper insulation can lead to the creation of the carbonized path (tracking) as discussed in chapter 2. Tracking on the paper insulation of tap changers is a dangerous defect which can cause failure of the power transformer. Star-connected tap changers are not prone to electrical tracking. The initiation of surface discharges requires a high tangential electric field at the surface of the paper insulating material. The electric field in star-connected tap changers is not sufficient in order to create tracking defects. Tracking defects can frequently appear in delta connected tap changers where the field can be large enough to cause PD activity on the surface of the paper insulating cylinder. The contamination of the surface by metallic particles enhances the tangential electric field over the surface and leads to creepage discharges. For that reason and according to experience, the maintenance of delta-connected tap changers is performed every three years whereas the maintenance of star-connected tap changers is performed every five years. Increased PD activity which can be identified as surface discharges and which occurs inside the tap changer can be used as a means of assessing the condition of the paper insulating cylinder. PD monitoring can be used as a diagnostic tool for the condition assessment of the paper insulation in the case of delta-connected tap changers and could prevent failures associated with tracking.

# 5

## Small scale experiments: Part 2

In this chapter, PD measurements that have been performed in a small single-phase tap changer are described. The experiments were initially performed in air. Following that, the single-phase tap changer was placed in a metallic drum which was filled with transformer oil. The metallic drum served as the metallic enclosure of the OLTC. The major insulation defect of on-load tap changers is tracking on the surface of the paper insulating cylinder, as discussed in chapter 4. This defect can frequently appear in delta-connected tap changers. For that reason, this chapter focuses on the measurements of surface discharges which can lead to tracking. The process by which tracking is created is examined. In addition, in the second part of chapter 6, a comparison between partial discharge detection by electrical sensors and partial discharge detection by acoustic sensors is presented. The purpose of this comparison is to investigate which is the most suitable detection method regarding PD measurements in an OLTC.

### 5.1 Single-phase tap changer

#### 5.1.1 Testing in air

A small scale experiment was designed with a single phase tap changer. The single-phase tap changer consists of 9 contacts. The distance between two adjacent contacts is approximately 60 mm. The single-phase tap changer is presented in Figure 5.1.





Figure 5.1. The single-phase tap changer. Outside part (left) and inside part (right).

### 5.1.1.1 Test procedure

In the first part of the experiments the single-phase tap changer was tested in air. To create surface discharges without endangering the paper insulation of the tap changer, contacts with 120 mm distance were tested. This means that one contact was left to float between the other two contacts from which one was under high voltage and the other was grounded. A schematic diagram of the test set up is presented in Figure 5.2.

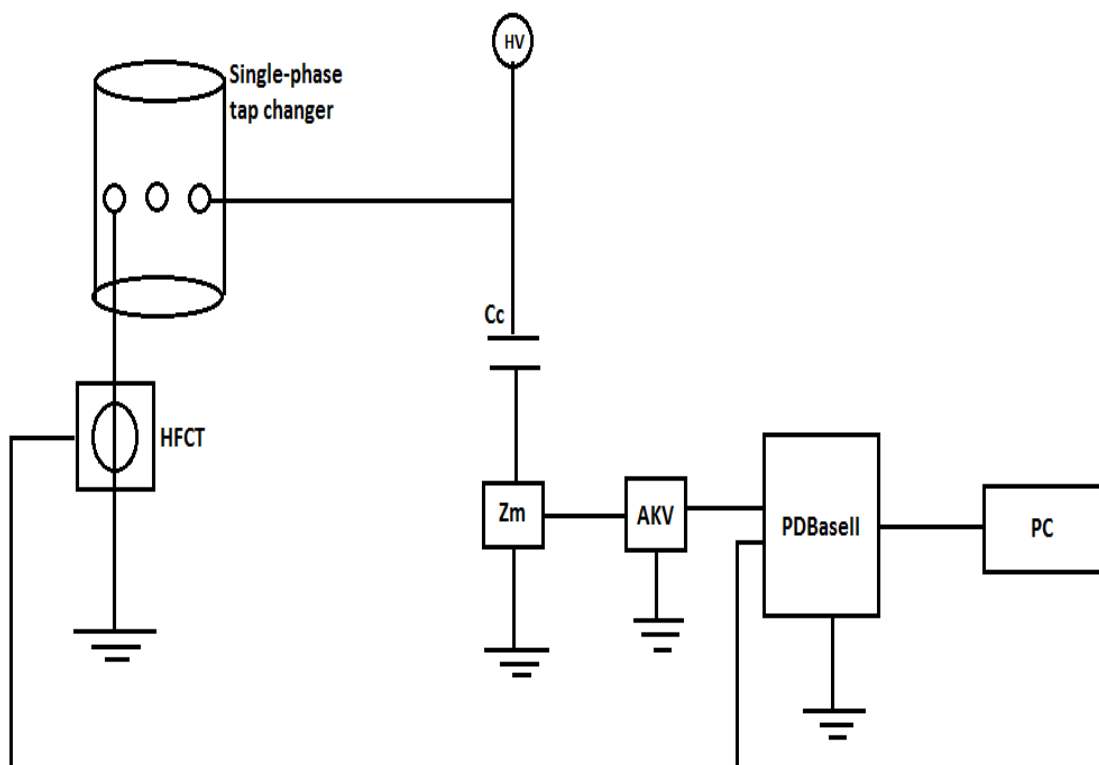


Figure 5.2. Schematic diagram of the test set up.

The AKV unit provides an output for the PD pulse created by the measuring impedance  $Z_m$ . In addition, the AKV unit was used for the voltage synchronization of PDBasell. This synchronization is essential in order to obtain the PRPD pattern. PD activity appeared at 5.3 kV. The PRPD pattern of the pulses is presented in Figure

## 5 Small-scale experiments: Part 2

5.3. The identification of the PD source provided by PDBasell is also presented in Figure 5.3. The acquisition mode that was used in this experiment was IEC 60270.

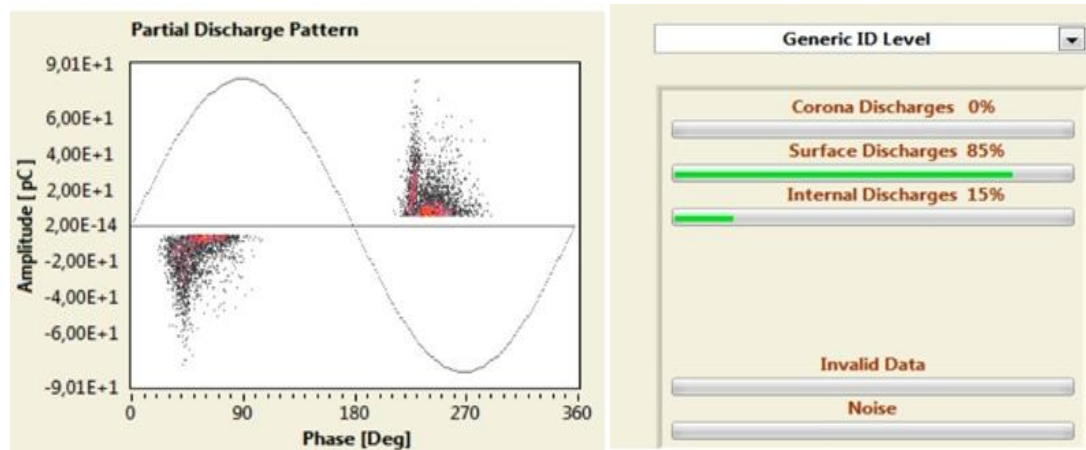


Figure 5.3. PRPD pattern of the pulses and PD source identification.

It must be noticed that the pattern has the opposite polarity than normal. In the HFCT sensor, an arrow indicates the direction of the output voltage in comparison to the direction of the input current. When the sensor is installed, the arrow must be directed towards the ground. In that case the detected voltage signal has the same phase with the input current [34].

The PRPD pattern of Figure 5.3 was obtained with the arrow of the HFCT sensor directed to the opposite direction from the ground. The PRPD pattern of Figure 5.3 is symmetrical for the positive and the negative half cycle of the voltage. The discharges occur before the voltage peaks both in the positive and the negative half cycle of the voltage. In addition, the scatter in the PD magnitudes is large. The characteristics of the PRPD pattern correspond to a pattern created by surface discharges. The experiment that was performed in air was a preliminary stage before the tap changer was placed in oil. This experiment was held as a first stage experiment to investigate the effect of the insulating oil on the PD activity of the tap changer.

### 5.1.2 Testing in oil

#### 5.1.2.1 Test procedure

The single-phase tap changer was later placed in a metallic drum which was filled with transformer oil. A needle was used to create surface discharges on the surface of the paper insulation of the tap changer. The needle was attached to one of the contacts and touched the paper insulation at an acute angle. The contact where the needle was attached was at high voltage. One of the adjacent contacts was grounded. The set up is presented in Figure 5.4.

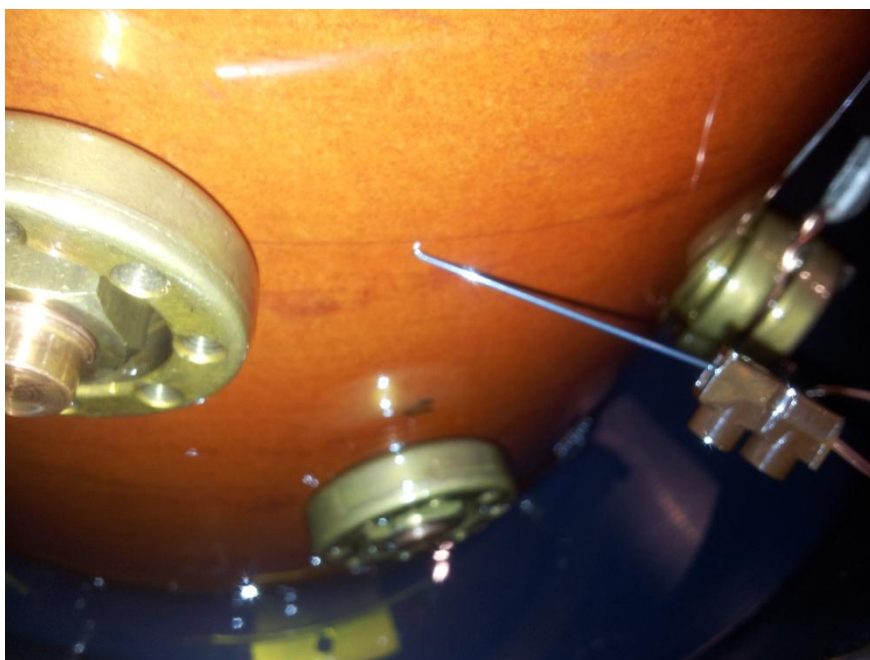


Figure 5.4. Test set up.

The distance between the point where the needle touched the paper insulation and the grounded contact was 25 mm. The acquisition was performed by using the WB detection mode and thus the set up was not calibrated. Discharges appeared at approximately 40 kV. The magnitude and the repetition rate of the PD pulses are presented in Table 5.1. The PRPD patterns at the different voltage levels are presented in Figure 5.5. Figure 5.6 presents the trend of the magnitude and the repetition rate of the PD pulses over the applied voltage.

Table 5.1. PD magnitude and repetition rate over the applied voltage.

<b>Voltage level [kV]</b>	<b>PD magnitude Q<sub>max</sub> 95% [mV]</b>	<b>Repetition rate [Pulses/Period]</b>
41	65	5
45	80	4
50	85	5.5
55	53	6

## 5 Small-scale experiments: Part 2

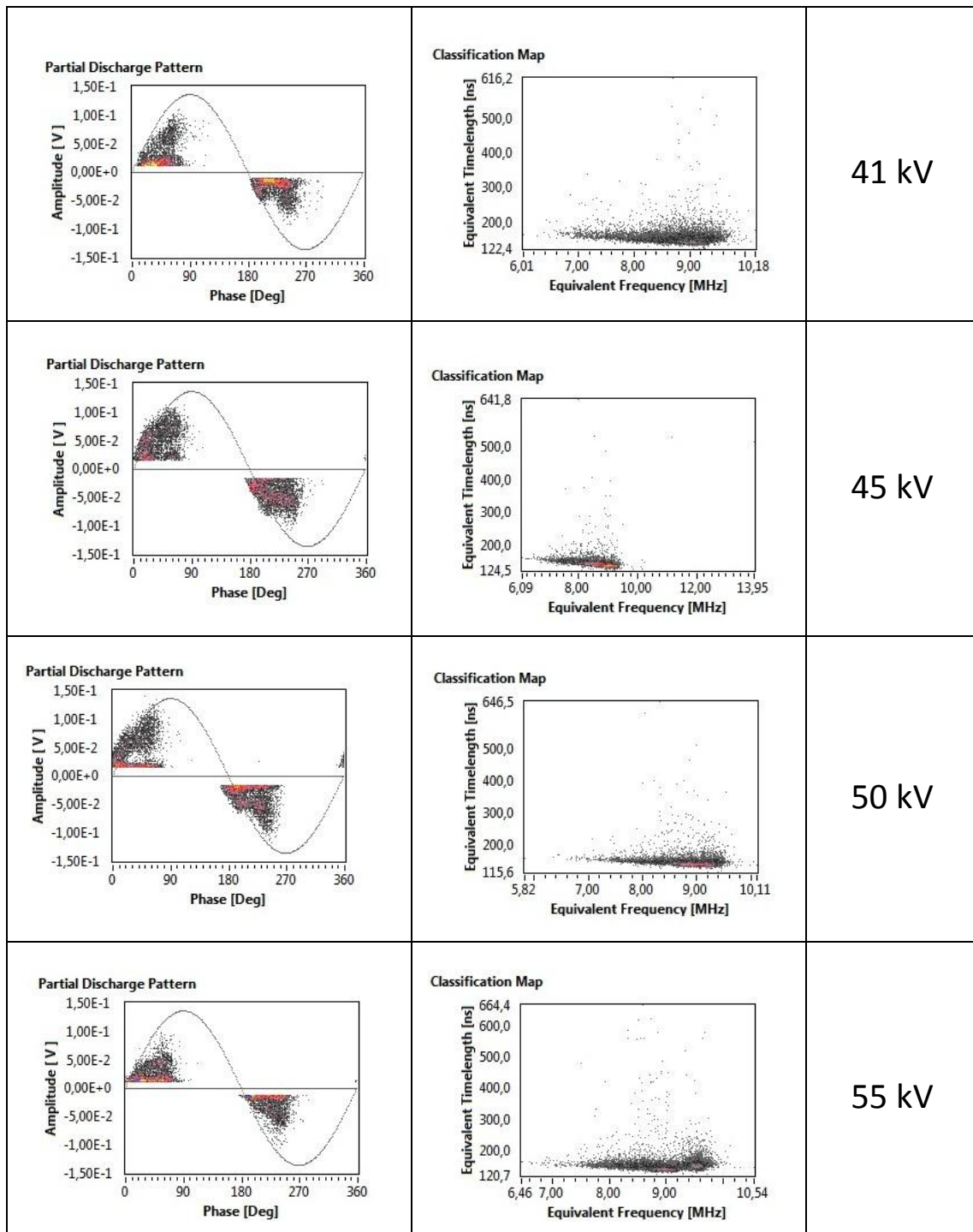


Figure 5.5. The PRPD pattern of the pulses.

## 5 Small-scale experiments: Part 2

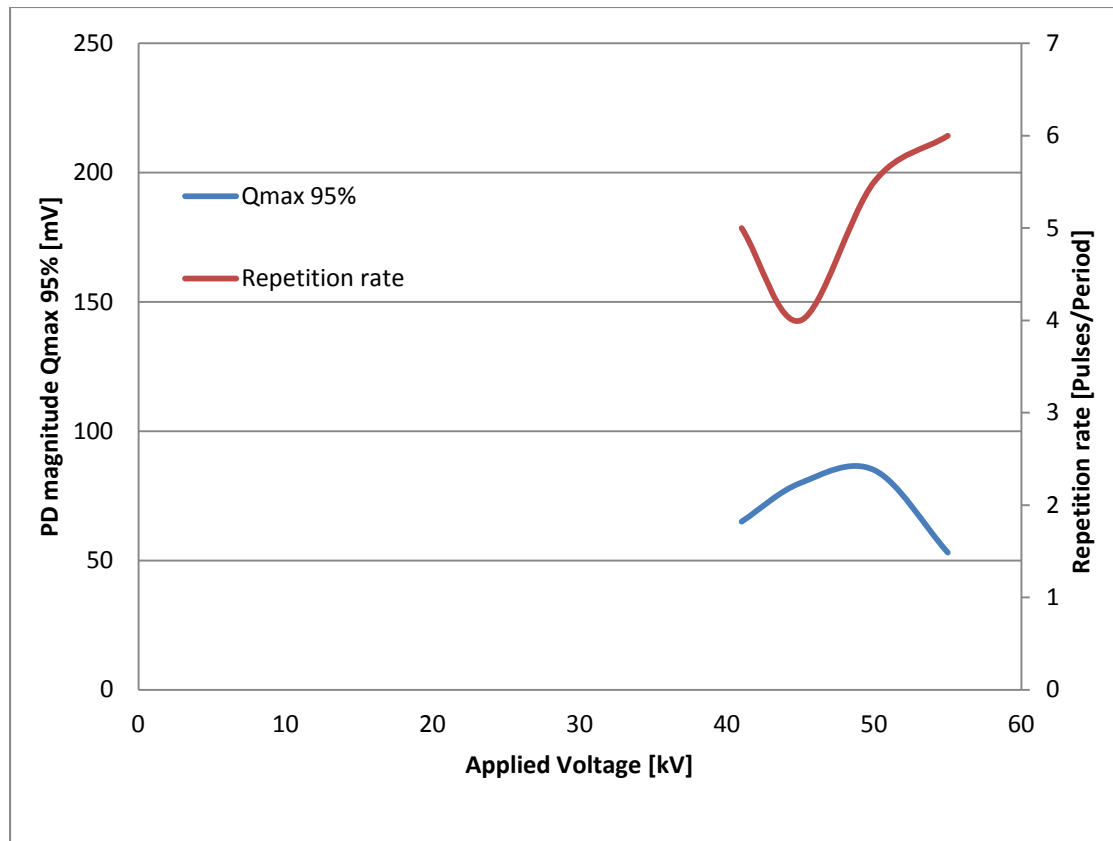


Figure 5.6. Repetition rate and PD magnitude over the applied voltage.

The defect that was introduced in the single-phase tap changer was a needle which touched the paper insulation at an acute angle. A schematic diagram of the set up is presented in Figure 5.7.

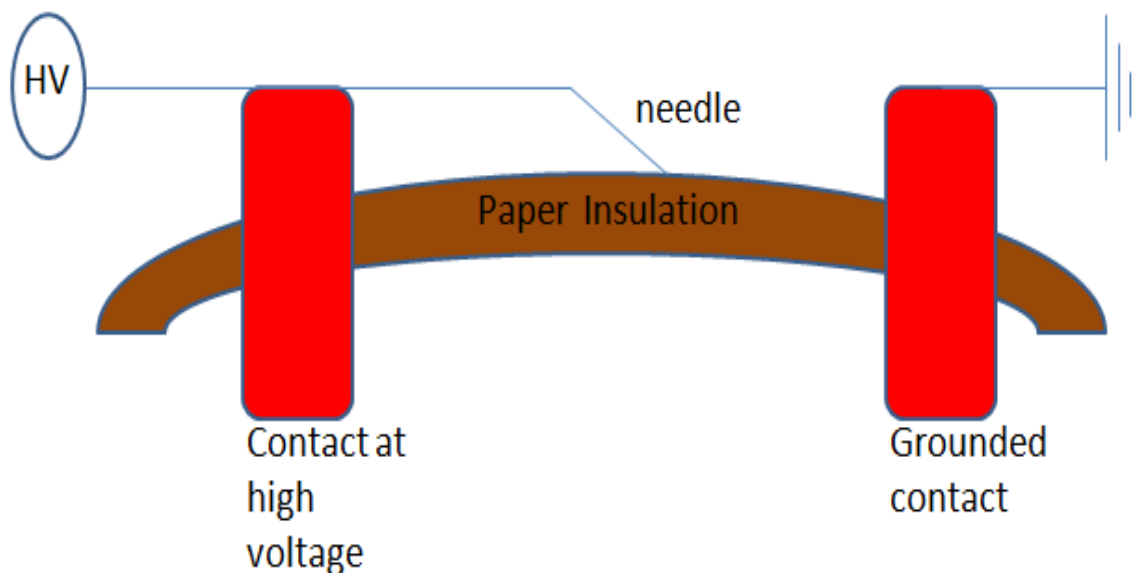


Figure 5.7. Schematic diagram of the set up.

The contacts go through the paper insulation as shown in Figure 5.7. As a result, the paper insulation is stressed by the electric field also internally and not

## 5 Small-scale experiments: Part 2

only on the surface. Therefore, the possibility of internal cavities as a potential PD source cannot be ignored. The pattern of Figure 5.5 looks like a mixture of internal and surface discharges. The TF map confirms that there is only one cluster of discharges. Therefore, there is only one source which causes the PD activity. The introduced defect should create a strong field over the surface of the paper insulation. Nevertheless, a cavity in the paper insulation could be regarded as a possible source of the partial discharge activity. For that reason, the electric field which stresses the paper insulation internally should be minimized, whereas the electric field over the surface of the paper insulation should be maximized. To limit the electric field strength inside the paper insulation the set up of Figure 5.8 was devised.

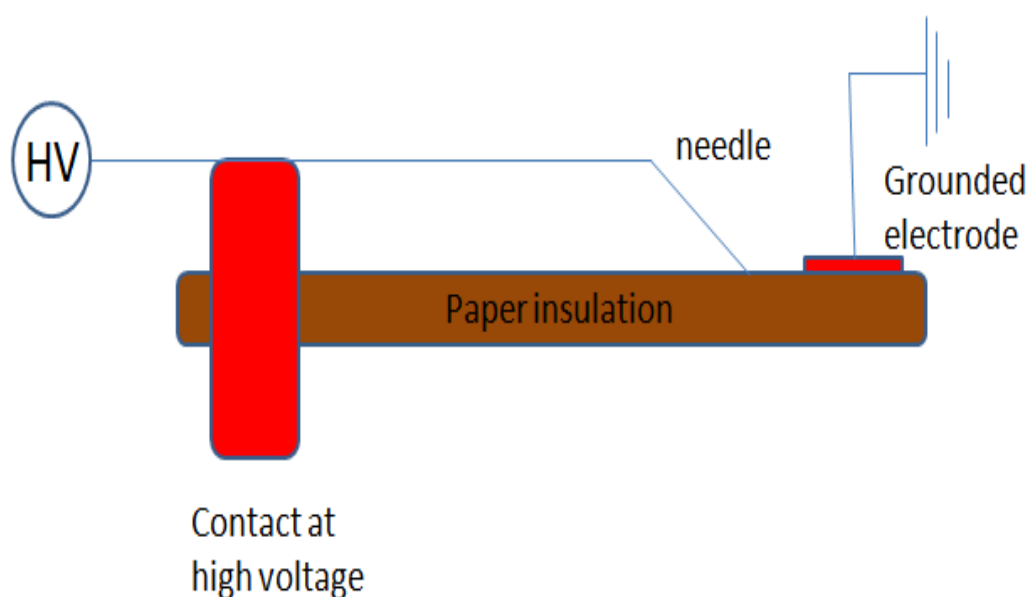


Figure 5.8. Set up to reduce the E field inside the paper.

As shown in Figure 5.8, the grounded contact has been replaced by a surface grounded electrode. The thickness of the bar is approximately 1.5 mm. In addition the contact which is connected to the high voltage is located 20 cm away from the grounded bar. The distance between the point where the needle touches the paper insulation and the grounded bar is approximately 10 mm. The patterns obtained in this experiment are presented in Figure 5.9.



## 5 Small-scale experiments: Part 2

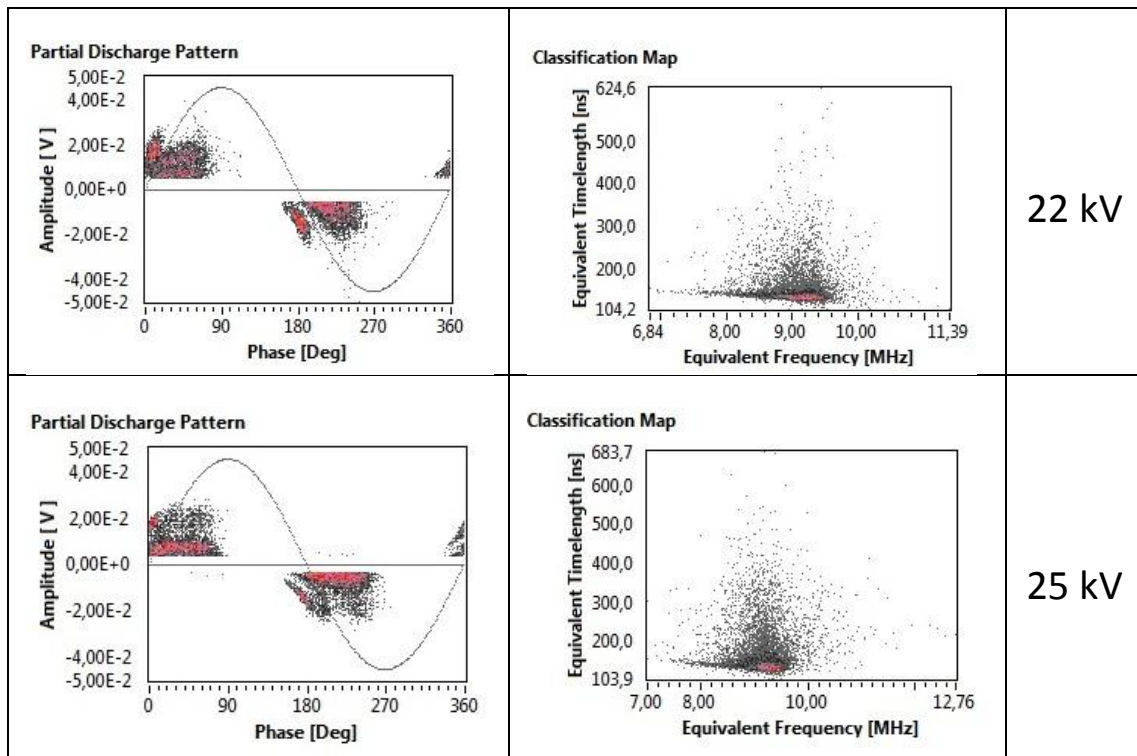


Figure 5.9. The PRPD pattern of the pulses.

An important observation was obtained during the experiments. At 25 kV and after a short period of time a flashover occurred. After inspection of the test set up, black spots were observed on the paper insulation as presented in Figure 5.10.

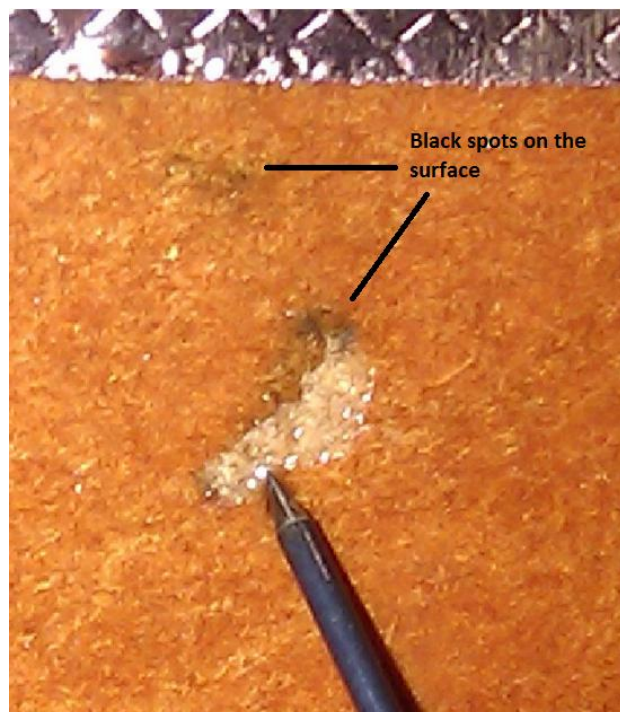


Figure 5.10. Black spots on the surface of the paper insulation.

The black spots that are created on the surface of the paper insulation are carbonized marks. The carbonized marks eventually create a conductive or semi-conductive carbon path over the surface of the paper insulation. This process is

called tracking. The process by which tracking is created in on-load tap changers can be explained as follows: The surface of the paper insulation of an OLTC can become contaminated by oil ageing by-products or more frequently by conducting particles. The conducting particles are present in the OLTC due to the contact wear after every tap selection process. The conducting particles can accumulate on the surface and can cause a significant distortion of the electric field over the surface of the paper insulation. The distortion of the field can lead to the appearance of creepage discharges. A creepage discharge is a surface discharge in the oil of the tap changer across the paper insulation. The characteristics and the features of creepage discharges will be determined by the materials which are affected, namely, the cellulose of the paper insulation and the oil insulation [35].

If the energy of the discharges is high enough, the molecules of the oil and the paper can be split and carbon by-products are formed. The burning of the paper and the oil due to the discharges, leads to deposition of carbon on the surface of the solid insulation. The dielectric strength of the solid insulation is reduced and the PD inception voltage is lower. The creepage discharges keep afflicting the paper insulation, thus leading to the elongation of the carbonized path. The path is elongated until the point when a large distance of the insulating paper between two contacts of different phases has been bridged. The remaining insulation distance is not sufficiently strong to withstand the applied voltage and a flashover between the contacts will occur. An important parameter which affects the process of creepage discharges is moisture. According to [35], moisture can decrease the PD inception voltage, thus, increasing the PD activity.

The visual inspection of the set up strengthens the assumption that the partial discharge activity takes place on the surface and not inside a cavity of the paper insulation. By comparing Figure 5.5 and Figure 5.9, it can be observed that the TF maps of the obtained pulses are approximately equal. The frequency spectrum and the timelengths of the obtained pulses from the two different experiments are approximately the same. The larger dispersion observed in the TF map of Figure 5.9 could be created by the software of the PDBasell detector. In some cases the software could be incapable of calculating the correct timelength of the pulse. It was observed that when the repetition rate increased significantly, the acquisition window of the software sometimes had acquired more than one pulse as shown in Figure 5.11.



## 5 Small-scale experiments: Part 2

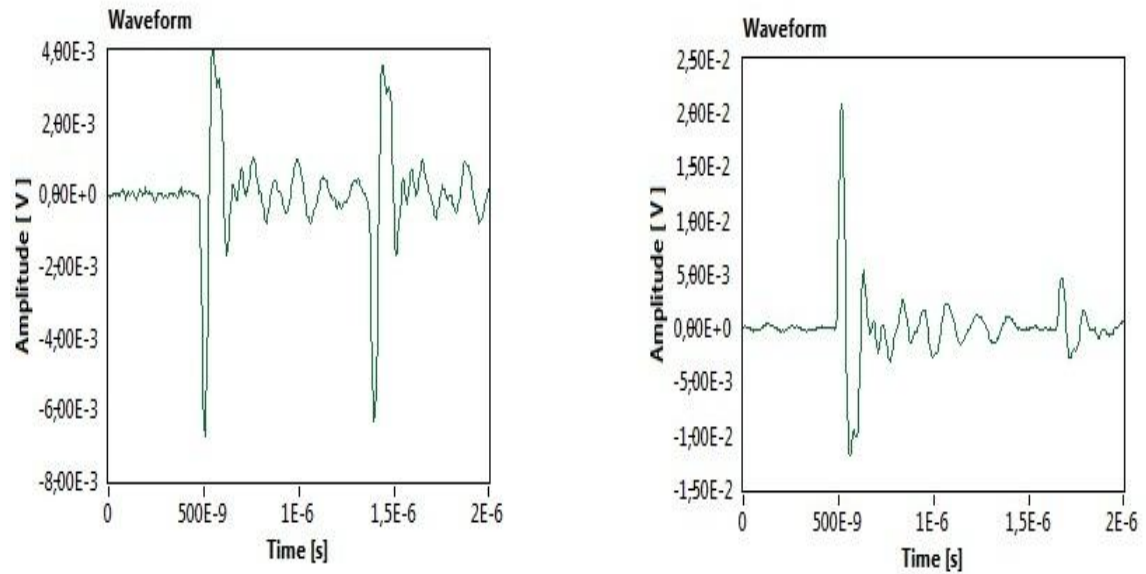


Figure 5.11. Pulse shape acquired in WB.

As shown in Figure 5.11, the acquisition window contains more than one PD pulses. In the cases where more than one pulse is displayed in the window, the timelength was not calculated correctly. The large dispersion in the timelengths of the pulses could have been the result of the discussed observation. The repetition rate over the applied voltage is presented in Figure 5.12.

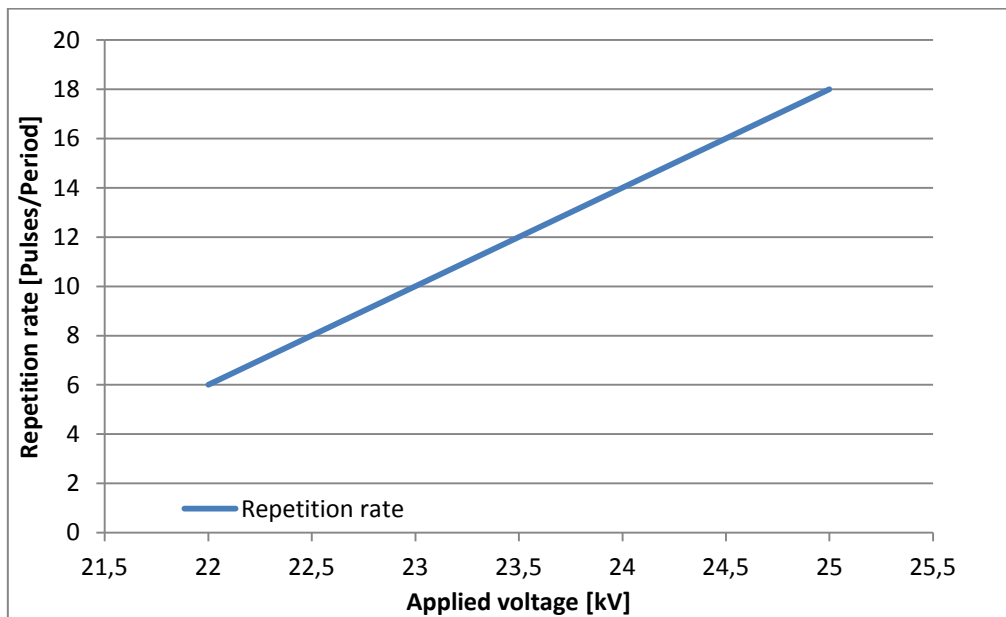


Figure 5.12. Repetition rate of the pulses obtained by the set up of Figure 5.8.

The repetition rate of the discharges is three times higher at 25kV than at 22 kV. The repetition rate increases from 6 pulses/period to 18 pulses/period. The increased repetition rate of the discharges could explain the creation of the black spots that were observed after breakdown.

The behavior of the pattern and especially the discharges at the zero voltage crossings could be attributed to the presence of space charge in the oil or in the paper insulation. The accumulation of space charge can alter the electric field over the surface. As a result, it could be possible that partial discharges also occur close or at the zero voltage crossings. The black spots that are observed in Figure 5.10 lead to the creation of tracking on the surface of the paper insulation. Tracking is a major insulation defect in delta-connected tap changers. Special consideration must be made in case of delta connected tap changers and especially when the line voltage is high.

### 5.2 Detection of the discharges

The major defects that can cause PD activity in an OLTC were discussed thoroughly. During the experiments, the detection of the discharges was performed by using electrical methods. The sensor that was used was the HFCT which must be connected to the grounding point of the equipment.

In Europe the OLTC is most frequently located in the same enclosure as the transformer. In addition, a resistor type OLTC is usually connected in the HV side of the transformer. The OLTC can be connected either in star or in delta, depending on the connection of the main transformer winding. Figure 5.13 presents the connection of on-load tap changers to star and delta connected windings. It is very important to locate the position where the discharge takes place. The location of the defect is important in order to decide the appropriate maintenance for the equipment.

In the case of star-connected tap changers, a common neutral for the OLTC and the transformer is built, as shown in Figure 5.13. The OLTC shown in Figure 5.13 (connections of the red arrows) which is connected to the star-connected winding (S1, S2, S3) of the transformer is placed at the neutral side of the transformer. The HFCT sensor can be placed at the grounding point of the common neutral of the OLTC and the transformer, as shown in Figure 5.13. This means that the HFCT sensor will detect PD activity that occurs both in the OLTC and the transformer. A separation of the discharges regarding their location is not possible when using the HFCT sensor. An HFCT sensor can provide information about the magnitude of the discharges and the PRPD pattern of the discharges but it cannot provide any information about the location of the PD source. The pattern can be used to identify the source of the discharges but not to locate the defect inside the complex system of the transformer and the OLTC. As a result, it can be concluded that the HFCT sensor is not the appropriate sensor to monitor the PD activity in star connected tap changers because discharges will be detected from both the power transformer and the OLTC without the possibility of separating the discharges that occur in the transformer from the discharges that occur in the OLTC.

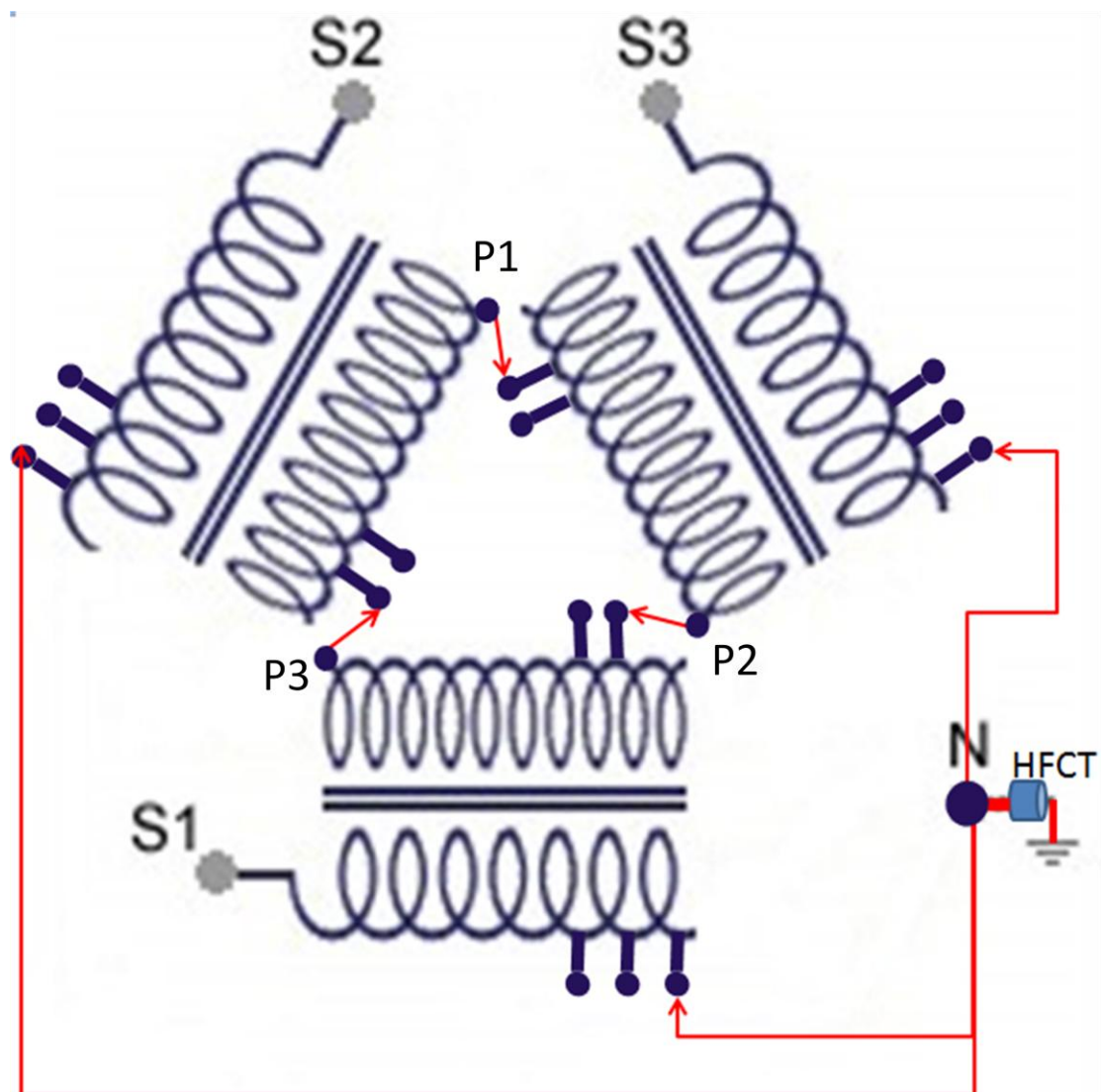


Figure 5.13. OLTC connection in star and delta connected windings.

A different type of problem occurs in delta-connected tap changers. PD activity can be initiated more frequently in delta-connected on-load tap changers. An OLTC connected to a delta-connected transformer winding (P1, P2, P3) is also presented in Figure 5.13. In delta-connected tap changers the grounding point is not present, as shown in Figure 5.13. As a result, the HFCT sensor cannot be used to detect PD activity occurring in the OLTC. Therefore, the HFCT sensor is not the best choice because in the case of delta-connected tap changers, interphase faults which can cause PD activity, like tracking, will not be detected by the HFCT sensors. A possible solution could be to place capacitive sensors at the bushings of the power transformer. The same problem as for star-connected tap changers would also appear in that case. PD activity can be detected from the OLTC as well as the transformer at the same time. The location of the PD source in the OLTC-transformer system cannot be found.

## 5 Small-scale experiments: Part 2

In addition, surface discharges involving pressboard can also occur in power transformers [36]. This fact enlarges the necessity of locating the position of the source inside the OLTC-transformer system for delta-connected tap changers. A separation between discharges occurring in the OLTC and discharges occurring in the power transformer is crucial when designing a diagnostic system for on-load tap changers and especially for delta-connected tap changers which are more prone to PD activity.

These observations led to the conclusion that a different detection system would be more suitable in the case of on-load tap changers. The set up of Figure 5.14 was used.

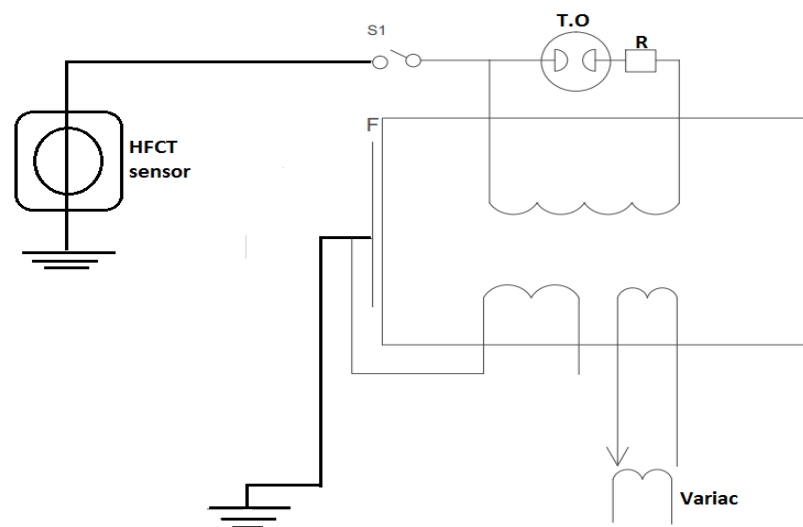


Figure 5.14. Set up used for acoustic measurements.

The set up of Figure 5.14 consists of a measuring transformer which was powered through a variac transformer. The test object (T.O) was a spark gap arrester connected in series with a 1.6 Mohm resistor. The spark gap arrester was left ungrounded (S1 open) during the experiment. The spark gap arrester represents a defect which gives rise to PD activity. The set up was placed inside a metallic drum which was filled with transformer oil. The spark gap arrester with the resistor connected in series and the transformer are presented in Figure 5.15. The sensor that was used in the experiments was an acoustic sensor manufactured by Physical Acoustics Corporation. The sensor was attached to the metallic enclosure as shown in Figure 5.16. The specifications of the sensor and the detection system are presented in detail in Appendix C.

## 5 Small-scale experiments: Part 2

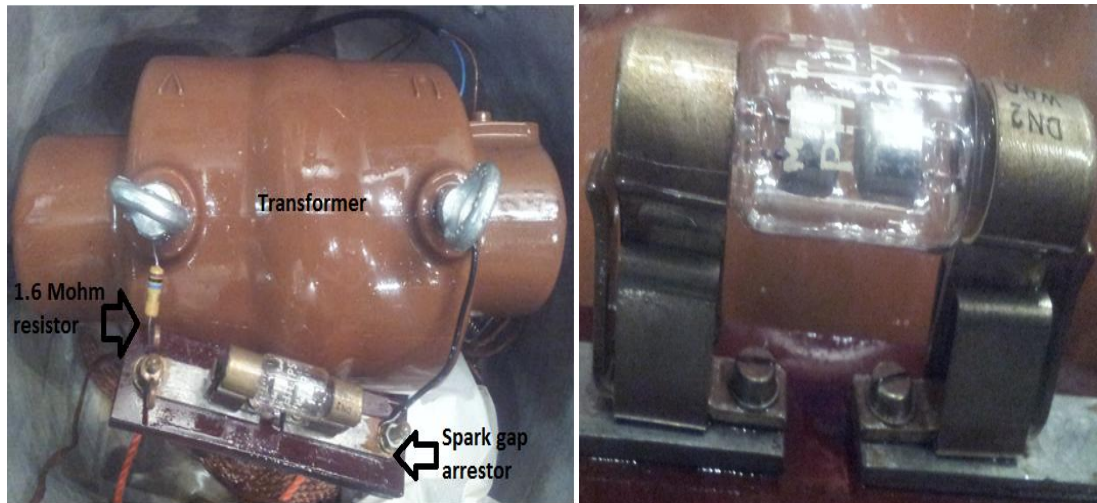


Figure 5.15. The test set up (left) – spark gap arrester (right).



Figure 5.16. Acoustic sensor attached to the metallic enclosure.

The first step of the experiment was the acquisition of the background noise pulses. Then the pulses originating from the spark gap arrester were acquired. Figure 5.17 presents the pulses of the background noise. Figure 5.18 presents the pulses that were acquired after voltage was applied to the spark gap arrester.



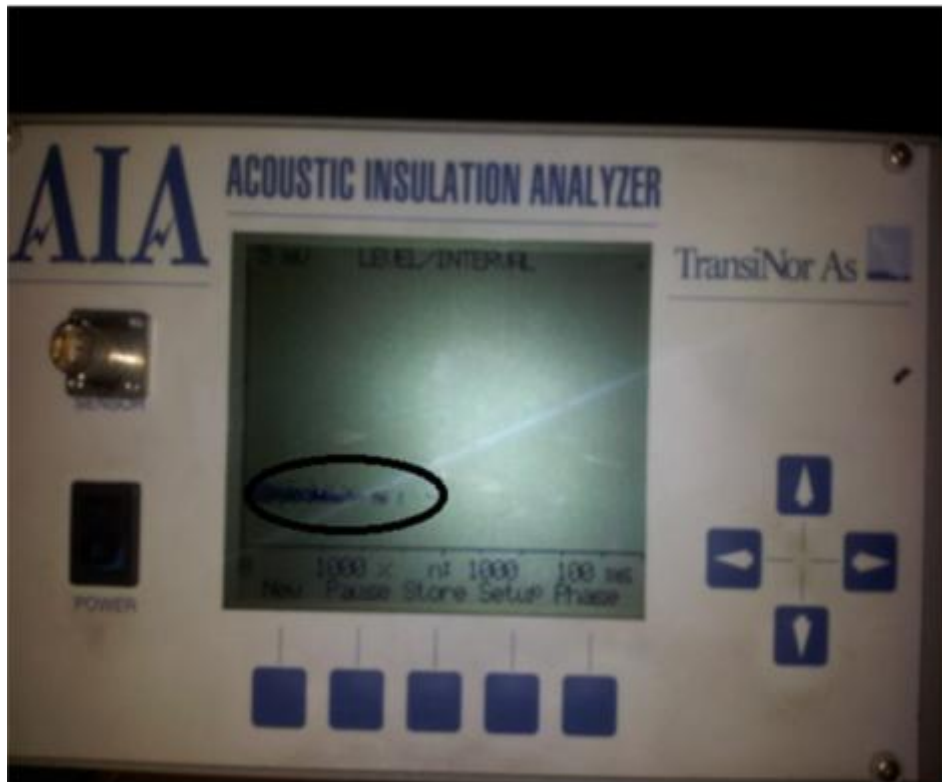


Figure 5.17. Acquisition of the background noise.



Figure 5.18. Acquisition of the pulses from the spark gap arrester.

The pulses that originated from the spark gap arrester display a different pattern than the pulses of the background noise. In addition, the result was confirmed by listening to the different types of acoustic signal. The magnitude of the sound signal significantly increased after voltage was applied and the spark gap

arrestor started discharging. Acoustic monitoring systems can be very sensitive and are widely used to detect PD activity in transformers [15].

### 5.3 Summary

In this chapter, a small single-phase tap changer was tested. The first experiments were performed in air while later the single-phase tap changer was placed in a metallic drum which was filled with transformer oil. The purpose of the experiment was to investigate the creation of tracking on the paper insulation. To reduce the electric field inside the paper insulation a grounded bar electrode was used. A needle was used to create surface discharges. The needle touched the paper at an acute angle. The grounded bar electrode (see Figure 5.8) ensured that the tangential field over the surface was dominant and the electric field inside the paper insulation was significantly reduced. The applied voltage caused a flashover. The most probable cause was that the oil between the needle and the grounder bar electrode broke down. After inspection of the single phase tap changer black carbon spots were observed on the surface of the paper insulating material.

The PRPD patterns of the discharges were acquired just before the breakdown. The discharge magnitudes and the discharge patterns strongly depend on the material of the needle and the humidity of the paper insulation as presented in [37]. The applied voltage is also a contributing factor to the creation of tracking which is generally defined as an electric discharge phenomenon that takes place on the surface of solid insulating materials and creates conductive or semi-conductive paths which usually consist of carbon, leading to a reduction in the dielectric strength of the insulation [35]. For that reason, delta-connected tap changers are more prone to electrical tracking while star-connected tap changers are less prone to tracking. Moreover, it was observed that the repetition rate of the discharges significantly increased when the voltage increased and just before break down. The increase in the repetition rate of the discharges could explain the creation of the black spots on the surface of the paper insulation because the increase in the repetition rate implies an increase in the energy dissipated at the spot of the discharge. The increased heat can lead to the burning of the material and the creation of the carbon marks.

In the second part of the chapter the applicability of the HFCT sensors for PD monitoring in star and delta-connected tap changers was investigated. In addition, a spark gap arrestor was used as a test object. The spark gap arrestor was left ungrounded. With the spark gap arrestor ungrounded, an acoustic PD detection system was used. The HFCT sensors do not provide the most suitable detection features for power transformers. A much better approach is to use acoustic signals detection by acoustic sensors [15] or electromagnetic signals detection by UHF antennas [16]. Acoustic sensors and UHF antennas can also provide information

about the location of the defect in the OLTC-power transformer system. In [38], different techniques of PD source location in power transformers by measuring the arrival time of electromagnetic signals are presented.

Finally, the experiments of chapter 4 in combination with the experiments performed in this chapter led to the conclusion that star-connected tap changers are less prone to PD activity than delta-connected tap changers. PD activity could occur in specific cases where a large step voltage is required and the selector/diverter switch of the tap changer can perform a large number of steps. On the other hand, experience has showed that tap changers rarely perform a large number of steps. In delta connected tap changers, PD activity can be more easily initiated because of the large voltage difference between different phases. The large voltage differences and the accumulation of conductive particle on the surface of the paper insulation can lead to creepage discharges. The discharge activity leads to the creation of the carbonized path which can eventually lead to OLTC failure. Delta-connected tap changers are prone to tracking defects. Other types of defects (see chapter 4) are not harmful for the insulation of the tap changer neither for star nor for delta-connected tap changers.



# 6

## Testing the 3-phase OLTC

A three phase, star-connected, selector switch type OLTC was tested for PD activity in the high voltage lab. An attempt was made to introduce the insulation defects that can cause partial discharge activity, which were presented in chapter 4, to the selector switch of the OLTC. The measurements were first performed in air. In the next part the selector switch was filled with oil. The OLTC was not inside a metallic enclosure filled with insulating oil (see Figure 6.1), as it is the case under real operating conditions. The introduction of the defects and the measurement of the PD activity created by the insulation defects in the three phase tap changer are presented in this chapter.

### 6.1 Experimental procedure (IN AIR)

The OLTC which was tested in the lab (see Figure 6.1) was a three-phase star connected tap changer. The OLTC consists of two compartments, the selector switch and the change-over switch. The selector switch is placed on the top part of the tap changer. The change-over switch is placed on the bottom of the tap changer. The selector switch was easily accessible, while the change over switch was not accessible. The tap changer was tested in two ways. In the first part of the experiments, the defects were placed between adjacent tap positions of the same phase. In the second part, the defects were placed between contacts of different, adjacent phases. In this part of the experiments, the defects were tested in air.

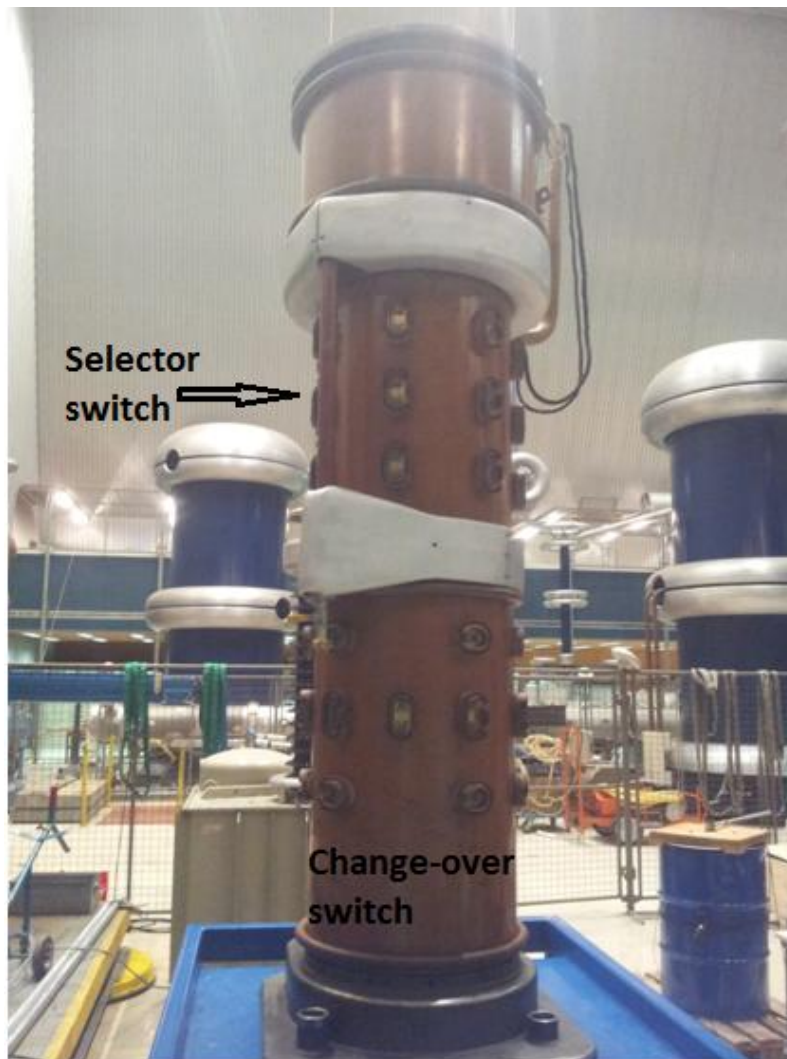


Figure 6.1. The three phase star connected tap changer.

### 6.1.1 Defects between adjacent tap positions

#### Corona discharges

The first defect that was introduced in the three phase tap changer was a wire attached to one contact of the tap changer and facing towards the contact of the next tap position. The wire was approximately 10 cm long with an almost flat tip, simulating a wire of a broken resistor. The almost flat wire is shown in Figure 6.2. Figure 6.3 presents the schematic diagram of the first test set up.

## 6 Testing the 3-phase OLTC

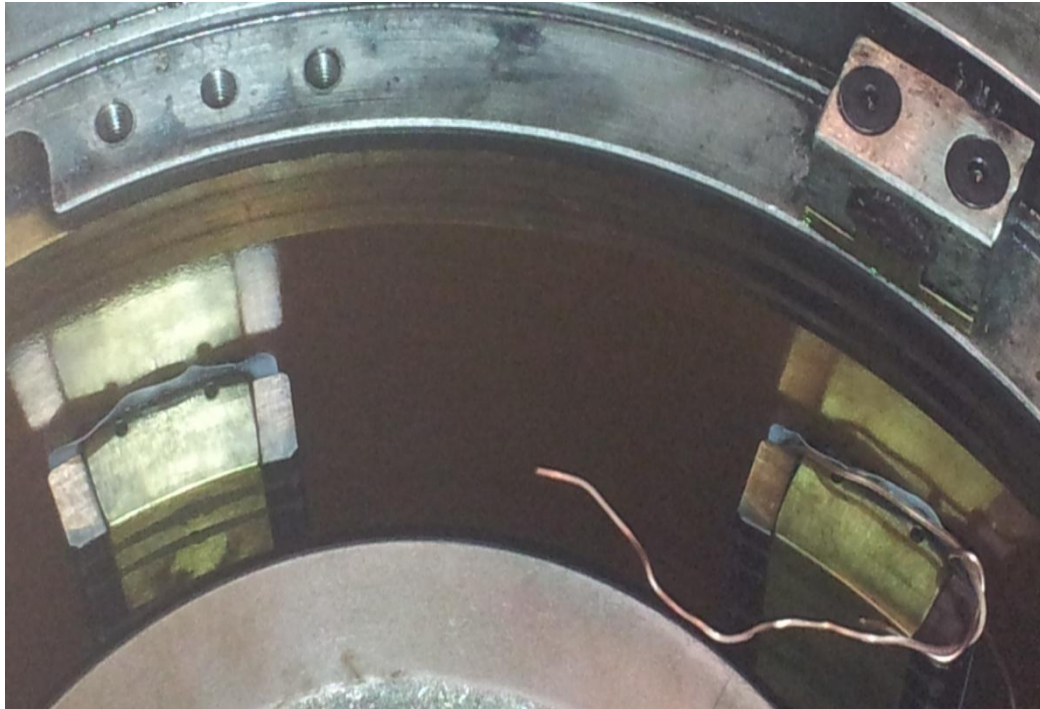


Figure 6.2. Sharp wire between adjacent tap positions.

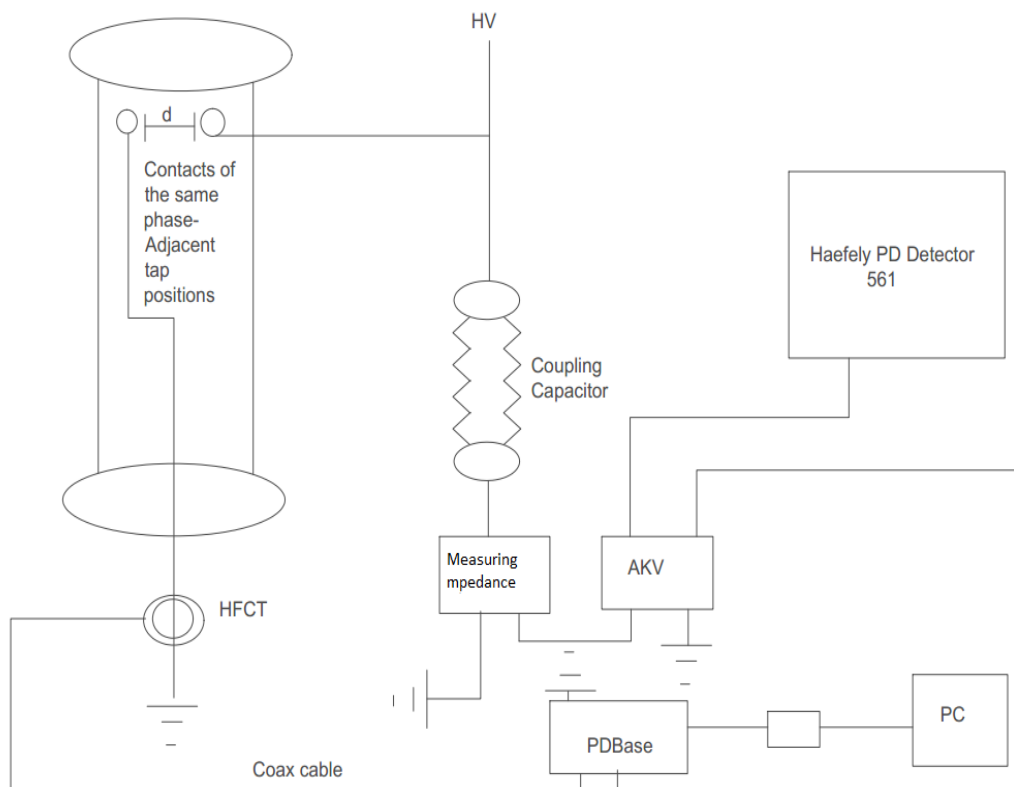


Figure 6.3. Schematic diagram of the test set up – Testing adjacent tap positions of the same phase.

The distance between adjacent tap positions of the same phase is 220mm. The results of the first experiment are presented in Table 6.1. The inception voltage of

## 6 Testing the 3-phase OLTC

the discharges was 5.75 kV, the same as the extinction voltage. This fact is characteristic of corona discharges. The PRPD pattern of the pulses at 6.9kV is presented in Figure 6.4. The acquisition mode used in this experiment is IEC 60270.

Table 6.1. PD magnitude

	PD magnitude
Sharp wire (Applied voltage: 6.9kV)	- 45 pC

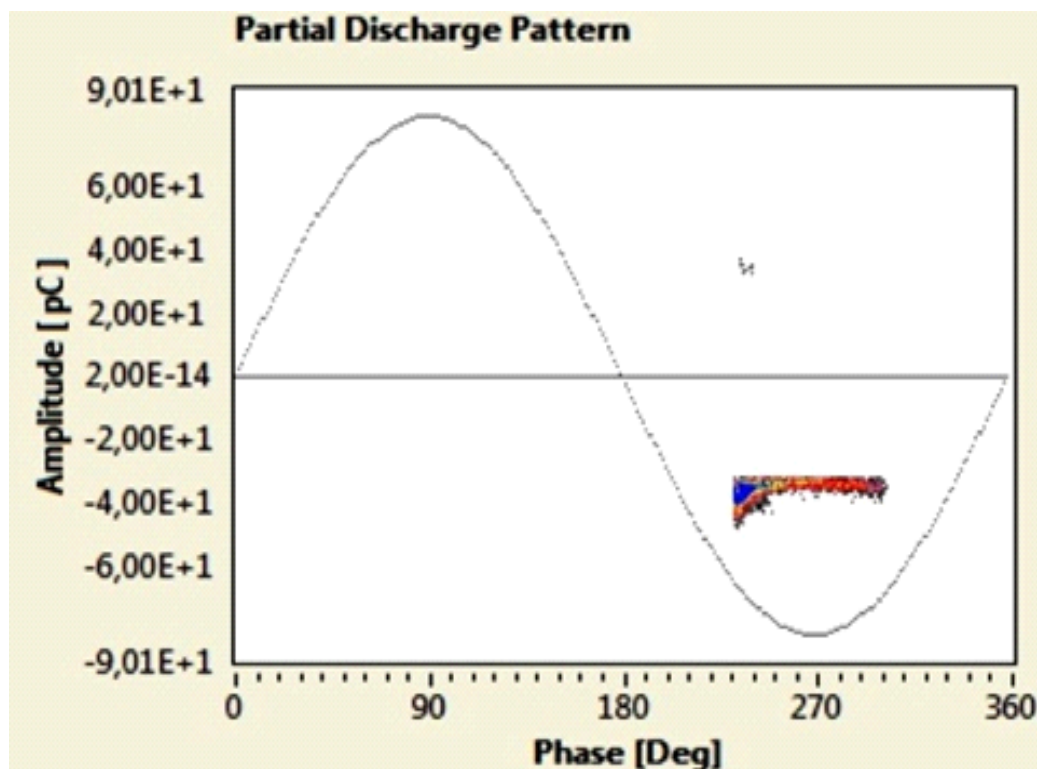


Figure 6.4. The PRPD pattern of the pulses.

The PRPD pattern that is shown in Figure 6.4 is a characteristic pattern of corona discharges. The pattern is flat without large differentiations of the PD magnitude. In addition, the negative pulses are placed around the peak of the applied voltage at 270°. When the wire is connected to the high voltage electrode, corona discharges in air depend mainly on the instantaneous value of the applied voltage [39]. When the wire is at negative high voltage, electron avalanches are starting from the tip of the wire where the field is the maximum. When the wire is at positive high voltage, starting electrons originate from within the gas and avalanches start at a distance from the tip of the wire where the field is lower. For that reason, the voltage must be further increased to get the required electric field to create corona discharges. As a result, positive corona appears at higher voltage levels than negative corona. The identification of the PD source creating the PRPD pattern of Figure 6.4, as provided by PDBasell is shown in Figure 6.5. The identification of PDBasell confirms that the PD source is negative corona.

## 6 Testing the 3-phase OLTC

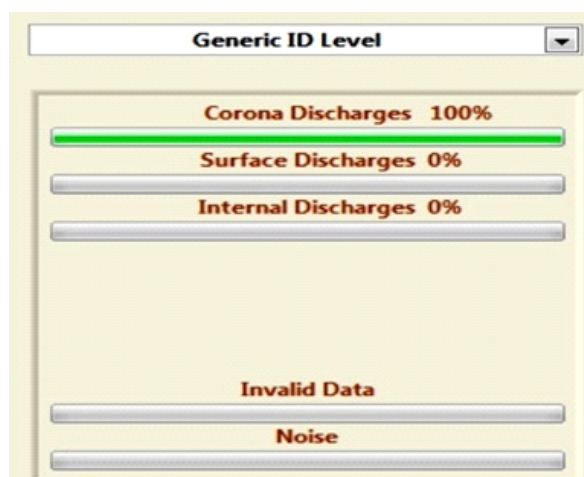


Figure 6.5. Identification of the PD source.

### Surface discharges

To create surface discharges, conductive tape was placed between the contacts of the tap changer as shown in Figure 6.6. The conductive tape was used instead of the needle that was used in the small scale experiments. The conductive tape was chosen because it would not endanger the paper insulation. A needle touching the paper insulation could damage the paper insulation of the OLTC.

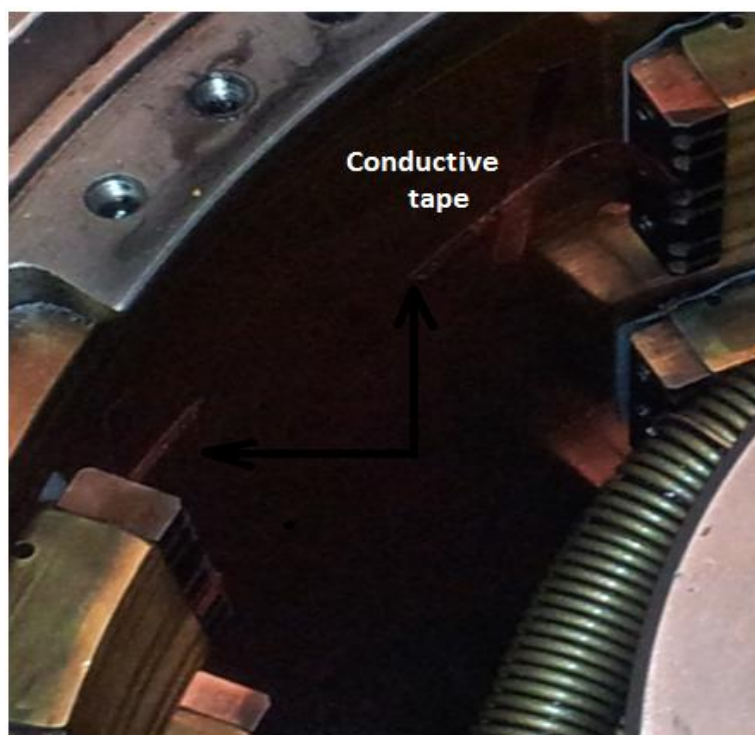


Figure 6.6. Conductive tape placed between adjacent tap positions.

The set up was initially tested for PD activity without introducing any defects. The applied voltage reached up to 21 kV and no PD activity was measured. After ensuring that the set up was PD free, the conductive tape was placed on the surface of the cylinder. The inception voltage of the PD activity was 6.8kV. The

## 6 Testing the 3-phase OLTC

results of this experiment are presented in Table 6.2. The PRPD pattern is presented in Figure 6.7.

Table 6.2. PD magnitude of the surface discharges.

Surface discharges (Tap to Tap)	PD magnitude [max]
At 7.7kV	310 pC

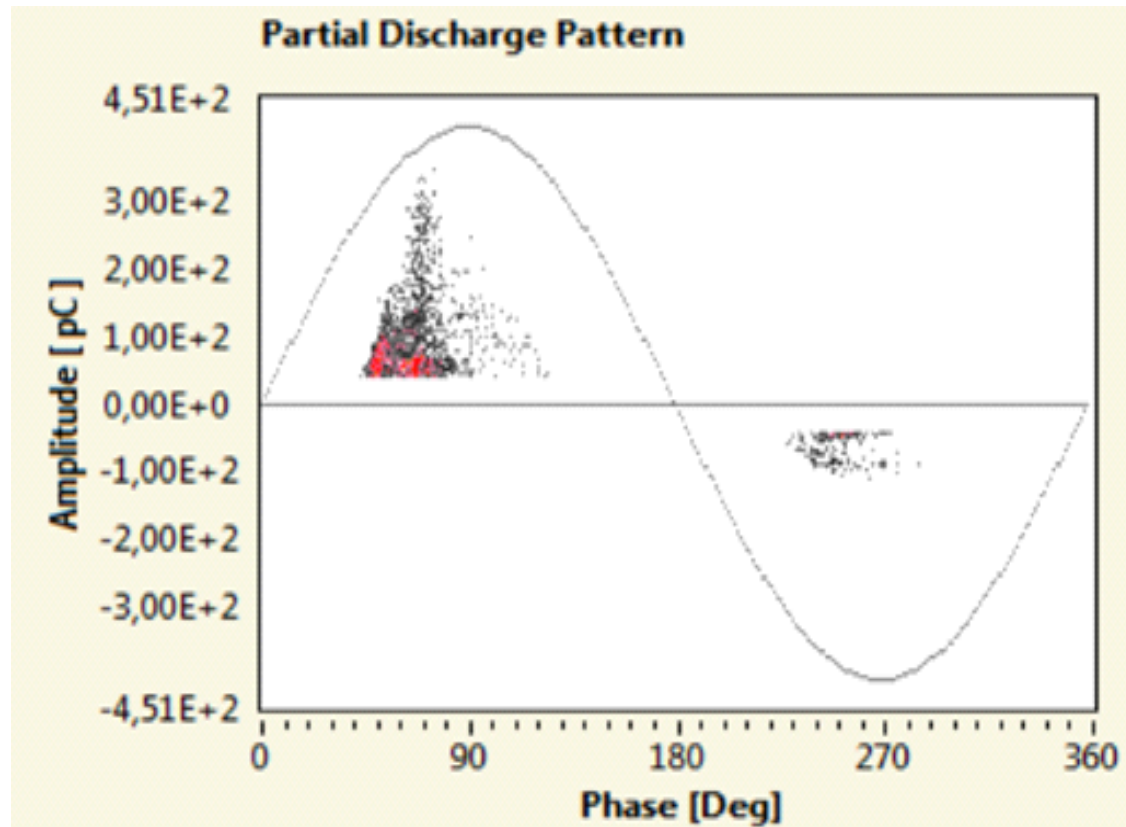


Figure 6.7. The PRPD pattern of the pulses.

The PRPD pattern of Figure 6.7, displays a large scatter of the PD magnitude especially in the positive half cycle of the applied voltage. Pulses with scattered magnitudes as in Figure 6.7, is a characteristic tendency displayed by surface discharges [29]. The number of pulses is larger in the positive voltage cycle with few negative pulses. The pattern is mostly concentrated between  $45^{\circ}$  and  $90^{\circ}$  in the positive cycle, in contrast to corona discharges which are concentrated around the peak of the applied voltage. In the negative cycle the discharges occur between  $230^{\circ}$  and  $280^{\circ}$ . The identification of the source from PDBasell shown in Figure 6.8 confirms that the source of the PD is surface discharges created by the conductive tape.



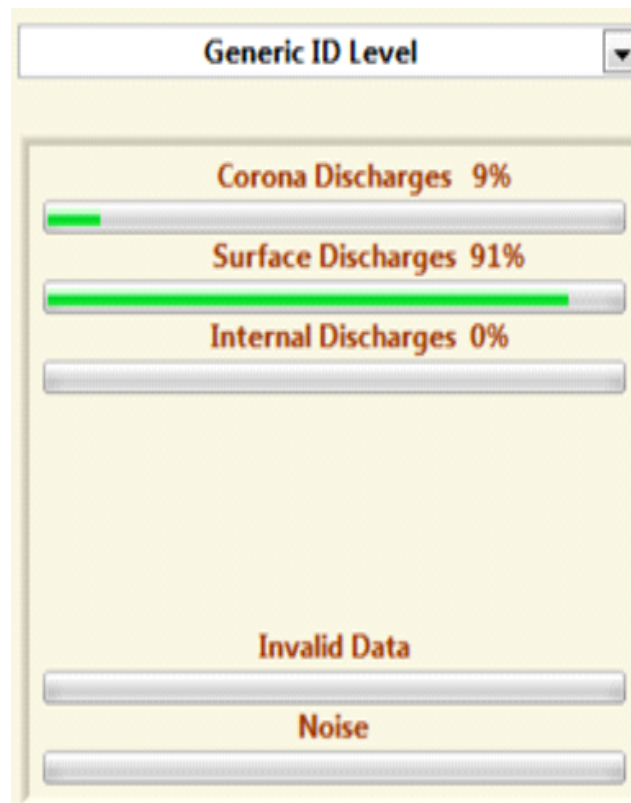


Figure 6.8. Identification of the PD source.

### 6.1.2 Defects between contacts of different phases.

In the second part of the experiments, the defects were placed between contacts of different phases. As explained in chapter 2, the electrical stress is higher between contacts of different phases. Especially for delta connected tap changers which have to insulate the whole line to line voltage, the electrical stress is maximal between contacts of different phases. The same defects were introduced, namely, a sharp wire and conductive tape.

#### Corona discharges

The position of the sharp wire is shown in Figure 6.9. The sharp wire is connected to one contact and faces towards the contact of a different phase. The schematic diagram of the test set up is presented in Figure 6.10.

## 6 Testing the 3-phase OLTC

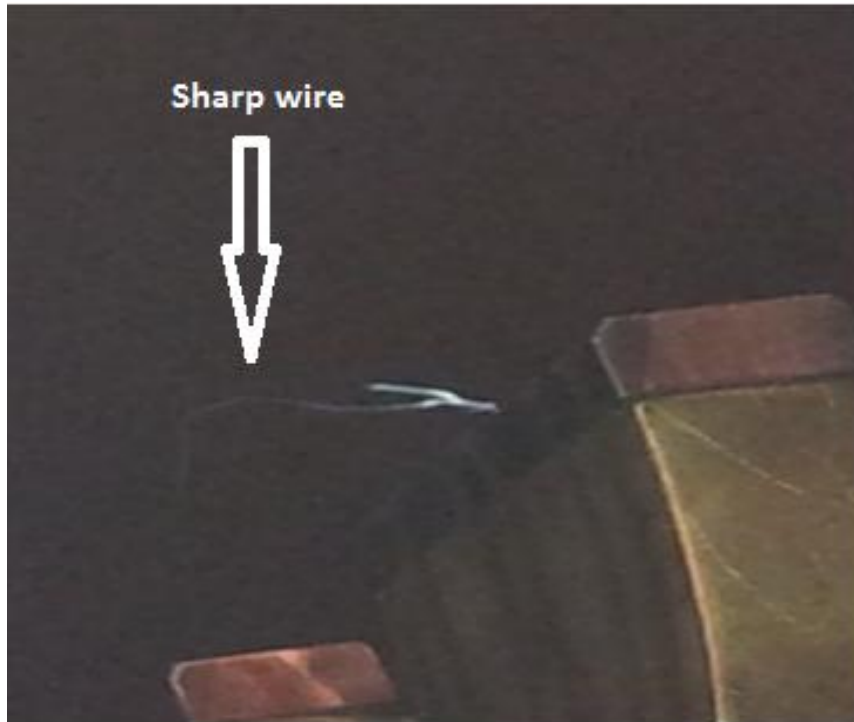


Figure 6.9. Sharp wire between contacts of different phases.

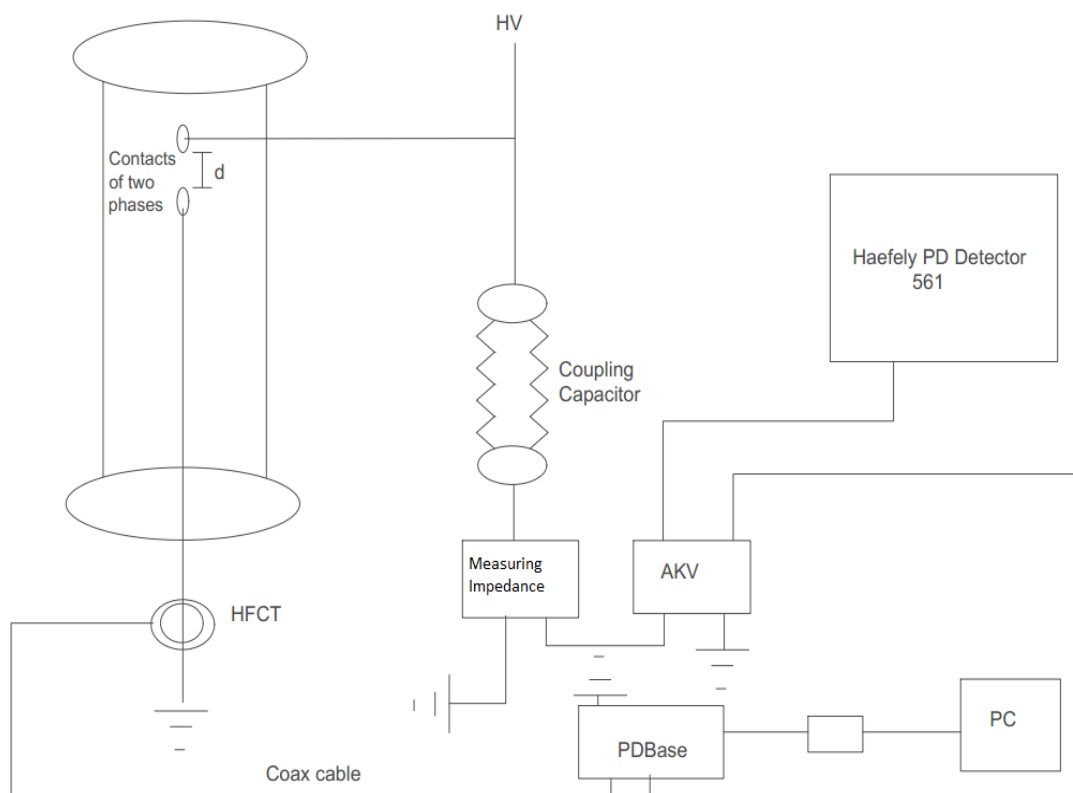


Figure 6.10. Schematic diagram of the test set up – Testing between contacts of different phases.



## 6 Testing the 3-phase OLTC

The noise level as measured by PDBasell is presented in Figure 6.11. The maximum value in the acquisition window is 110 pC and the trigger level is at 3.3 pC.

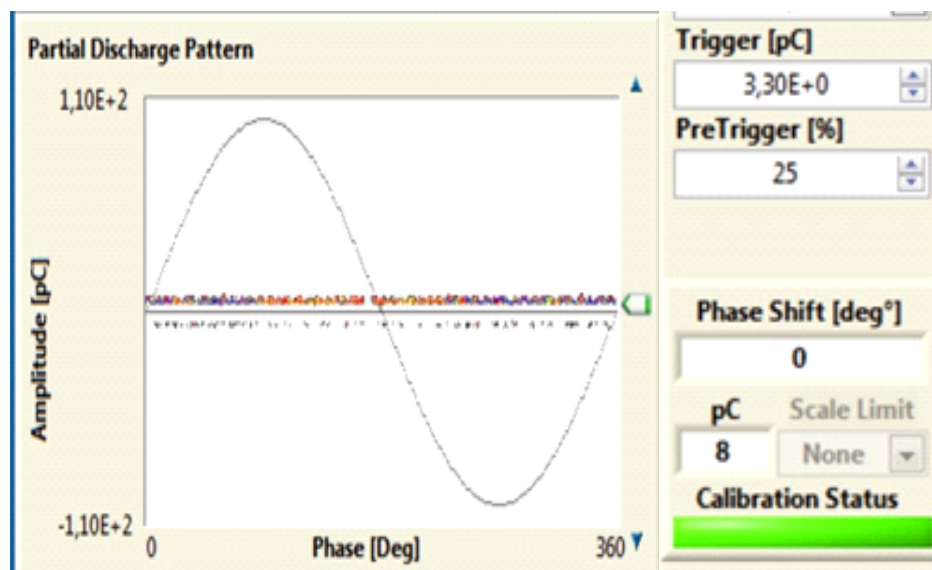


Figure 6.11. Noise level.

Table 6.3 and Table 6.4 present the results of this experiment. The inception voltage of the discharges was 5.8 kV as shown in Table 4.5. The extinction voltage was the same as the inception voltage. This behavior is characteristic of corona discharges. The PRPD pattern at 6.9 kV is presented in Figure 6.12. The detection mode used in this case is IEC 60270.

Table 6.4. Inception voltage of the discharges.

	Inception voltage
Sharp wire in air	5.8 kV

Table 6.5. PD magnitude.

	PD magnitude
Sharp wire in air (Applied voltage: 6.9 kV)	101pC (PDBasell)

## 6 Testing the 3-phase OLTC

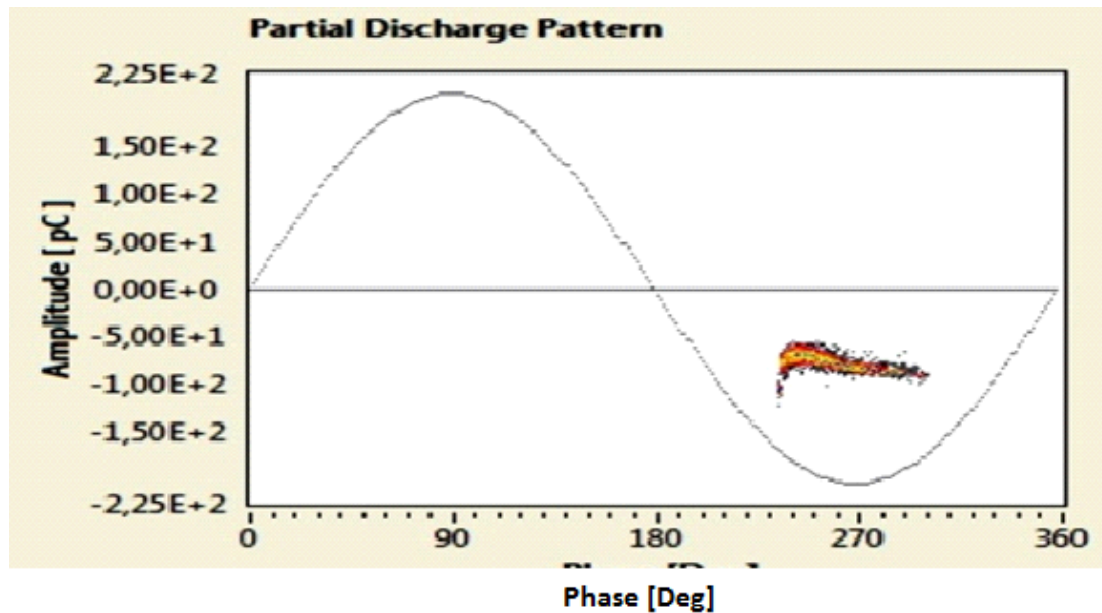


Figure 6.12. The PRPD pattern of the pulses obtained from a wire between contacts of different phases.

The PRPD pattern is flat and centered around the peak of the voltage waveform. Moreover, the discharge magnitudes do not show great differentiations in value. The pattern observed in Figure 6.12 is a characteristic pattern of corona discharges. The sharp wire is placed at the contact which is connected to the high voltage. For that reason, negative corona appears first. Increased voltage would lead to the appearance of positive corona. The PD source identification as obtained by PDBasell is presented in Figure 6.13. Figure 6.14 presents one waveform of the acquired PD pulses.

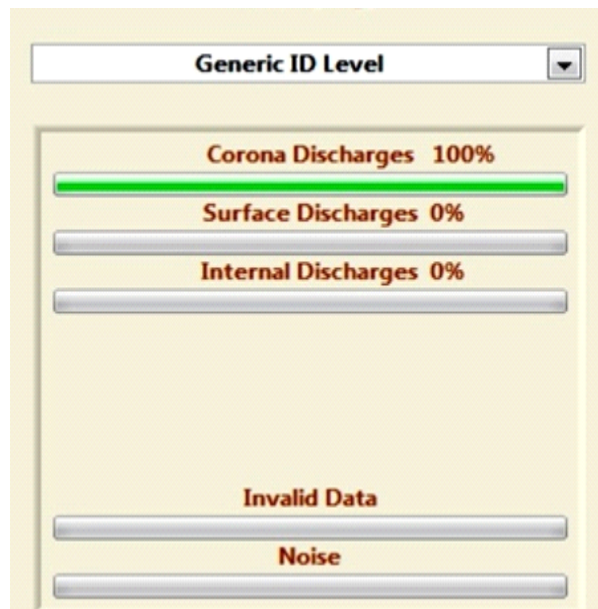


Figure 6.13. Identification of the PD source for a wire between contacts of different phases.

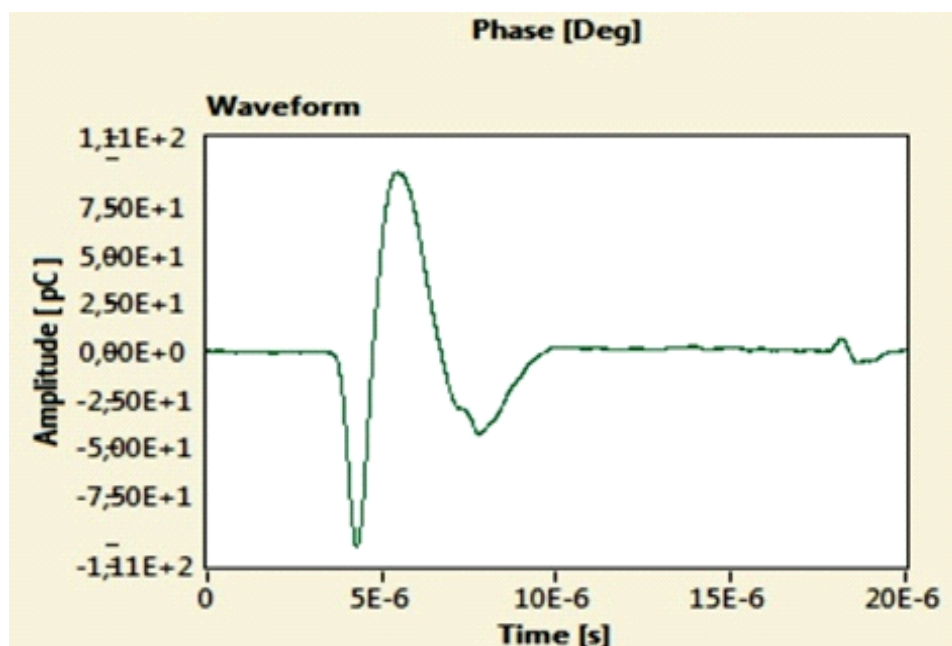


Figure 6.14. Waveform of the PD pulse.

The pulse shape of Figure 6.14 is obtained by using the IEC 60270 identification mode. The features of the IEC detection mode are presented in chapter 4. The PRPD pattern of Figure 6.12 consists of negative discharges. In Figure 6.14, the waveform of the PD pulse consists of two peaks, one positive peak and one negative. The classification of the discharge as positive or negative is performed by detecting the polarity of the first peak of the pulse. In Figure 6.14, the first peak is negative and of approximately the same value as the positive peak. The fact that the first peak is negative classifies the PD pulse as a negative pulse.

### Surface discharges

In the next part of the experiments, the first step was again to test - without introducing any defects - if the set up was PD free. The voltage was increased up to 21 kV but no PD activity was measured. Conductive tape was then placed partially between contacts of different phases. The inception voltage of the PD activity was 6.6 kV. The results of this experiment are presented in Table 6.6.

Table 6.6. PD magnitude-Surface discharges.

Surface discharges (Phase to Phase)	PD magnitude (mean value)
At 6.9kV	57pC
At 8.6kV	190pC

The PRPD pattern of the pulses is presented in Figure 6.15. The applied voltage is 8.6 kV. The PRPD pattern at a voltage of 6.9 kV is presented in Figure 6.16.

## 6 Testing the 3-phase OLTC

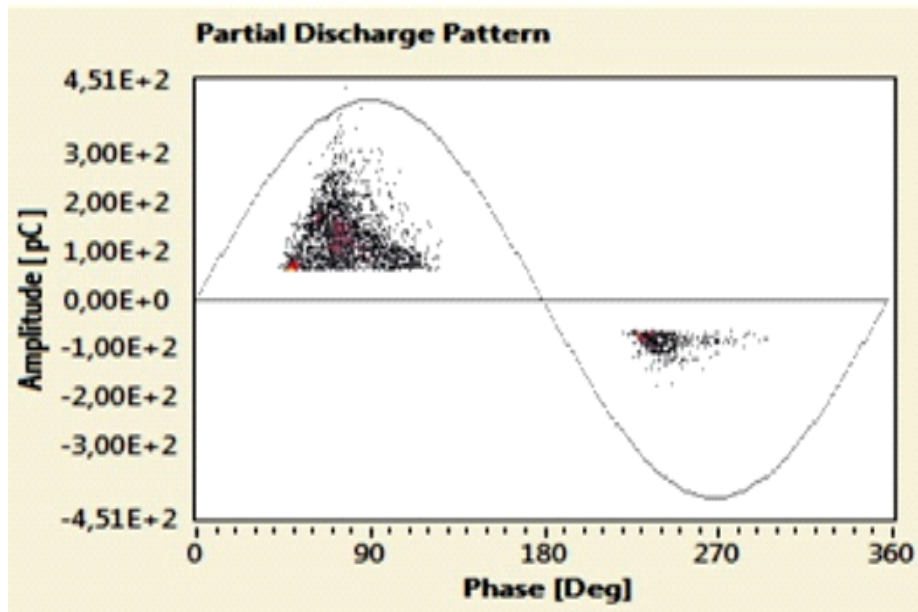


Figure 6.15. PRPD pattern of the pulses, obtained by placing conductive tape on the paper insulation between contacts of different phases, at 8.6 kV.

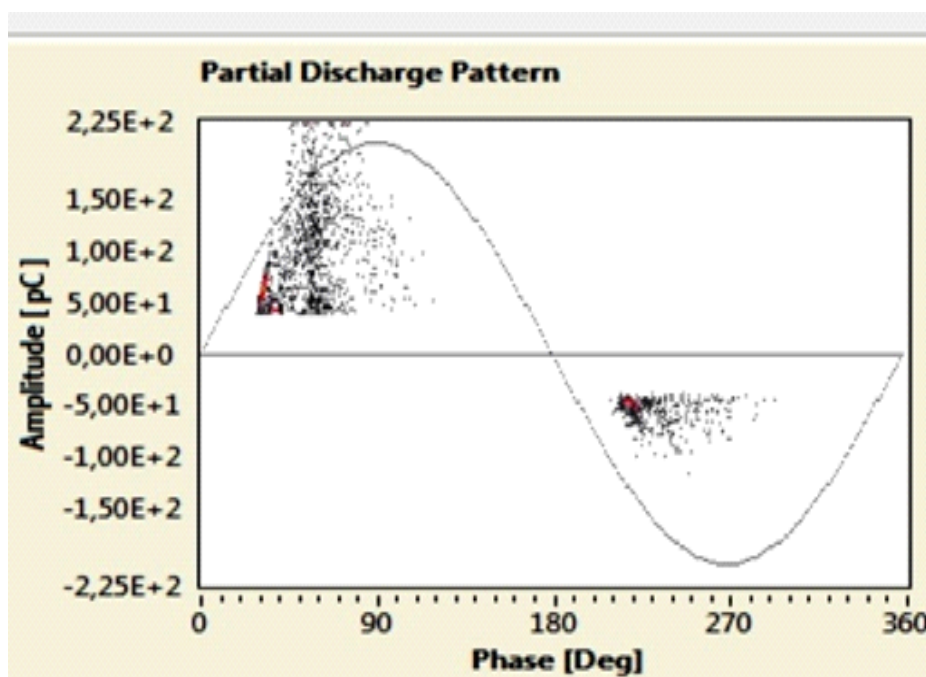


Figure 6.16. PRPD pattern of the pulses, obtained by placing conductive tape on the paper insulation between contacts of different phases, at 6.9 kV.

The PRPD patterns of Figure 6.15 and 6.16 are characterized by a large scatter in the PD magnitudes. In addition, discharges in the positive voltage cycle and the negative voltage cycle are present. The number of positive discharges is larger than the number of negative discharges. In addition, an increase in the applied voltage leads to an increase in the magnitude of the PD pulses (see Table 6.6). The patterns of Figures 6.15 and 6.16 are characteristic of surface discharges.

## 6.2 Experimental procedure (IN OIL)

The selector switch of the tap changer was filled with oil. The goal of the experiments was to investigate the effect of the oil insulation on the PD activity. In real conditions the tap changer is placed inside a steel enclosure which is filled with oil. In-tank tap changers are placed in the same enclosure as the power transformer. Tap changers can also be placed in a separate steel enclosure. In both cases the tap changer is located in a steel enclosure which is filled with insulating oil.

The OLTC, that was planned to be tested in the high voltage lab, was not placed in a steel enclosure. Filling the selector switch with oil does not prevent surface discharges from appearing on the outside part of the paper insulating cylinder. A test was performed at different positions - where no defects were present - to investigate if surface discharges would appear on the outside part of the tap changer. The surface was initially cleaned with alcohol. In some positions surface discharges appeared on the surface as shown in Figure 6.17.

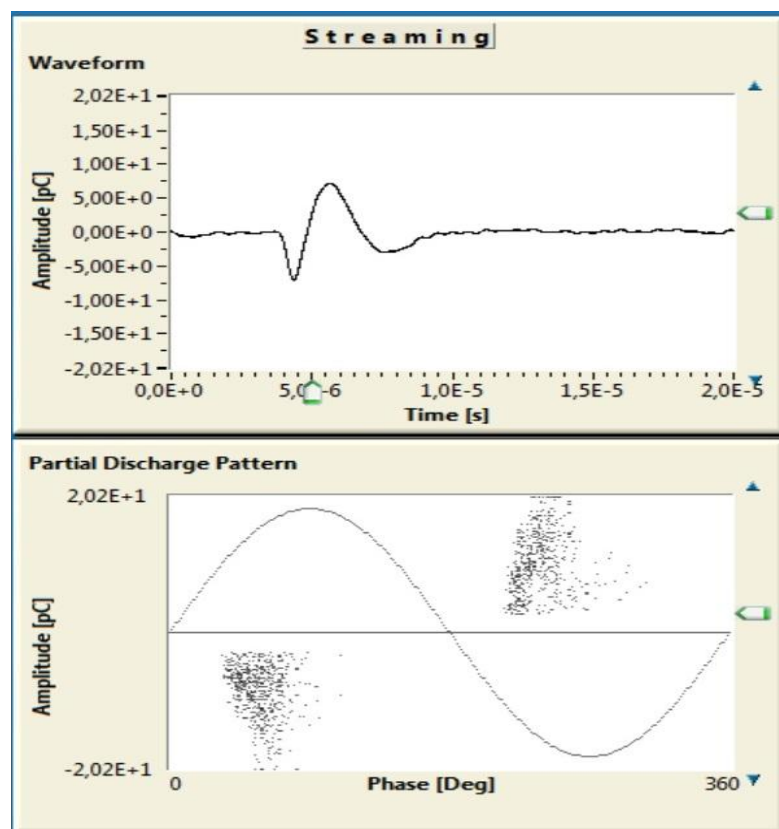


Figure 6.17. Discharges occurring on the outside of the tap changer.

The wire that was tested in air was placed in a position where surface discharges did not appear. The position was between adjacent tap positions as shown in Figure 6.2. The voltage was increased up to 60 kV. Above 60 kV, internal discharges appeared in the high voltage transformer. In addition, the voltage was not further increased due to the risk of a flashover between the contacts of the tap changer. Up to 60 kV, no PD activity was measured in the tap changer. The quality of

## 6 Testing the 3-phase OLTC

the new, dry oil and the fact that the insulating oil was not contaminated at any degree, could explain why the defects that were tested in air did not give rise to any PD activity in the insulating oil.

Finally, it was not attempted to introduce larger defects that could create the large PD sources that were required, as it was performed in the small scale experiments. For example, tracking which is a major defect especially for delta connected tap changers could not be created in the tap changer. The process depends on the applied voltage and time but more importantly the damage on the paper insulation would be non repairable and it was not intended to damage the OLTC. In addition, other types of defects like gas bubbles in oil could not be tested in the three phase tap changer for practical reasons.

### 6.3 Summary

The experiments that were performed in air provided a good insight into the probable locations within the tap changer where PD activity can be initiated. The most important conclusion drawn from the performed experiments is that PD activity is highly unlikely to be initiated between adjacent tap positions. The inception voltage for corona and surface discharges in air (5.75 kV and 6.8 kV) is larger than the maximum step voltage of on-load tap changers. The maximum step voltage can be as much as 5 kV. The presence of insulating oil will obviously improve the insulation of the tap changer. It is logical to assume that defects that are present between adjacent taps do not pose a significant threat for the insulation of the OLTC. PD activity could occur when insulation defects are found between contacts of different phases where the electrical stress is higher. Therefore, the small scale set up was correctly built in a way that it simulated the conditions between adjacent contacts of different phases.

The experiments that have been performed when the selector switch of the three-phase tap changer was filled with oil could not provide much information about the PD activity occurring in OLTCs. The problems that were experienced during the experiments were a big obstacle to overcome. Nevertheless, an indication about the PD activity occurring in on-load tap changers can be extracted from the experiments. Wires in the oil of the tap changer between adjacent tap positions did not cause PD activity when the voltage was raised up to 60 kV. This could be attributed to the quality of the oil which was new, dry and not contaminated. It also demonstrated the fact that wires from broken resistors in OLTC would hardly cause PD activity in star-connected tap changers with new dry oil. The possibility of PD occurrence due to broken resistors is higher for delta connected tap changers depending on the voltage difference between the contacts of the different phases and the quality of the oil. The possibility of PD occurrence increases when the oil is contaminated with metallic particles. The PD inception voltage when the oil is

## 6 Testing the 3-phase OLTC

contaminated with conducting particles can significantly decrease as presented in [40]. Nevertheless, in star-connected tap changers, corona discharges are more unlikely to occur because of the low voltage difference between the contacts of different phases (see chapter 2) than in delta-connected tap changers where the voltage between contacts of different phases equals the line voltage (see chapter 2).

## Conclusions and recommendations

In this chapter, the conclusions that were drawn from the experiments are presented. The results of the PD measurements that were performed in the small scale set up, in the single phase tap changer and in the three-phase, selector switch type OLTC are discussed in section 7.1. In section 7.2, some recommendations for further research regarding the PD monitoring of on-load tap changers are presented.

### 7.1 Conclusions

#### OLTC examination and experiments on the three phase OLTC

The OLTC is responsible for regulating the output voltage of a power transformer. After every operation of the OLTC, the voltage output of the power transformer is increased or decreased by the step voltage. The first conclusion that was drawn from the experiments and from a thorough examination of a star connected tap changer is that PD activity cannot be initiated between adjacent tap positions. The maximum step voltage of an OLTC was found to be 5 kV. Considering the large distance between adjacent tap positions, the occurrence of partial discharges between contacts of the same phase is considered highly unlikely.

On the other hand, the voltage difference between contacts of different phases is higher. For delta connected tap changers, the voltage difference between contacts of different phases equals the line voltage at the point where the power transformer is connected. Star connected tap changers are stressed by only a part of the line to neutral voltage.

In addition, the distance between contacts of different phases is smaller than the distance between adjacent tap positions. Therefore, the OLTC is maximally stressed between adjacent contacts of different phases.



### PD experiments

The major insulation defects that can lead to PD appearance in on-load tap changers were presented. The major insulation defects include:

- 1) *Corona discharges*. A rare scenario that can occur in an OLTC is a broken transition resistor. The wire of the transition resistor can cause a local increase in the electric field. As a result, corona discharges in the insulating oil could appear. From the experiments, it was concluded that corona discharges from broken transition resistors can hardly occur in star connected tap changers with new dry oil. This fact can be attributed to the low voltage difference between contacts of different phases. On the other hand, the voltage between contacts of different phases in delta connected tap changers is much higher. Therefore, the probability of PD activity due to a broken resistor is increased for delta connected tap changers. The probability of PD activity is also increased when the oil is contaminated with conducting particles. The insulating oil of the OLTC is frequently contaminated with metallic particles. As a result, the PD inception voltage can be significantly reduced.
- 2) *Gas bubbles* in oil. During the operation of the tap changers, arcs are created and extinguished in the insulating oil. Due to the arcing process, gas bubbles are formed in the insulating oil of the tap changer. Increased amounts of gas bubbles in the insulating oil means an excessive arcing period during the operation of the tap changer. In other words, increased PD activity originating from gas bubbles in the insulating oil could provide information about excessive arcing periods. The applicability of PD measurements as a tool to assess the arcing process was investigated. The conclusion drawn from the experiments is that the arcing process of the on-load tap changers cannot be assessed by PD measurements because the electric field strength is not high enough to cause the appearance of PD activity in spherical gas bubbles of 1mm diameter in star-connected tap changers ( $E \ll 2.56 \text{ kV/mm}$ ). In delta-connected tap changers PD activity in spherical gas bubbles of 1mm diameter could appear only if the gas bubble could be trapped for a significant amount of time in an area where the electric field is  $E > 2.56 \text{ kV/mm}$ . Even then the measured PD activity could not be used to assess the arcing process occurring in the selector switch of the OLTC because the gases created during the arcing periods are quickly removed from the insulating oil by using a vent system.

## 7 Conclusions and recommendations

- 3) *Tracking* on the paper insulation. From the performed experiments and according to the experience of Smit Transformer Services, it was concluded that tracking on the paper insulation is the most dangerous defect especially for delta connected tap changers. The contamination of the surface of the paper insulation with conducting particles in combination with the large voltage between the contacts of different phases can lead to a significant field enhancement. The local high electric field at the surface of the paper insulation can lead to creepage discharges on the surface of the solid insulation. A carbonized path can be created on the surface of the paper insulation and can ultimately lead to OLTC failure. Star connected tap changers are not prone to electrical tracking.

The results that were obtained from the experiments showed that PD activity is more likely to appear in delta connected tap changers. The most probable PD source in delta connected tap changers is tracking on the paper insulation. PD monitoring can be used to identify tracking defects in delta connected tap changers and to prevent possible failures associated with tracking.

### **Detection system**

The PD measurements were performed by means of electrical detection methods. In the final part of the experiments, a comparison was made between PD measurements by electrical methods and acoustic PD measurements. Detection of PD activity by electrical methods provides essential information about the PD source. The most important information is the PRPD pattern of the discharge pulses. The PRPD pattern can be used to identify the defect which causes the PD activity. The major disadvantage of electrical detection is that the location of the defect cannot be found. In star-connected windings, a common neutral is built for the OLTC and the transformer. An HFCT sensor installed around the grounding point of the common neutral will detect discharges occurring in both the OLTC and the transformer. A separation of the discharges occurring in the OLTC from the discharges occurring in the transformer is not possible. In delta-connected tap changers the ground point is not present and HFCT sensors cannot be used. By using capacitive sensors mounted on the bushings of the transformer, the same difficulty as in the case of star-connected tap changers will be encountered.

It was concluded that acoustic PD measurements or measurements of electromagnetic waves via UHF antennas is a better approach regarding on-load tap changers, considering that the major insulation defects appear more frequently in delta connected tap changers, because PD monitoring by using acoustic sensors or

UHF antennas provides the capability of finding the location of the source which is a principal requirement for the power transformer-OLTC system.

### 7.2 Recommendations for further research

The experiments that were performed in this research project constitute an initial step towards the direction of establishing a PD monitoring system for on-load tap changers. Further research should be more focused on:

- Delta connected tap changers. PD activity will more frequently appear in delta connected tap changers. The main insulation defect for delta connected tap changers is the tracking on the paper insulation. Additional research is required in that topic. More specifically, the conditions that lead to tracking on the paper insulation must be further investigated. Additional experiments must be performed in order to acquire more phase resolved PD patterns associated with tracking. The effect of the shape and the conductivity of the carbonized path on the phase resolved PD patterns should be investigated. It is necessary to perform additional experiments with different types of tracking defects (shape, conductivity) in order to create a larger database of PRPD patterns associated with tracking. In that way, the different types of tracking can be more easily identified and the process by which tracking defects are created on the surface of the paper insulation in on-load tap changers can be further comprehended.
- PD detection methods which use acoustic sensors or UHF antennas. The applicability of different detection sensors in on-load tap changers must be further investigated. In that way a detection system which can locate the position of the defect in the transformer-OLTC system can be designed.
- On-line PD measurements. On-line PD measurements should be performed in power transformers under operation. The obtained PD patterns should be compared with known patterns that were created by the insulation defects that were tested in the lab and it should also be attempted to locate the position of the PD source in the OLTC-transformer system.

# Appendix A

## OLTC technologies

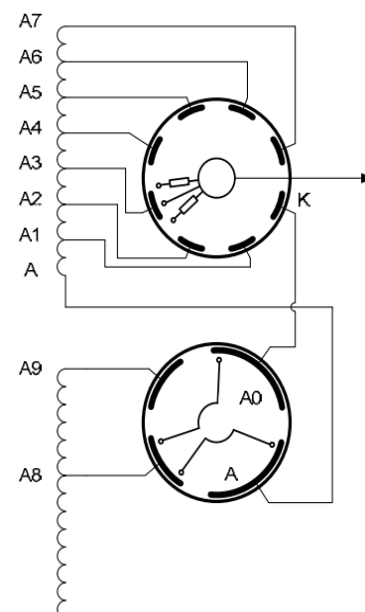
In this appendix, the operation of the different OLTC technologies is presented in more detail. The operation of a selector switch type OLTC, a diverter switch type OLTC and a vacuum switch type OLTC are presented.

### A. 1 The different OLTC technologies

In chapter 2, the basic principles of the different OLTC technologies were described. As mentioned in chapter 2, three basic technologies can be found. The three technologies are the sector switch, the diverter switch and the arising technology of vacuum switch type tap changers. The transition period where the tap changer moves its contacts from one tap position to the next one will be described in more detail in this section.

#### A. 1. 1 Selector switch type OLTC

A selector switch type OLTC with a coarse change-over selector is presented in Figure A.1. The selector switch is found on the top part of the tap changer and is easily accessible for inspection. The change-over selector which is placed on the bottom part of the tap changer is not easily accessible. The selector switch and the changeover selector consist of a stator where the fixed contacts are mounted. The fixed contacts are connected to the tap positions on the transformer winding (see Figure A.1). The rotor of the tap changer is placed inside the stator. A drive system is responsible for rotating the rotor of the OLTC. The rotor is responsible for making the connection of the stator contacts to the tap positions of the main winding. As shown in Figure A.1, the tap changer has selected the main winding on tap A8. The current is flowing through the rotor of the change-over selector (contact A in Figure A.1) and reaches the selector switch. The selector switch has selected the contacts of the third tap position (contact A3 in Figure A.1).



The current leaves the tap changer through a slip ring. The transition from one position to the next one consists of a number of steps as shown in Figure A.2.

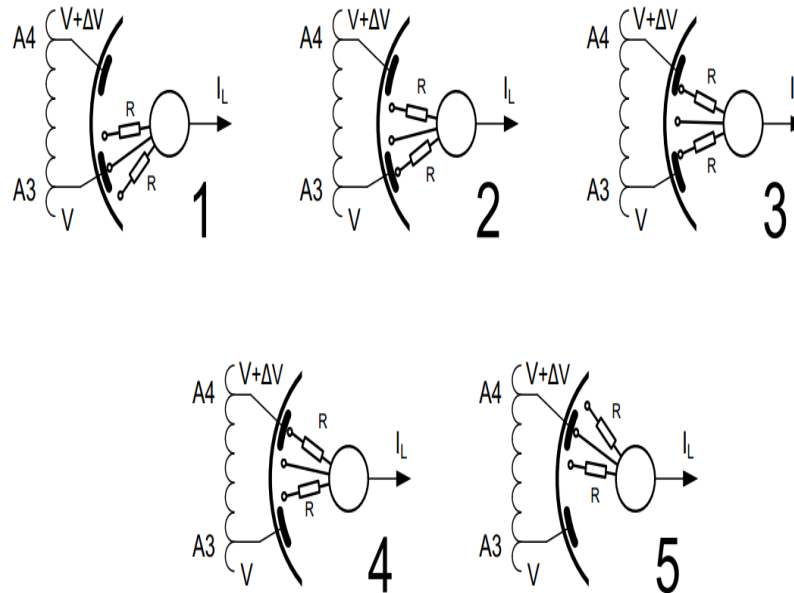


Figure A.2. The transition process [5].

There are 4 contacts per phase mounted on the rotor, as shown in Figure A.3: the main roller contact, two transition contacts which are connected in series with a resistor and one set of contacts which connect each phase to a slipring. The rotor contacts are made of wolfram to prevent excessive damage during arcing periods. The stator contacts are made from copper and are equipped with wolfram edges. The wolfram contacts are called arcing contacts. When the selector switch moves its contacts from contact A3 to contact A4, the load current flows through the first transition resistor while the main contact has left contact A3 (position 2 in Figure A.2). The rotor moves further and the second transition contact touches contact A4. The load current is in this position (position 3 in Figure A.2) split between the two transition resistors. The transition resistors ensure the uninterrupted flow of the low current. In addition, the transition resistors prevent a short-circuit between two adjacent taps of the tapped winding. When the second transition contact touches contact A4 a circulating current starts flowing. The circulating current is  $I_c = \Delta V/2R$ . The circulating current depends on the step voltage and the transition resistance. Then, the rotor moves further, the first transition contact leaves contact A3 and the main contact touches tap A4 (position 4 in Figure A.2). Finally, the main contact will



Figure A.3. Rotor contacts

move to tap A4 (position 5 in Figure A.2) and the load current will flow through the main roller contact.

A vector diagram representing the load current and the voltage during the transition period is presented in Figure A.4. The OLTC increases the output voltage by the step voltage  $\Delta V$  through the five steps of Figure A.2.

The voltage will initially drop because of the voltage drop over the transition resistor. When both the transition contacts are connected, the voltage drop will be half because the resistors are connected in parallel with respect to the load current. Then again the load current flows through only one transition resistor. The vector of the output voltage follows a flag cycle as presented in Figure A.4. The tap changer operation is thus called flag-cycle operation. In on-load tap changers which transfer the load current from the main contacts before creating the circulating current the voltage output always follows the flag cycle diagram.

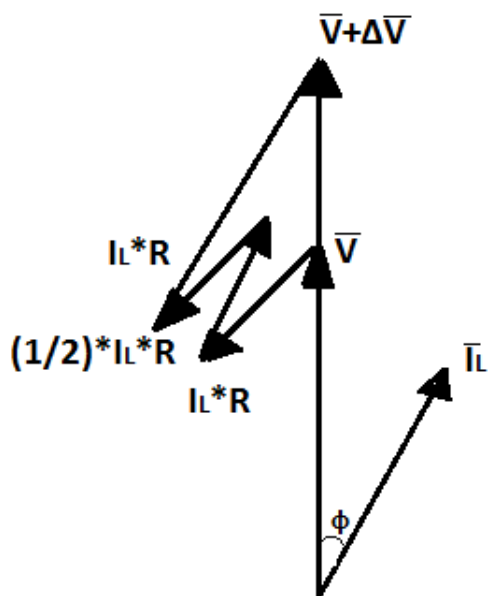


Figure A.4. Vector diagram of a selector switch type OLTC.

When increasing the number of turns in the circuit, the selector switch will pass successively through taps A1 to A7 (Figure A.5). The tappings are connected one after the other to the line terminal or to the neutral depending on the connection of the transformer windings. If the transformer winding is connected in delta, then the tappings are in their turn connected to the line terminal. For star-connected transformer windings, the tappings are in their turn connected to the neutral point. When all the tap windings have been selected by the selector switch (see Figure A.5-A), a tap winding in the change-over selector switch must be selected. Then, the selector switch can continue its operation. The selection of the next tap position in the change-over selector is depicted in Figure A.5. When the selector switch has included all the tap windings in the circuit (roller contacts in position A7 – see Figure A.5-A), the voltage has been increased by 7 times the step voltage  $\Delta V$ . Before the selector switch can perform the next switching operation, the roller contact 1 of the change over switch moves from position A8 to position A9 (see Figure A.5-B). The voltage of the slipping A0 and consequently the voltage of contact A0 of the tap selector increase by 8 times the step voltage  $\Delta V$ . For that period roller contact 2 of the change-over switch remains in the position A8.

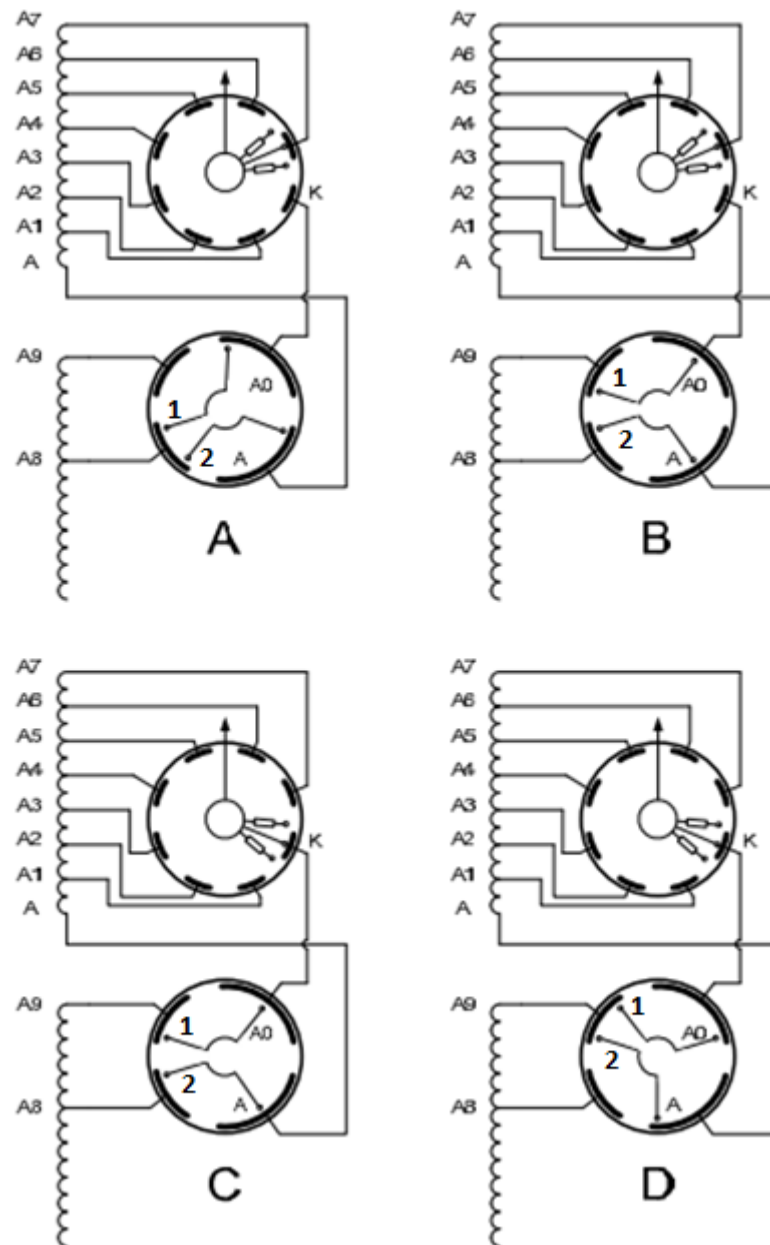


Figure A.5. The transition process of the change-over selector [5].

The voltage difference between contacts A0 and A7 is again the step voltage  $\Delta V$ . The selector switch moves to contact k (see Figure A.5-C), thus sensing only one step difference  $\Delta V$ .

The load current is flowing through roller contact 1 and the change-over selector contact A0. The roller contact 2 of the change-over switch moves from A8 to A9 (see Figure A.5-D) before the selector switch roller contact moves from A0 to A1. After switching the change-over selector switch, the selector switch can perform the next cycle of operations.

### A. 1. 2 Diverter switch type OLTC

The diverter switch type OLTC technology combines a diverter switch and a tap selector. Figure A.6 presents the schematic diagram of a diverter switch type OLTC combined with a tap selector. It can be seen in Figure A.6 that the tap selector consists of two sets of contacts. One contact operates under load. The next contact is responsible for selecting the next tap position. The contact which selects the next tap position does not switch any current. When the next tap position is determined, the diverter switch moves its contacts from their current position to other contact which has selected the next tap position. The tap selector can be combined with a change over selector if the expansion of the OLTC's range is required. The change-over selector can be used as a coarse change over selector or as a reversing change-over selector.

The transition between two contacts in a diverter switch type OLTC is presented in Figure A.7. The load current initially flows through the main contact  $MCa$  (Figure A.7-A). The switch of  $MCa$  opens and the current starts flowing through the main switching contact  $MSCa$  (Figure A.7-B). The switch of the first transition contact closes and the switch of  $MSCa$  opens (Figure A.7-C). The load current is now flowing through the first transition contact  $TCa1$  (Figure A.7-D). The switch of the second transition contact  $Tcb1$  closes and the load current is split between the two transition resistors (Figure A.7-E). A circulating current  $I_c$  is also created (Figure A.7-E). The switch of the contact  $TCa1$  opens and the load current flows through  $Tcb1$  (Figure A.7-F). The switch of the main switching contact of the next tap position closes and takes over the load current. At the same time the switch of  $Tcb1$  opens (Figure A.7-G). The switch of the main contact of the next tap position closes (Figure A.7-H) and the load current has been successfully transferred to the main contact of the next tap position  $MCb$  (Figure A.7-I). The voltage has been increased/decreased by the step voltage  $\Delta V$ . The transition period is now complete.

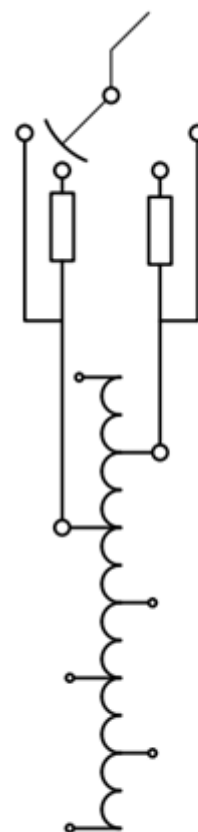


Figure A.6. Diverter switch type OLTC with tap selector [5].



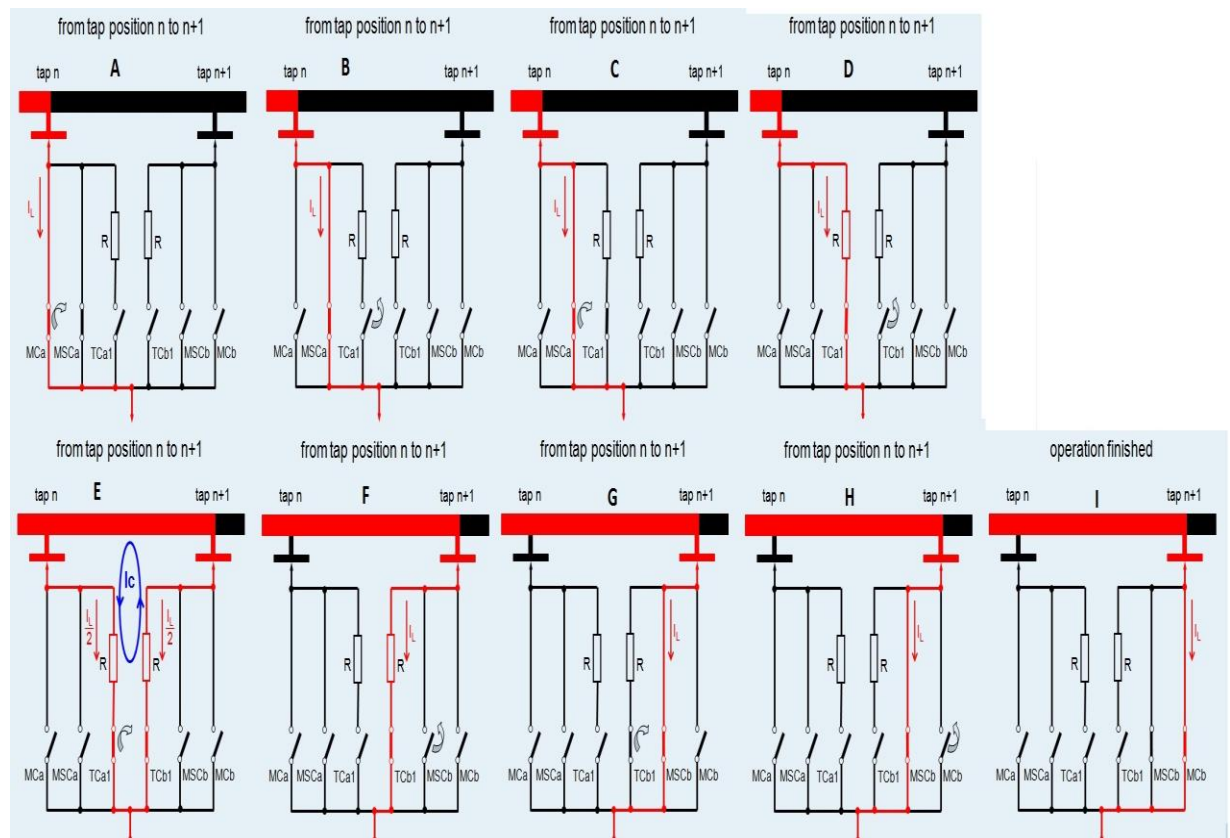


Figure A.7. Transition period in diverter switch type OLTC [6].

### A. 1.3 Vacuum switch type OLTC

A new technology arising fast at the last few years is the vacuum switch type OLTC. The arcs in that type of OLTC are extinguished inside a vacuum chamber. The vacuum type OLTC displays some important advantages over the conventional oil type OLTC. The advantages were thoroughly discussed in chapter 2. The operation of the vacuum switch type OLTC is presented in Figure A.8.

The OLTC is equipped with two vacuum chambers per phase. When the transition contact which is connected in series with a transition resistor approaches the next tap position, an arc is created and extinguished in the vacuum chamber (Figure A.8-3). The arc is created because when the transition contact touches the next tap position a circulating current starts flowing (Figure A.8-5). Then the main contact leaves the tap position and an arc is created and extinguished inside the vacuum chamber. The arc is created because the circulating current stops flowing. The load current flows through the transition contact (Figure A.8-7). Then the main contact touches the next tap position and takes over the load current (Figure A.8-9).

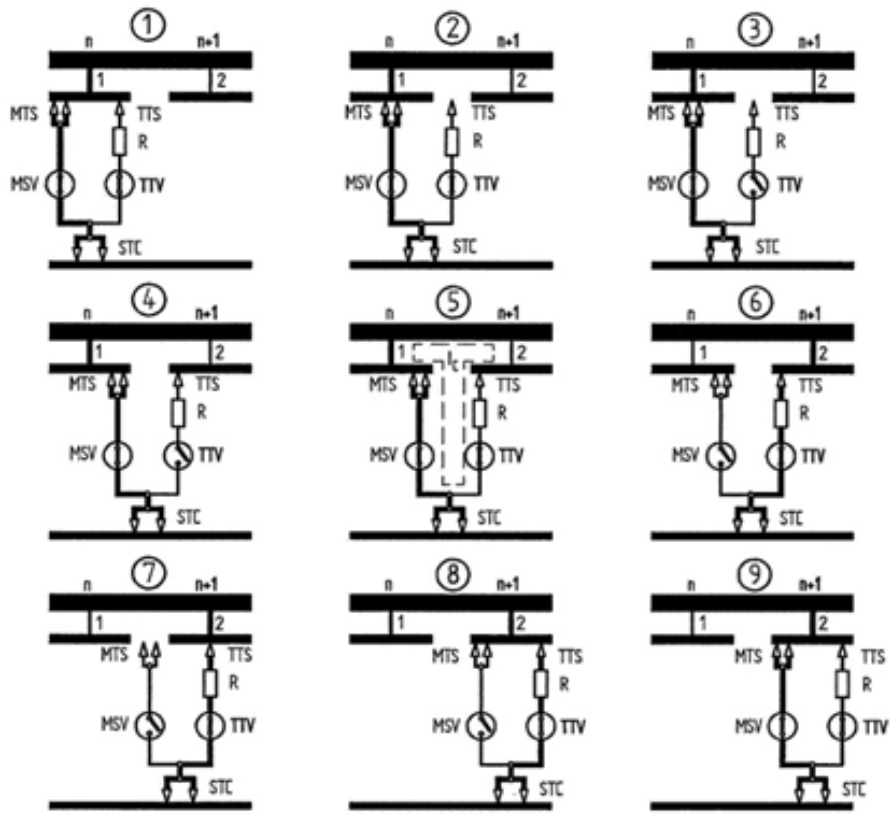


Figure A.8. Operation of the vacuum type OLTC [6].

# Appendix B

## PDBasell Check

The PD detector that was used in this research project was PDBasell manufactured by TechImp Spa. This particular PD detector provides the user with different acquisition modes and different representations of the PD pulses. Some of the features that are provided by PDBasell were presented in chapter 4. In this appendix the different acquisition modes will be compared.

### B.1 Acquisition modes

PDBasell is equipped with different acquisition modes. The acquisition window of PDBasell is presented in Figure B.1.

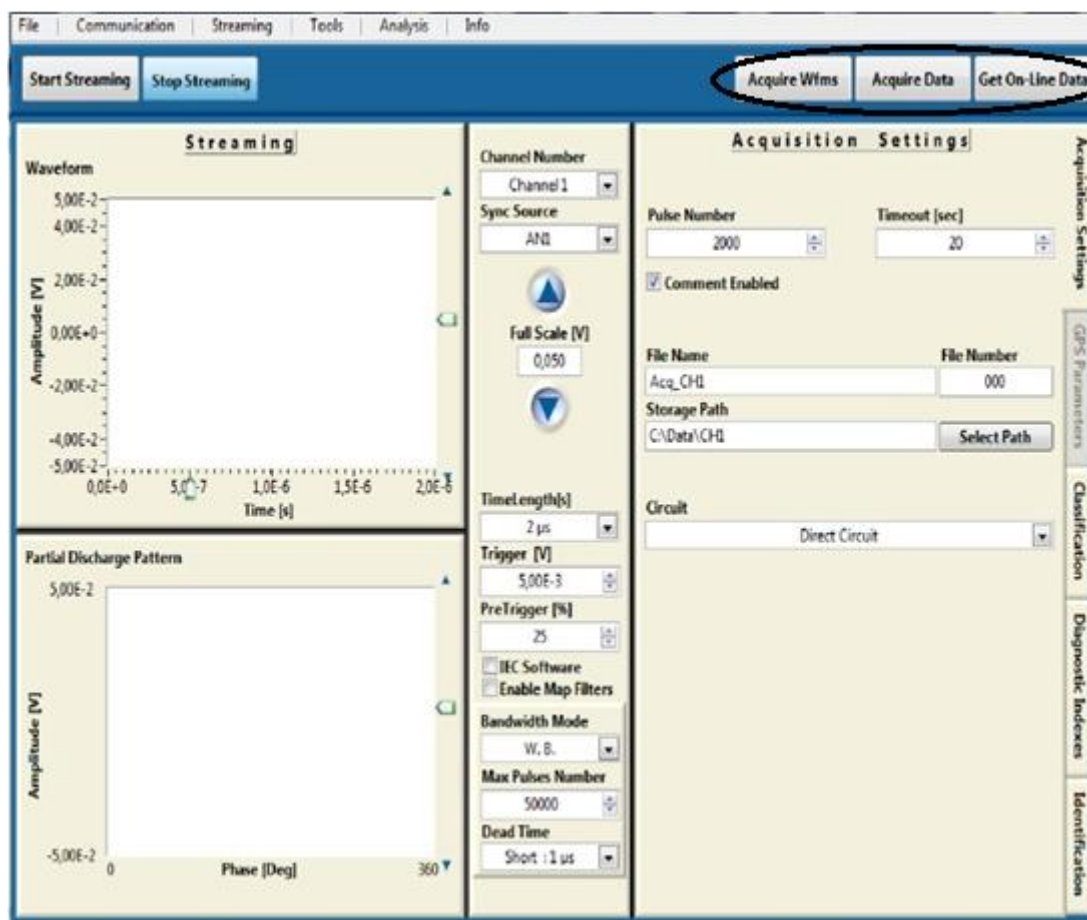


Figure B.1. Acquisition window of PDBasell.

## Appendix B

In the Acquisition window of Figure B.1 the different features of the detector are presented. The detector provides three different acquisition modes depending on the frequency bandwidth of the mode. The different acquisition modes are:

- 4) W.B (Wide Band): The range of frequency acquisition is from 16 kHz to 48 MHz.
- 5) W.B + HPF (High Pass Filter): is the wide band plus a 2.5 MHz high pass embedded filter. The range of frequency acquisition is from 2.5 MHz to 48 MHz.
- 6) IEC 60270: is the IEC standard bandwidth. The range of frequency acquisition is from 115 to 440 kHz.

In addition, for each mode, the user can select between the acquisitions of different types of data. The acquisition can be performed by using the three options which are highlighted in the black ellipse of Figure B.1. The different options are: the *'acquire waveforms'* option and the *'acquire data'* option. In the IEC 60270 acquisition mode, the *'acquire data'* option presents only the phase resolved pattern of the pulses. The option *'acquire waveforms'* displays the phase resolved pattern, the shape of the PD pulse and the frequency spectrum of the pulse. To compare the different types of acquisition, the set up of Figure B.2 was devised.

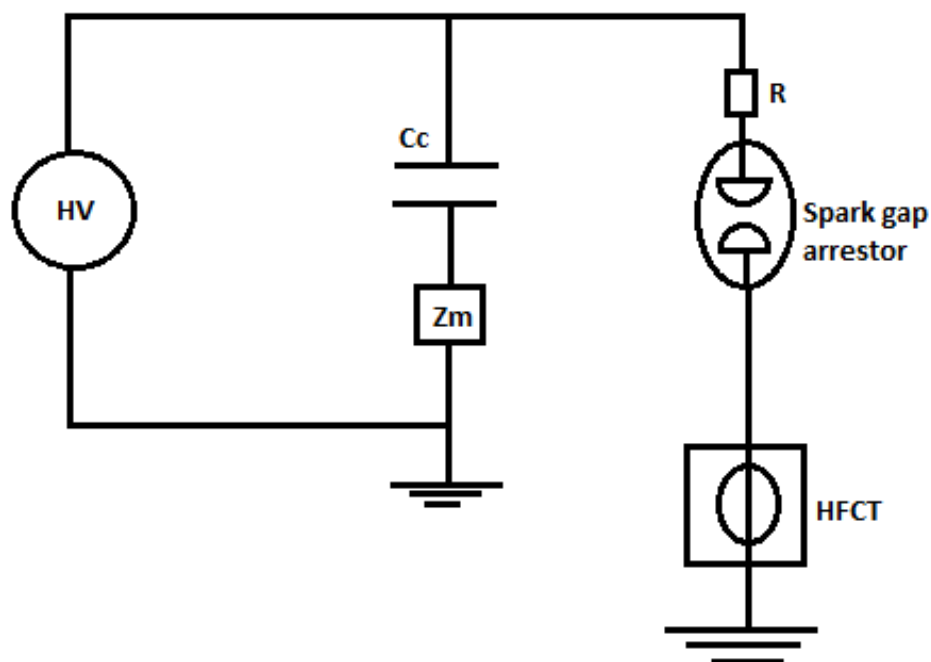


Figure B.2. Spark gap arrester used to test PDBaseII.

A spark gap arrester was used to represent a PD source. A resistor of 1.6 Mohms was connected in series with the spark gap arrester to protect it. The acquisition was performed using the IEC 60270 frequency bandwidth. A comparison was made between the *'acquire waveforms'* and the *'acquire data'* options. The acquisition of 5000 pulses was performed once using the *'acquire data'* option and

## Appendix B

once using the 'acquire waveforms' option in IEC 60270 detection mode. The results are presented in Figure B.3.

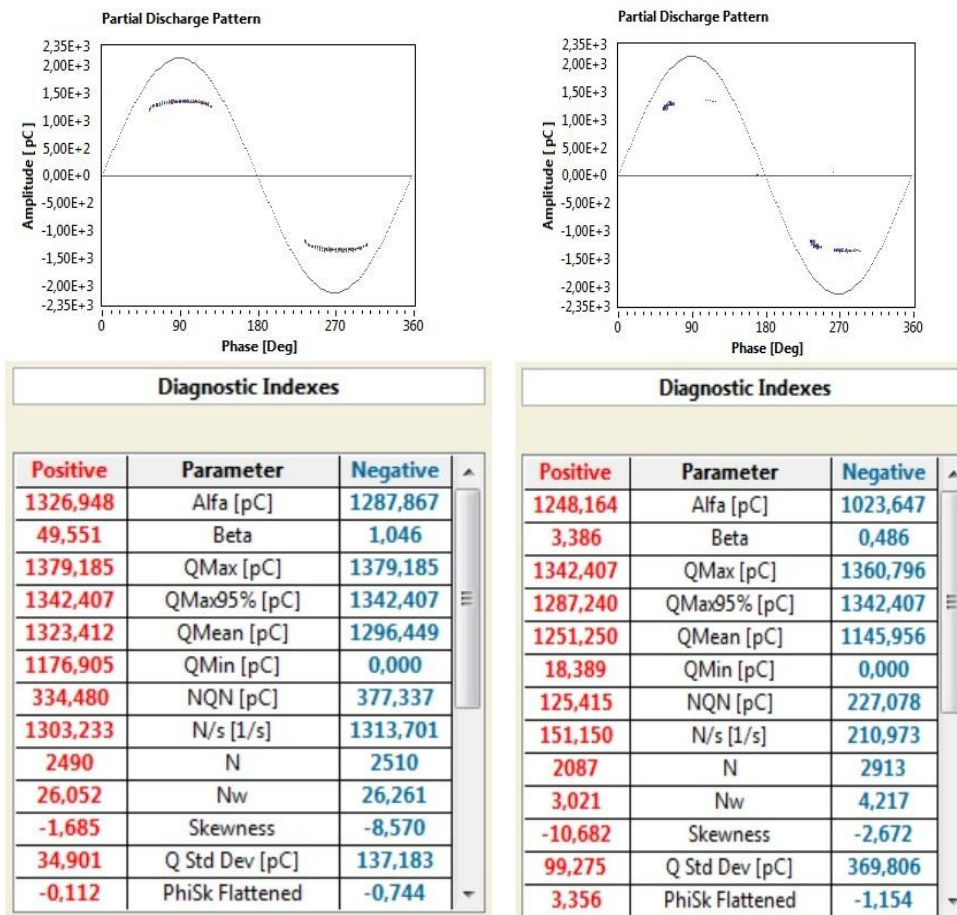


Figure B.3. 'Acquire data' (left) and 'Acquire waveforms' (right) using IEC 60270 detection mode.

The major difference between the two different options appears in the repetition rate. It can be observed from Figure B.3 that the value of the repetition rate is much smaller when using the 'acquire waveforms' option. This can be explained by the fact that the 'acquire waveforms' option enables all the features of the detector's software and must also use more memory in order to present all the different displays of the pulses. The acquisition process is thus slower and the calculated repetition rate is not the correct one. The miscalculation of the repetition rate when 'acquire waveforms' is used, is caused by the larger time required to acquire the 5000 pulses. The acquisition of 5000 pulses requires 2.26 seconds when the 'acquire data' option is used and 13.98 seconds when the 'acquire waveforms' option is used. In Figure B.3 the different acquisition parameters are presented. As shown in Figure B.3, there are also differences in other diagnostic parameters such as the Qmax 95% or the Qmean values. The major difference is observed when comparing the repetition rate that is calculated by the two different acquisition options.


# Appendix C

## Acoustic detection equipment

Table D.1. Acoustic Insulation Analyzer (AIA) [39].

	Manufacturer	Technical data
	TransiNor AS	<b>Dimensions:</b> (WxHxD) 25x15x31 cm
		<b>Weight:</b> Instrument Approximately 6 kg
		<b>Mains Voltage:</b> 230 VAC, 50/60 Hz 110 VDC Battery: 12 V, 4 Ah

Table D.2. Acoustic sensor [40].

	Manufacturer	Technical data
	Physical Acoustics Corporation (PAC)	<b>Acoustic emission sensor:</b> D9241A
		<b>Operating frequency:</b> 20-60 kHz
		<b>Peak sensitivity, Ref V/(m/s):</b> 82 dB
		<b>Resonant frequency, Ref V/(m/s):</b> 30 kHz

# Bibliography

- [1] P. Kang, D. Birtwhistle, J. Daley, D. McCulloch, "Non-invasive on-line condition monitoring of on load tap changers", IEEE proceedings on generation, transmission and distribution, Vol. 3, p. 2223-2228, January 2000.
- [2] A.Kramer, "On-load tap changers for power transformers; Operation principles, applications and selection", Maschinenfabrik Reinhausen GmbH, Regensburg Germany, ISBN 3-00-005948-2, 2000.
- [3] A. White, "Tapchanging – the transformer designer's perspective", IEE European Seminar on Developments of On-load Tap changers: Current Experience and Future, Regensburg Germany, p. 4/1-4/6, 9 November 1995.
- [4] "On-load tap changing equipment", WILLEM SMIT & CO'S, TRANSFORMATORENFABRIEK N.V, Nijmegen – Holland.
- [5] J.J. Erbrink, "On-load Tap Changer Diagnosis on High-Voltage Power Transformers using Dynamic Resistance Measurements", PhD Thesis, Delft University of Technology, March 2011.
- [6] WILLEM SMIT & CO'S, TRANSFORMATORENFABRIEK N.V, SMIT TRANSFORMATOR Service, Nijmegen – Holland.
- [7] J.J. Erbrink, E. Gulski, P.P. Seitz, R. Leich, "Advanced on-site diagnosis of transformer on-load tap changer", IEEE International Symposium on Electrical Insulation, Vancouver, Canada, p. 252-256, June 2008.
- [8] X. Chen, A. Cavallini, G. C. Montanari, "Improving High Voltage Transformer Reliability through Recognition of PD in Paper/Oil systems", International Conference on High Voltage Engineering and Application, Chongqing, China, November 9-13, 2008.
- [9] H. Zainuddin, P. M. Mitchinson, P. L. Lewin, "Investigation on the Surface Discharge Phenomenon at the Oil-pressboard Interface", IEEE International Conference on Dielectric Liquids, Trondheim, Norway, June 26-30, 2011.
- [10] V. Sokolov, Z. Berler, V. Rashkes, "Effective methods of assessment of insulation system conditions in power transformers: a view based on practical experience", Proceedings of the Electrical Insulation Conference and Electrical Manufacturing and Coil Winding Conference, Cincinnati, USA, p. 659-667, 26-28 October 1999.

- [11] N. Yoshimura, S. Kumagai, B. Du, "Research in Japan on the Tracking Phenomenon of Electrical Insulating Materials", IEEE Electrical Insulation Magazine, Vol. 13, No. 5, p. 8-19, October 1997.
- [12] P. M. Mitchinson, P. L. Lewin, B. D. Strawbridge, "Tracking and Surface Discharge at the Oil-Pressboard Interface", Annual Report Conference on Electrical Insulation and Dielectric Phenomena, October 14-17, 2012.
- [13] R. M. Schomper, "Condition assessment model for power transformers", Master thesis, Technical University of Delft, December 2004.
- [14] Cigre, "Life assessment techniques for power transformers", Working Group A2.18, Technical Brochure 227, June 2003.
- [15] S. Markalous, S. Tenbohlen, K. Feser, "Detection and Location of Partial Discharges in Power Transformers using Acoustic and Electromagnetic Signals", IEEE Transactions on Dielectrics and Electrical Insulation, Vol. 15, Issue: 6, p. 1576 – 1583, December, 2008.
- [16] S. Coenen, S. Tenbohlen, "Location of PD sources in Power Transformers by UHF and Acoustic Measurements", IEEE Transactions on Dielectrics and Electrical Insulation, Vol. 19, Issue: 6, p. 1934 – 1940, December, 2012.
- [17] G. Luo, D. Zhang, "Study On Performance of Developed and Industrial HFCT Sensors", 20<sup>th</sup> Australasian Universities Power Engineering Conference (AUPEC), 5 – 8 December, 2010.
- [18] Z. Wang, Y. Liu, P. J. Griffin, " Artificial intelligence in OLTC fault diagnosis using dissolved gas-in-oil information", IEEE Power Engineering Society Summer Meeting, Seattle, USA, Vol. 4, p. 2422-2427, 16-20 July 2000.
- [19] M. Duval, "The Duval triangle for load tap changers, non-mineral oils and low temperature faults in transformers", IEEE Electrical Insulation Magazine, Vol. 24, No 6, p. 22-29, November-December 2008.
- [20] IEEE Std C57.104-1991, "IEEE Guide for the interpretation of gases generated in oil-immersed transformers".
- [21] M. Wang, A. J. Vandermaar, K. D. Srivastava, "Review of condition assessment of power transformers in service", IEEE Electrical Insulation Magazine, Vol. 18, No.6, p. 12-25, November – December 2002.
- [22] R. Zijderduin, J. J. Erbrink, E. Gulski, J. J. Smit, R. Leich, " Condition Assessment of power transformers OLTC by DGA and dynamic resistance measurements", Proceedings of the 16<sup>th</sup> international symposium on high voltage engineering, Johannesburg, South Africa, 2009.



- [23] Kelman, "Transport X", Portable Dissolved Gas Analysis unit and Moisture in Oil, [www.kelman.co.uk](http://www.kelman.co.uk), viewed April 2013.
- [24] E. Lemke, S. Berlijn, E. Gulski, M. Muhr, E. Pultrum, T. Strehl, W. Hauschild, J. Rickmann, G. Rizzi, "Guide for Partial Discharge measurements in compliance to IEC 60270", Cigre 2008.
- [25] S. I. Cho, "On-line PD (Partial Discharge) Monitoring of Power system Components", Aalto, 2011.
- [26] R. O. Duda, P. E. Hart, "Pattern Classification and Scene Analysis", Wiley, 1973.
- [27] A. Krivda, "Automated Recognition of Partial Discharges", IEEE Transactions on Dielectrics and Electrical Insulation, Vol. 2, no. 5, p. 796 – 821, October, 2005.
- [28] A. Contin, A. Cavallini, G. Montanari, G. Pasini, F. Puletti, " Digital detection and fuzzy classification of partial discharge signals", IEEE Transactions on dielectrics and electrical insulation, Vol. 9, no. 3, 2002.
- [29] Electra, No. 11, Working Group 21.03, "Discharges", Study Committee No. 21, 1968.
- [30] A. Cavallini, G. C. Montanari, B. Codet, P. Vetu, "Condition assessment of instrument transformer by partial discharge analysis: A comprehensive approach", Transmission and Distribution Conference and Exhibition, 2005/2006 IEEE PES, 21-24 May, 2006.
- [31] H. Illias, T. S. Yuan, A. H. Abu Bakar, H. Mokhlis, "Partial Discharge Patterns in High Voltage Insulation", IEEE International conference on Power and Energy (PECon), 2 – 5 December, Kota Kinabalu Sabah, Malaysia, 2012.
- [32] G. C. Montanari, A. Cavallini, F. Ciani, "Partial discharges in internal voids: dependence on defect position with respect to electrodes", Conference on Insulation and Dielectric Phenomena, 14-17 October 2007.
- [33] F. Kreuger, "Industrial High Voltage", Volume I, Delft University Press, Delft, 1991.
- [34] TechImp, PD sensors, Inductive PD sensors, High Frequency Current Transformers, closed core version, [www.techimp.com](http://www.techimp.com), viewed March 2013.
- [35] J. Dai, Z. D. Wang, P. Jarman, "Creepage Discharge on Insulation Barriers in Aged Power Transformers", IEEE Transactions on Dielectrics and Electrical Insulation, Vol. 17, no. 4, p. 1327 - 1335, August, 2010.

- [36] J. Li, W. Si, X. Yao, Y. Li, "Partial Discharge Characteristics over differently Aged Oil/Pressboard Interfaces", IEEE Transactions on Dielectrics and Electrical Insulation, Vol. 16, no. 6, p. 1640 – 1647, 2009.
- [37] X. Yi, Z. D. Wang, F. Perrot, M. Lashbrook, "Surface Treeing on Pressboard Barriers in Synthetic and Natural Ester Liquids under AC Stress", IEEE International Conference on Dielectric Liquids (ICDL), 26-30 June, 2011.
- [38] H. R. Mirzaei, A. Akbari, E. Gockenbach, M. Zanjani, K. Miralikhani, "A Novel Method for Ultra-High-Frequency Partial Discharge Localization in Power Transformers Using the Particle Swarm Optimization Algorithm", IEEE Electrical Insulation Magazine, Vol. 29, no. 2, p. 26-37, March-April, 2013.
- [39] Suwarno, "In comparison between corona discharges in air and streamer discharge in silicone oil", International Conference on High Voltage Engineering and Application, Chongqing, China, November 9-13, 2008.
- [40] A. Cavallini, G. C. Montanari, F. Ciani, "Analysis of Partial Discharge Phenomena in Paper-Oil Insulation Systems as a Basis for Risk Assessment Evaluation", IEEE International Conference on Dielectric Liquids, June – July, 2005.
- [41] TransiNor AS, Acoustic Insulation Analyzer (AIA), [www.doble.com/products/acoustic\\_insulation\\_analyzer.html](http://www.doble.com/products/acoustic_insulation_analyzer.html), viewed May 2013.
- [42] Physical Acoustics Corporation (PAC), [www.pacndt.com/index.aspx?go=company](http://www.pacndt.com/index.aspx?go=company), viewed May 2013.

# Acknowledgments

There are many people who contributed to the completion of this research project. I feel obliged to thank each and every one.

Firstly, I would like to express my gratitude and appreciation to Dr. ir. Peter H.F. Morshuis. I am really grateful for the opportunity of working on such an interesting project. I also feel the need to thank Dr. ir. Morshuis for his support and help, especially, during the difficult times of this project. Our weekly meetings proved to be a source of motivation and encouragement for me.

I would also like to express my appreciation to Dr. ir. Armando Rodrigo Moreira, for his contribution to the completion of the research project. Dr. ir. Moreira was always willing to help during the experiments in the high voltage lab. In addition, I would like to say many thanks for our discussions when things got complicated.

I would like to acknowledge the help that was provided during the project by the staff of the High Voltage Lab. Ing. Paul van Nes and Mr. Wim Termorshuizen always found time to help me even when their schedule was extremely loaded. Their help in the construction of the small scale set ups was very significant.

I would like to thank Eng. Luca Fornasari of TechImp S.P.A for exchanging ideas with me during his visit at Delft and for reviewing my experimental results. In addition, I would like to thank PhD students Alex Tsekmes and Roman Kochetov because they both helped in their own ways. I would like to thank Roman for providing his expensive needles for the experiments. In addition, I would like to express my gratitude to PhD student Lukasz Chmura. Lukasz was always interested in my progress and he always had spare time to discuss and review my chapters despite his overloaded schedule.

It is important to me to thank my friends and my roommates. Kosta, Vanjel, Chris, Katerina and George thank you for a very funny year in Delft and for the psychological support. In addition, I would like to thank Roland, Marco and Ron for our collaboration in the high voltage lab. Very special thanks to my friend Ron. Despite our fights, working together was a pleasure. Kosta (mother), I want to thank you for everything you did for me this year.

Finally, I would like to thank my family. You are always an inspiration to me. Thank you for all your support: For the financial support during the difficult times back home but more importantly for the mental support. You always encouraged me to do the best and you are always there for me in every aspect of my life.